Inaugural - Dissertation

zur
Erlangung der Doktorwürde
der
Naturwissenschaftlich-Mathematischen
Gesamtfakultät der
Ruprecht-Karls-Universität
Heidelberg

Vorgelegt von
Dirk Robert Rehn, M.Sc.
aus Offenbach am Main

Datum der Mündlichen Prüfung: 26. November 2015

Development of Quantum Chemical Methods for Excited-State and Response Properties

Gutachter:

Prof. Dr. Andreas Dreuw
PD Dr. Markus Pernpointner

October 19, 2015

Meiner Mutter

Contents

List of Figures

List of Tables

Preface

Abstract

The interaction of light and matter is central in some of the most fundamental processes in nature. The theoretical description of these processes is essential for numerous applications in all fields of science. To gain an understanding of light-induced reactions at a microscopic scale, it is necessary to study quantum mechanical phenomena, for which quantum chemical methods are required.

Quantum chemical methods offer access to excitation energies, potential energy surfaces and excited-state properties, which are key for the description of photo-chemical reactions. A variety of well-established quantum chemical methods is available, but however, many of these methods have limited applicability due to their exceedingly large computational demands. In general a numerically exact description is only possible for molecules with few atoms. Yet, biologically or technically relevant systems comprise hundreds or thousands of atoms. Examples are protein-chromophore complexes, which take part in photosynthesis or the reception of light in the eyes of humans and animals.

An important part in the field of quantum chemistry is the development of suitable methods, which offer both, a sufficiently accurate description of the involved physical effects, and feasible computational requirements. Of the available methods, which fulfill the above-stated requirements, many suffer from severe drawbacks.

The central information obtained from quantum chemical calculations is the energy of electronic states. However, for many interesting questions, further properties of the electronic states are required. Hence, an important part of the development of quantum chemical methods is the derivation and implementation of methodologies for the description of excited state properties. A key property is the gradient of the energy. It is required to efficiently explore potential energy surfaces and for the theoretical modeling of experimental findings. Other important quantities are absorption cross-sections, which correspond to absorption coefficients in spectroscopical experiments.

In this thesis, the so-called algebraic diagrammatic construction (ADC) scheme for the polarization propagator is considered for the description of electronically excited states. It is a quantum chemical method, which has gained more attention over the last decade. It could be shown that ADC offers for many relevant systems a well-balanced mix of both accuracy and computational demand. In particular, in this thesis the derivation and implementation of excited state energy gradients is presented. Furthermore an approach to obtain optical properties using the so-called intermediate state representation (ISR) is discussed. The ISR/ADC approach for the computation of two-photon absorption cross-sections and its implementation are presented.

Both implementations are numerically tested and applied to two model sys-

tems, all-*trans*-octatetraene and *trans*-bithiophene. The results for *trans*-bithiophene are very promising, however, in the case of all-*trans*-octatetraene limitations for the description of the excited state geometry by the presented derivative approach are encountered.

Zusammenfassung

Die Wechselwirkung von Licht und Materie spielt eine zentrale Rolle in einigen der grundlegendsten Prozesse in der Natur. Die theoretische Beschreibung dieser Prozesse ist elementar für zahlreiche Anwendungen in allen Bereichen der Naturwissenschaften. Um lichtinduzierte Reaktionen auf mikroskopischer Ebene zu verstehen, ist die Beschreibung quantenmechanischer Phänomene notwendig. Für die Untersuchung dieser Phänomene werden quantenchemische Rechenmethoden benutzt.

Quantenchemische Rechenmethoden liefern die benötigten Informationen zur Beschreibung von photochemischen Reaktionen wie Anregungsenergien, Potentialhyperflächen und Eigenschaften angeregter Zustände. Eine Vielzahl von quantenchemischen Rechenmethoden ist verfügbar. Allerdings ist die Anwendung eines Großteils dieser Methoden aufgrund ihres enormen Rechenaufwandes stark eingeschränkt. Generell ist die Berechnung numerisch exakter Eigenschaften nur für Moleküle mit sehr wenigen Atomen möglich, wohingegen biologische Systeme oder Komplexe mit Relevanz für technische Anwendungen oft hunderte oder tausende Atome enthalten. Ein Beispiel dafür sind Proteine, die bei der Photosynthese oder dem Sehvorgang im Auge von Menschen und Tieren beteiligt sind.

Ein wichtiger Teil der Quantenchemie befasst sich mit der Entwicklung von Rechenmethoden, die zum einen anwendbar bei relevanten Systemen sind und zum anderen eine ausreichende Genauigkeit in der Beschreibung der beteiligten physikalischen Effekte liefern. Von den existierenden Methoden, die der oben genannten Beschreibung entsprechen, haben viele teils schwerwiegende Nachteile.

Die zentrale Größe, die quantenchemische Rechenmethoden liefern, ist die Energie von elektronischen Zuständen. Darüber hinaus sind jedoch weitere Eigenschaften der elektronischen Zustände wichtig für zahlreiche Fragestellungen und die Berechnung dieser Eigenschaften stellt eine wichtige Herausforderung dar. Dazu müssen methodische Ansätze entwickelt und in Computerprogrammen implementiert werden. Eine wichtige Eigenschaft sind Ableitungen der Energie elektronischer Zustände. Ableitungen werden benötigt, um stationäre Punkte in Potentialhyperflächen zu lokalisieren und experimentelle Spektren zu simulieren. Weitere wichtige Eigenschaften um spektroskopische Experimente zu beschreiben sind Absorptionswahrscheinlichkeiten.

In dieser Arbeit wird das sogenannte algebraisch-diagrammatische Konstruktionsverfahren (ADC) für den Polarisations-Propagator für die Beschreibung von elektronisch angeregten Zuständen benutzt. ADC ist eine quantenchemische Rechenmethode, die in den letzten Jahren mehr Beachtung gefunden hat. Es konnte gezeigt werden, dass ADC eine ausgewogene Mischung aus Genauigkeit und Rechenaufwand für viele relevante Systeme darstellt.

Im Detail werden in dieser Arbeit die Herleitung und die Implementierung von

Ausdrücken für die Ableitung der Energie von angeregten Zustandständen vorgestellt. Zusätzlich wird ein theoretisches Verfahren zur Beschreibung von optischen Eigenschaften über die sogenannte Darstellung in intermediären Zuständen (ISR) dargestellt. Der ADC/ISR-Ansatz wird für die Berechnung von Zweiphotonenquerschnitten angewendet und die Implementierung der hergelteiteten Ausdrücke wird beschrieben.

Mit den entwickelten Programmen werden numerische Testrechnungen durchgeführt und die Anwendbarkeit beider Programmentwicklungen wird am Beispiel von zwei Modellsystemen demonstriert. Als ein Modellsystem wird das Bithiophenmolekül gewählt und die erhaltenen Ergebnisse stimmen mit experimentellen Befunden überein. Im Fall des zweiten Modellsystems, *trans*-Oktatetraen, werden Schwierigkeiten bei der korrekten Beschreibung der angeregten Zustandsgeometrie durch die neuimplementierten Ableitungen festgestellt.

Chapter 1

Introduction

The theoretical investigation of electronically excited states of molecular systems is necessary to study the interaction of light and matter at a microscopic scale and is one of the major challenges for contemporary quantum chemistry. Processes following light absorption are studied or utilised in all areas of science, i.e. physics, chemistry, biology, medicine and material sciences and it is difficult to overstate the importance of light-induced phenomena and their consequences for all areas of life. Certainly, the most important example is photosynthesis. The photo-initiated conversion of water and carbon dioxide to oxygen and carbohydrates performed by plants, algae and bacteria [1] forms the basis for almost all life on earth. Another important biological example is vision of humans and animals involving a structural change in the rhodopsin protein caused by the enclosed retinal pigment molecule undergoing an isomerisation reaction [2]. Similar light-controlled activation or release reactions of drugs have medical applications or facilitate *in vivo* studies [3]. Technical examples with extremely high relevance are the conversion of solar energy in photovoltaic cells and the reverse process of converting electric energy into light in light-emitting diodes. Especially the design and development of efficient low-cost solar cells is a goal with strong societal repercussions [4, 5].

Photo-initiated processes are triggered by the initial absorption of light by a molecular system, promoting the system to an electronic excited state. The excitation is followed by a variety of possible scenarios depending on the properties of the system. These possibilities include chemical reactions, electron emission, emission of a photon, and the dissipation of the excess energy into heat. To describe

and predict the evolution of the excited molecular system, the detailed knowledge of the involved electronically excited states and their properties is crucial [6].

Experimentally, excited-state properties can be studied using absorption and emission spectroscopy. Some features like excitation and fluorescence energies of optically-allowed states can easily be accessed with simple steady-state spectroscopy. Obtaining signals of so-called dark states or the investigation of the excited-state dynamics require more elaborate experiments. Today, a large selection of highly sophisticated spectroscopic methods is available. For example ultra-fast transient absorption spectroscopy can be used to study light-induced chemical reactions on a femtosecond timescale [7]. However, the resulting spectra are often complex and difficult to interpret, since the signals of many different effects can interfere with each other. Naturally, the complexity of the spectra increases for the study of bigger and more complex systems and in many cases models based on accompanying quantum chemical calculations are inevitable for the interpretation of the experimental findings.

The development of a theoretical model of the excited-state dynamics of photo-initiated processes, requires the calculation of the energies of the involved electronic excited states with quantum chemical methods. However, numerically exact computations are strongly limited to exceedingly small systems with few atoms. Still, systems of interest usually comprise of hundreds or even more atoms. Different strategies are pursued to enable accurate computations of larger systems. One scheme is to split the system into a quantum chemically treated subsystem, for example the pigment molecule in a protein, and include the remaining system through a computationally cheaper model, i.e., classical mechanics. Nevertheless, such schemes may require the quantum chemical treatment of up to 200 atoms, which is still too large for many highly accurate methods. For the electronic ground state such calculations have become standard using density-functional theory (DFT), while the development of applicable computational methods with sufficient accuracy for the description of electronically excited states remains an important challenge.

Nowadays, several quantum chemical methods exist which facilitate the calculation of excited states and their properties. Yet, most of them cannot be applied to large molecular systems, since they are exceedingly computationally demanding.

The remaining methods are [6, 8]: semi-empirical approaches [9–11], configuration interaction singles (CIS) [12, 13], time-dependent Hartree-Fock (TD-HF) [14], complete active space self-consistent field (CASSCF) [15, 16] and time-dependent density functional theory (TDDFT) [17, 18]. All of them can be applied to systems of at least several hundred atoms. However, the application of these methods is limited due to severe drawbacks, such as large errors in excitation energies, incorrect description of the excited states, or the requirement of a priori knowledge about the excited states of the systems. Especially the lack of predictability demands extensive testing of the computed excited states against experimental data or more reliable quantum chemical methods to allow for thorough interpretation of the results. More accurate methods can be employed for small or medium-sized molecules and are often used for benchmark calculations on model systems with reduced size. Such methods can compute excitation energies with errors of less than 0.4 eV and can be applied to molecules up to hundred atoms. Coupled cluster (CC) [19] methods are among those respective methods and another approach, which has been given more attention over the last decade is the algebraic diagrammatic construction (ADC) scheme for the polarization propagator [20].

All quantum chemical methods constitute approximations of the molecular Schrödinger equation and most of them only treat its electronic part. The solution of the electronic Schrödinger equation in these approximative schemes yields energies of electronic states and gives access to the electronic wavefunction. The difference in energy between electronic states corresponds to the absorption or emission wavelength in spectroscopic measurements. In addition, the simulation of optical spectra requires, depending on the experiment, different properties which are obtained through different methodologies. For example the oscillator strength corresponds to the extinction coefficient in absorption spectra and multi-photon cross-sections are required for the simulation of laser-driven non-linear spectroscopy. Different techniques to obtain these properties are required for different quantum chemical models and their derivation and implementation is an important part of the development of new methods.

Another key property for the description of various optical phenomena and the understanding of chemical reactions is the gradient of the electronic energy and its efficient evaluation using analytical derivative expressions is an important trait for

quantum chemical methods. Since the early work of Pulay [21] analytical energy derivatives have become a standard tool in quantum chemistry. As Pulay wrote in a recent review article [22]: '*Analytical calculation of energy derivatives with respect to nuclear coordinates revolutionized applied molecular quantum mechanics by allowing the routine calculation of molecular structures and related properties.*'

Energy derivatives are employed in almost all *in silico* quantum chemical studies. A prominent example is the use of derivatives with respect to nuclear coordinates to explore potential energy surfaces (PES) of molecular systems, which are essentiell for the description of dynamical effects. For many properties of molecular systems only the stationary points of PES are relevant, which can be obtained with energy gradients through optimization. For example, the minima in the PES of the lowest electronic state represent equilibrium structures of molecules, which are required to access thermodynamical properties of chemical reactions or to simulate steady-state absorption spectra. Likewise, the minimum of the first electronically excited singlet state is required to simulate steady-state fluorescence spectra. In addition, gradients offer access to so-called minimal energy pathways, which reveal mechanisms of chemical reactions and they can be used to minimize the difference between the PES of two electronic states to study so-called conical intersections, which play important parts in light-induced processes.

Gradients of any energy functional can simply be obtained via finite differences for each component of the perturbation. However, the applicability of numerical derivatives of quantum chemical energy functions is limited for different reasons. A limiting factor is the required number of single point energy calculation of at least two points for each component of the perturbation. If the perturbation is a geometrical distortion and the system has N atoms, than (in absence of symmetry) at least $3N-6$ single point energy calculations have to be performed. Additionally, numerical differentiation suffers from numerical instabilities which can lead to slow or failing convergence. In contrast to finite differences, analytical derivatives are numerically stable and can for many quantum chemical methods be performed at a computationally cost comparable to a single energy calculation[22, 23].

This thesis is organized as follows: in the first part, the development and implementation of excited state properties, i.e., excited state gradients and nonlinear optical properties, using the algebraic diagrammatic construction scheme is

discussed and in the second part applications on molecular systems are presented. First, the basic approximations inherent in all quantum chemical methods are introduced in chapter 2. In chapter 3, the algebraic diagrammatic construction scheme for the polarization propagator is presented and the working equations for its second order variant are derived. In the subsequent chapter 4 an introduction to analytical derivatives for *ab initio* methods is given and analytical gradient expressions for the energy of the second and third order ADC approximations are obtained. Chapter 5 deals with the computation of optical properties using the so-called intermediate state representation approach. The first part of this thesis is concluded by chapter 6, which covers details on the implementation of the presented methodologies. In the first chapter of the second part, test calculations are presented and in the subsequent chapter 8 the implemented features are applied to study two medium-sized molecular systems. The thesis is concluded giving an outlook on further developments

Part I

Theoretical methods

Chapter 2

Theoretical foundations

2.1 Basic approximations

Quantum chemical methods are approaches to solve the molecular time-independent Schrödinger equation (SE), which yields the energies of the molecular system E as eigenvalues:

$$\hat{\mathcal{H}}(\mathbf{r},\mathbf{R})|\Psi(\mathbf{r},\mathbf{R})\rangle = E|\Psi(\mathbf{r},\mathbf{R})\rangle, \tag{2.1}$$

Here, the Hamiltonian $\hat{\mathcal{H}}$ and the wavefunction $|\Psi\rangle$ depend on the electronic coordinates $\mathbf{r}$ and the nuclear coordinates $\mathbf{R}$. Since the SE in general cannot be solved analytically, numerical approximations have to be introduced.

2.1.1 Born-Oppenheimer approximation

The first, most basic approximation, which is inherent in most quantum chemical methods, is the Born-Oppenheimer approximation [24]. Since electrons and nuclei differ in mass by at least three orders of magnitude, the electrons can assumed to be moving through a constant electric field generated by the resting nuclei. Thus, the electronic part can be treated as a separate problem and the nuclear coordinates enter the electronic Schrödinger equation as parameters. The solution of the electronic SE

$$\hat{\mathcal{H}}_{el.}(\mathbf{r};\mathbf{R})|\Psi(\mathbf{r},\mathbf{R})\rangle = \varepsilon(\mathbf{R})|\Psi(\mathbf{r};\mathbf{R})\rangle, \tag{2.2}$$

yields so-called electronic states and state energies. However, the electronic SE is still too complicated to be solved analytically and the main goal of quantum chemistry is to find suitable schemes to obtain sufficiently accurate approximate solutions.

2.1.2 Hartree-Fock

One of the most basic approaches to obtain the electronic state with the lowest energy, the so-called ground state, is the Hartree-Fock (HF) approximation [24]. Here, as an ansatz for the N-particle ground-state wavefunction $|\Psi_0\rangle$, a so-called Slater determinant of single-particle wavefunctions (orbitals) $\phi_1(\mathbf{r}), \ldots, \phi_N(\mathbf{r})$ is introduced. The electronic SE, which is a partial differential equation of N coupled electrons, is split into systtem of N single-electron differential equations, which yield the orbitals as solutions. The orbitals are constructed as a linear combination of usually atom-centered basis functions $\{\chi_\mu(r)\}$:

$$\phi(r)_p = \sum_\mu C_p \chi_\mu(r). \tag{2.3}$$

The coefficients $\{C_p\}$ are determined by solving the Hartree-Fock equations [24]. Here, the electron spin has been omitted, which otherwise requires an additional spin index for ϕ_p. The single-electron equations are still coupled through the electron-electron interaction and the solutions of each differential equation depends implicitly on all orbitals. These coupled non-linear single-electron equations are solved self-consistently through an iterative procedure. This iterative procedure minimizes the expectation value of the Slater determinant with respect to the electronic Hamiltonian, based on the variational principle under the constraint of orthonormal single-particle wavefunctions:

$$\int d\mathbf{r} \phi_i^\star(\mathbf{r}) \phi_j(\mathbf{r}) = \langle \phi_i | \phi_j \rangle = \delta_{ij} \tag{2.4}$$

As a result, a set of n single-electron wavefunctions, so-called molecular orbitals (MO), is obtained. The MO are transformed from the atom-centered basis (AO) through the orbital transformation matrix $\mathbf{C}$, of which the elements have been introduced in equation 2.3, and n is the number of basis functions in the AO basis.

In addition, a set of n orbital energies is obtained, which together with the MO can be used to calculate the HF ground-state energy:

$$E_{HF} = \sum_{i}^{N} h_{ii} + \frac{1}{2}\sum_{ij}^{N}\langle ij|ij\rangle - \langle ij|ji\rangle = \sum_{i}^{N}\epsilon_i - \frac{1}{2}\sum_{ij}^{N}\langle ij||ij\rangle \tag{2.5}$$

Here, the one-electron integrals $\{h_{pq}\}$ and the two-electron integrals $\langle pq|rs\rangle$, which depend on the orbitals, have been introduced together with the symmetrized two-electron integrals $\langle pq||pq\rangle$, which are defined as:

$$\langle pq||rs\rangle = \langle pq|rs\rangle - \langle pq|sr\rangle \tag{2.6}$$

The index i in equation 2.5 is limited to the lowest first N orbitals. These are the so-called occupied orbitals, because they are occupied by the N electrons of the N-electron wavefunction in the electronic ground state. The remaining $n - N$ orbitals are unoccupied and the so-called virtual orbitals. In general, in this work indices $i, j, k, \ldots$ refer to occupied orbitals, $a, b, c, \ldots$ refer to virtual orbitals and $p, q, r, \ldots$ refer to general orbitals (both occupied and virtual).

In the HF approach, the electron-electron interactions are approximated. Instead of the full potential, each individual electron only experiences a static charge distribution generated by all other electrons. Therefore, dynamic effects due to changes in the electron movement are neglected. Though this approximation might appear crude, it usually recovers 95% of the electronic energy. However, the remaining 5% are often crucial for the theoretical description of chemical effects, since the thermodynamics of chemical reactions are driven by energy differences of the same order of magnitude. The difference between the (numerically) exact energy and the HF energy is called the correlation energy $E_{corr.} = E_{exact} - E_{HF}$ and post-HF methods, which are also called correlated or wavefunction-based methods, aim at improving the HF results.

2.2 Second quantization

The formalism of second quantization [24, 25] offers a convenient way to introduce and discuss post-HF methods. Here, a complete set of orthonormal single-particle

states (orbitals) and occupation numbers n_p for each orbital ϕ_p are used to represent many-particle states $|n_1, n_2, \ldots, n_\infty\rangle$. This formalism can be used for both fermionic and bosonic systems, however, in this work only electronic systems are discussed and the occupation numbers can only assume the values 0 or 1. In addition, any state must be antisymmetric with respect to permutation of two electrons. For many-electron states based on the HF orbitals, the set of single-electron states is finite $|n_1, n_2, \ldots, n_m\rangle$, with m being the number of HF orbitals.

2.2.1 Creation and annihilation operators

All many-electron states can be obtained from the so-called vacuum state $|0, 0, \ldots, 0\rangle$, in which all single-electron states are unoccupied, by applying so-called creation and annihilation operators. However, for the discussion of post-HF methods, the vacuum state is usually replaced by the HF ground state

$$|\Psi_{HF}\rangle = |n_i, n_j, \ldots, n_N, n_a, n_b, \ldots, n_m\rangle, \tag{2.7}$$

with N being the number of electrons and $n_i = n_j = \cdots = n_N = 1$, $n_a = n_b = \cdots = n_m = 0$. The creation and annihilation operators act on a many-electron state by changing the occupation number of a given orbital while preserving the required symmetry. The creation operator $\hat{c}_p^\dagger$ acts on the many-electron state $|n_1, \ldots, n_m\rangle$ by occupying orbital ϕ_p, i.e. changing its occupation number to 1, and yields 0 if ϕ_p was already occupied.

$$\hat{c}_p^\dagger |n_1, \ldots, n_m\rangle = -1^{(\sum_\tau^{p-1} n_\tau)} \delta(n_p, 0) |n_1, n_2, \ldots, n_{p-1}, 1, n_{p+1}, \ldots, n_m\rangle \tag{2.8}$$

The adjoint operator $\hat{c}_p$ removes the electron in orbital p, i.e. sets n_p to 0, and yields 0 if ϕ_p was already unoccupied.

$$\hat{c}_p |n_1, \ldots, n_m\rangle = -1^{(\sum_\tau^{p-1} n_\tau)} \delta(n_p, 1) |n_1, n_2, \ldots, n_{p-1}, 0, n_{p+1}, \ldots, n_m\rangle \tag{2.9}$$

It is important to note the anti-commutation relations of the creation and annihilation operators, which follow from the definitions in equations 2.8 and 2.9:

$$\hat{c}_p^\dagger \hat{c}_q^\dagger = -\hat{c}_q^\dagger \hat{c}_p^\dagger, \qquad \hat{c}_p \hat{c}_q = -\hat{c}_q \hat{c}_p, \qquad \hat{c}_p^\dagger \hat{c}_q = \delta_{pq} - \hat{c}_q \hat{c}_p^\dagger. \tag{2.10}$$

2.2.2 Arbitrary operators

The creation and annihilation operators are used to represent the action of arbitrary operators on many-electron states. For example a single-particle operator $\hat{\mathcal{O}}$ has in second quantization the form:

$$\hat{\mathcal{O}} = \sum_{pq} \langle \phi_p | \hat{\mathcal{O}} | \phi_q \rangle \hat{c}_q^\dagger \hat{c}_q = \sum_{pq} o_{pq} \hat{c}_p^\dagger \hat{c}_q \tag{2.11}$$

and $\langle \phi_p | \hat{\mathcal{O}} | \phi_q \rangle = o_{pq}$ are the matrix elements of $\hat{\mathcal{O}}$ in the single-electron basis. In the same way the electronic Hamiltonian, which will be called $\hat{H}$ in the following can be expressed as:

$$\hat{\mathcal{H}}_{el} = \hat{H} = \sum_{pq} h_{pq} \hat{c}_p^\dagger \hat{c}_q + \frac{1}{4} \sum_{pqrs} \langle pq||rs\rangle \hat{c}_p^\dagger \hat{c}_q^\dagger \hat{c}_s \hat{c}_r \tag{2.12}$$

2.3 Møller-Plesset perturbation theory (MP)

Perturbation theory offers a way to improve over the HF results. Møller-Plesset perturbation theory (MP) [26] is a well-established quantum chemical method. It is a special variant of Rayleigh-Schrödinger perturbation theory [27, 28], which is discussed first in this section before the explicit Hamiltonian splitting of MP is introduced.

2.3.1 Rayleigh-Schrödinger perturbation theory

In Rayleigh Schrödinger perturbation theory, the full Hamiltonian $\hat{H}$ is split into a part $\hat{H}_0$ of which the complete spectrum is known and the remaining part $\hat{H}_1 = \hat{H} - \hat{H}_0$, which is assumed to be a small perturbation.

$$\hat{H}_0 |\Psi_I^{(0)}\rangle = E_I^{(0)} |\Psi_I^{(0)}\rangle \tag{2.13}$$

Introducing an auxiliary parameter λ the Hamiltonian is written as:

$$\hat{H} = \hat{H}_0 + \lambda \hat{H}_1. \tag{2.14}$$

It is assumed, that both the exact eigenvalues of $\hat{H}$, E_I, and the eigenstates $|\Psi_I\rangle$ can be expressed in a series expansion:

$$E_I = \sum_{n=0}^{\infty} \lambda^n E_I^{(n)} \qquad\qquad |\Psi_I\rangle = \sum_{n=0}^{\infty} \lambda^n |\Psi_I^{(n)}\rangle \tag{2.15}$$

By inserting these series expansions in the eigenvalue equation for $\hat{H}$:

$$\left(\hat{H}_0 + \lambda \hat{H}_1\right) \sum_{n=0}^{\infty} \lambda^n |\Psi_I^{(n)}\rangle = \left(\sum_{n=0}^{\infty} \lambda^n E_I^{(n)}\right) \left(\sum_{n=0}^{\infty} \lambda^n |\Psi_I^{(n)}\rangle\right) \tag{2.16}$$

and collecting all terms with the same exponent of λ, the Schrödinger equation can be split into multiple equations:

$$\hat{H}_0|\Psi_I^{(0)}\rangle = E_I^0|\Psi_I^{(0)}\rangle \tag{2.17}$$

$$\hat{H}_0|\Psi_I^{(1)}\rangle + \hat{H}_1|\Psi_I^{(0)}\rangle = E_I^{(0)}|\Psi_I^{(1)}\rangle + E_I^{(1)}|\Psi_I^{(0)}\rangle \tag{2.18}$$

$$\hat{H}_0|\Psi_I^{(2)}\rangle + \hat{H}_1|\Psi_I^{(1)}\rangle = E_I^{(0)}|\Psi_I^{(2)}\rangle + E_I^{(1)}|\Psi_I^{(1)}\rangle + E_I^{(2)}|\Psi_I^{(0)}\rangle \tag{2.19}$$

$$\cdots .$$

It is useful to request that $|\Psi_I^{(0)}\rangle$ is normalized and orthogonal to higher order contributions:

$$\langle\Psi_I^{(0)}|\sum_{n=0}^{\infty} \Psi_I^{(n)}\rangle = \langle\Psi_I^{(0)}|\Psi_I^{(0)}\rangle = 1. \tag{2.20}$$

By multiplying the equations 2.17 - 2.19 from the left with $\langle\Psi_I^{(0)}|$ one obtains the equations determining the energy contributions of different order:

$$E_I^{(0)} = \langle\Psi_I^{(0)}|H_0|\Psi_I^{(0)}\rangle \tag{2.21}$$

$$E_I^{(1)} = \langle\Psi_I^{(0)}|H_1|\Psi_I^{(0)}\rangle \tag{2.22}$$

$$E_I^{(2)} = \langle\Psi_I^{(0)}|H_1|\Psi_I^{(1)}\rangle \tag{2.23}$$

$$\cdots .$$

In a similar way the corrections to the wavefunction can be found by multiplying equations 2.18 - 2.19 from the left by $\langle\Psi_J^{(0)}|$, with $I \neq J$. For example the first

order contribution is defined by:

$$\langle\Psi_J^{(0)}|\hat{H}_0|\Psi_I^{(1)}\rangle + \langle\Psi_J^{(0)}|\hat{H}_1|\Psi_I^{(0)}\rangle = \langle\Psi_J^{(0)}|E_I^{(0)}|\Psi_I^{(1)}\rangle + \langle\Psi_J^{(0)}|E_I^{(1)}|\Psi_I^{(0)}\rangle. \tag{2.24}$$

Using $\langle\Psi_J^{(0)}|\Psi_I^{(0)}\rangle = \delta_{IJ}$ equation 2.24 simplifies to:

$$E_J^{(0)}\langle\Psi_J^{(0)}|\Psi_I^{(1)}\rangle + \langle\Psi_J^{(0)}|\hat{H}_1|\Psi_I^{(0)}\rangle = E_I^{(0)}\langle\Psi_J^{(0)}|\Psi_I^{(1)}\rangle, \tag{2.25}$$

from which follows:

$$\frac{\langle\Psi_J^{(0)}|\hat{H}_1|\Psi_I^{(0)}\rangle}{E_I^{(0)} - E_J^{(0)}} = \langle\Psi_J^{(0)}|\Psi_I^{(1)}\rangle. \tag{2.26}$$

Thus, the first order correction to the wavefunction is given as:

$$|\Psi_I^{(1)}\rangle = \sum_{J\neq I} |\Psi_J^{(0)}\rangle \frac{\langle\Psi_J^{(0)}|\hat{H}_1|\Psi_I^{(0)}\rangle}{E_I^{(0)} - E_J^{(0)}} \tag{2.27}$$

and higher order corrections can be determined using the same procedure.

2.3.2 MP partitioning of the Hamiltonian

In MP the Hartree-Fock Hamiltonian $\hat{F}$ is chosen as zeroth order Hamiltonian, which is given as:

$$\hat{F} = \sum_{pq} f_{pq}\hat{c}_p^\dagger\hat{c}_q = \sum_{pq} h_{pq}\hat{c}_p^\dagger\hat{c}_q + \sum_{pq}\sum_k \langle pk||qk\rangle\hat{c}_p^\dagger\hat{c}_q \tag{2.28}$$

and is diagonal in the basis of MO orbitals $f_{pq} = \epsilon_p\delta_{pq}$. Thus $\hat{H}_0$ is defined as

$$\hat{H}_0 = \sum_p \epsilon_p\hat{c}_p^\dagger\hat{c}_p \tag{2.29}$$

and the remaining perturbation $\hat{H}_1$ is defined by equation 2.12 as:

$$\hat{H}_1 = -\sum_{pq}\sum_k \langle pk||qk\rangle\hat{c}_p^\dagger\hat{c}_q + \frac{1}{4}\sum_{pqrs}\langle pq||rs\rangle\hat{c}_p^\dagger\hat{c}_q^\dagger\hat{c}_s\hat{c}_r. \tag{2.30}$$

The eigenstates of $\hat{H}_0$ are the HF ground state $|\Psi_0^{(0)}\rangle$ and all other N-electron states, the so-called excited determinants. These are obtained from the HF ground state by replacing occupied orbitals by virtual orbitals, which is done by applying excitation operators $\hat{C}_I \equiv \{c_a^\dagger c_i; c_a^\dagger c_b^\dagger c_i c_j, a < b, i < j; \dots\}$:

$$|\Psi_I^{(0)}\rangle = \hat{C}_I |\Psi_0^{(0)}\rangle. \tag{2.31}$$

Depending on how many occupied orbitals have been replaced by virtual orbitals, these excited determinants are referred to as singly-excited $|\Psi_i^a\rangle$, doubly-excited $|\Psi_{ij}^{ab}\rangle$ and so on. Inserting these definitions in the expressions derived earlier in section 2.3.1 yields the expressions for the MP energy and wavefunction corrections:

$$\begin{aligned} E_0^{(0)} &= \sum_p \langle \Psi_0^{(0)} | \epsilon_p \hat{c}_p^\dagger \hat{c}_p | \Psi_0^{(0)} \rangle \\ &= \sum_i \epsilon_i \end{aligned} \tag{2.32}$$

$$\begin{aligned} E_0^{(1)} &= -\sum_{pq} \sum_k \langle pk||qk\rangle \langle \Psi_0^{(0)} | \hat{c}_p^\dagger \hat{c}_q | \Psi_0^{(0)} \rangle \\ &\quad + \frac{1}{4} \sum_{pqrs} \langle pq||rs\rangle \langle \Psi_0^{(0)} | \hat{c}_p^\dagger \hat{c}_q^\dagger \hat{c}_s \hat{c}_r | \Psi_0^{(0)} \rangle \\ &= -\frac{1}{2} \sum_{ij} \langle ij||ij\rangle \end{aligned} \tag{2.33}$$

$$\begin{aligned} E_0^{(2)} &= -\sum_{pq} \sum_k \langle pk||qk\rangle \langle \Psi_0^{(0)} | \hat{c}_p^\dagger \hat{c}_q | \Psi_0^{(1)} \rangle \\ &\quad + \frac{1}{4} \sum_{pqrs} \langle pq||rs\rangle \langle \Psi_0^{(0)} | \hat{c}_p^\dagger \hat{c}_q^\dagger \hat{c}_s \hat{c}_r | \Psi_0^{(1)} \rangle \end{aligned} \tag{2.34}$$

Collecting all terms up to to first order yields the Hartree-Fock energy given in equation 2.5 and thus, first-oder MP (MP(1)) provides no improvement over the HF result and the second-order term is the first correction to the HF energy. Before the second-order energy contribution can be evaluated, the first-order correction to the wavefunction $|\Psi_0^{(1)}\rangle$ has to determined, which has according to equation 2.27

the form:

$$|\Psi_0^{(1)}\rangle = \sum_{ia} |\Psi_i^a\rangle \frac{\langle \Psi_i^a | \hat{H}_1 | \Psi^0 \rangle}{E_0^{(0)} - E_{\Psi_i^a}} + \sum_{\substack{i<j \\ a<b}} |\Psi_{ij}^{ab}\rangle \frac{\langle \Psi_{ij}^{ab} | \hat{H}_1 | \Psi^0 \rangle}{E_0^{(0)} - E_{\Psi_{ij}^{ab}}} + \sum_{\substack{i<j<k \\ a<b<c}} |\Psi_{ijk}^{abc}\rangle \frac{\langle \Psi_{ijk}^{abc} | \hat{H}_1 | \Psi^0 \rangle}{E_0^{(0)} - E_{\Psi_{ijk}^{abc}}} + \cdots \tag{2.35}$$

To simplify the expression for $|\Psi_0^{(1)}\rangle$, Brillouin's theorem can be applied, which states that the matrix element of the Hamiltonian between the HF ground state and singly-excited determinants vanishes:

$$\langle \Psi_0^{(0)} | \hat{H} | \Psi_i^a \rangle = \langle \Psi_i^a | \hat{H} | \Psi_0^{(0)} \rangle = 0. \tag{2.36}$$

Inserting the partitioned Hamiltonian into equation 2.36 yields:

$$\langle \Psi^{(0)} | \hat{H}_0 + \hat{H}_1 | \Psi_i^a \rangle = \langle \Psi^{(0)} | \hat{H}_0 | \Psi_i^a \rangle + \langle \Psi^{(0)} | \hat{H}_1 | \Psi_i^a \rangle = 0. \tag{2.37}$$

The first term can be evaluated as

$$\langle \Psi_0^{(0)} | \hat{H}_0 | \Psi_i^a \rangle = \sum_p \langle \Psi_0^{(0)} | \epsilon_p c_p^\dagger c_p | \Psi_i^a \rangle = \sum_i \epsilon_i \langle \Psi_0^{(0)} | \Psi_i^a \rangle = 0 \tag{2.38}$$

from which follows that:

$$\langle \Psi_0^{(0)} | \hat{H}_1 | \Psi_i^a \rangle = \langle \Psi_i^a | \hat{H}_1 | \Psi_0^{(0)} \rangle = 0. \tag{2.39}$$

In addition, it can readily be seen, that matrix elements of single-particle operators between determinants that differ by more than one excitation vanish. The same applies to matrix elements of two-particle operators, in which the determinants have more than two different excitations. Thus, the first order MP correction to the wavefunction is given by:

$$|\Psi_0^{(1)}\rangle = \sum_{\substack{i<j \\ a<b}} |\Psi_{ij}^{ab}\rangle \frac{\langle \Psi_{ij}^{ab} | \hat{H}_1 | \Psi^0 \rangle}{E_0^{(0)} - E^{(0)}}. \tag{2.40}$$

Using the definition of $|\Psi_0^{(1)}\rangle$, the second order energy correction can be found as:

$$E_0^{(2)} = \sum_{\substack{i<j \\ a<b}} \frac{\langle \Psi_{ij}^{ab} | \hat{H}_1 | \Psi^0 \rangle}{E_0^{(0)} - E^{(0)}} \frac{1}{4} \sum_{pqrs} \langle pq||rs\rangle \langle \Psi_0^{(0)} | \hat{c}_p^\dagger \hat{c}_q^\dagger \hat{c}_s \hat{c}_r | \Psi_{ij}^{ab} \rangle. \tag{2.41}$$

2.4 Wick's theorem

Wick's theorem [29] can be employed to evaluate matrix elements in second quantization as they occur for example in the expressions for MP in the previous section 2.3.2. To introduce Wick's theorem, first the contraction of two operators $\hat{A}^\bullet \hat{B}^\bullet$ is defined as:

$$\hat{A}^\bullet \hat{B}^\bullet = \hat{A}\hat{B} - \{\hat{A}\hat{B}\}. \tag{2.42}$$

In equation 2.42 the normal ordering of two operators $\{\hat{A}\hat{B}\}$ has been introduced. The normal ordering of an operator string is defined by the following requisition: the expectation value of the HF ground state with respect to the normal-ordered operator string must vanish:

$$\langle \Psi^{(0)} | \{\hat{A}\hat{B}\hat{C}\dots\} | \Psi^{(0)} \rangle = 0. \tag{2.43}$$

From the definition of the normal ordering follows, that in a normal-ordered string of creation and annihilation operators all creation operators of virtual orbitals $\hat{c}_a^\dagger, \hat{c}_b^\dagger, \dots$ and annihilation operators of occupied orbitals $\hat{c}_i, \hat{c}_j, \dots$ are on the left-hand side and all creation operators of occupied orbitals $\hat{c}_i^\dagger, \hat{c}_j^\dagger, \dots$ and annihilation operators of virtual orbitals $\hat{c}_a, \hat{c}_b, \dots$ are on the right-hand side of the operator string.

Wick's theorem states, that an operator string can be expressed as a sum of

all possible normal-ordered contractions of the operator string:

$$\begin{aligned}\hat{A}\hat{B}\hat{C}\hat{D}\hat{E}\hat{F}\ldots =& \{\hat{A}\hat{B}\hat{C}\hat{D}\hat{E}\hat{F}\ldots\} \\ &+ \sum_{\substack{\text{single}\\ \text{contractions}}} \{\hat{A}^{\bullet}\hat{B}^{\bullet}\hat{C}\hat{D}\hat{E}\hat{F}\ldots\} \\ &+ \sum_{\substack{\text{double}\\ \text{contractions}}} \{\hat{A}^{\bullet}\hat{B}^{\bullet}\hat{C}^{\bullet\bullet}\hat{D}^{\bullet\bullet}\hat{E}\hat{F}\ldots\} \\ &\ldots \\ &+ \sum_{\substack{\text{full}\\ \text{contractions}}} \{\hat{A}^{\bullet}\hat{B}^{\bullet}\hat{C}^{\bullet\bullet}\hat{D}^{\bullet\bullet}\hat{E}^{\bullet\bullet\bullet}\hat{F}^{\bullet\bullet\bullet}\ldots\}.\end{aligned} \tag{2.44}$$

The key implication of Wick's theorem can be realized by evaluating the expectation value of the HF ground state on both sides of equation 2.44:

$$\begin{aligned}\langle\Psi^{(0)}|\hat{A}\hat{B}\hat{C}\hat{D}\hat{E}\hat{F}\ldots|\Psi^{(0)}\rangle =& \langle\Psi^{(0)}|\{\hat{A}\hat{B}\hat{C}\hat{D}\hat{E}\hat{F}\ldots\}|\Psi^{(0)}\rangle \\ &+ \sum_{\substack{\text{single}\\ \text{contractions}}} \langle\Psi^{(0)}|\{\hat{A}^{\bullet}\hat{B}^{\bullet}\hat{C}\hat{D}\hat{E}\hat{F}\ldots\}|\Psi^{(0)}\rangle \\ &+ \sum_{\substack{\text{double}\\ \text{contractions}}} \langle\Psi^{(0)}|\{\hat{A}^{\bullet}\hat{B}^{\bullet}\hat{C}^{\bullet\bullet}\hat{D}^{\bullet\bullet}\hat{E}\hat{F}\ldots\}|\Psi^{(0)}\rangle \\ &\ldots \\ &+ \sum_{\substack{\text{full}\\ \text{contractions}}} \langle\Psi^{(0)}|\{\hat{A}^{\bullet}\hat{B}^{\bullet}\hat{C}^{\bullet\bullet}\hat{D}^{\bullet\bullet}\hat{E}^{\bullet\bullet\bullet}\hat{F}^{\bullet\bullet\bullet}\ldots\}|\Psi^{(0)}\rangle.\end{aligned} \tag{2.45}$$

All terms on the right-hand side of equation 2.45 except the fully contracted expressions vanish, because they contain uncontracted normal-ordered operators. Hence, the expectation value of the HF ground state with respect to an operator string can be expressed as the expectation value of all possible full contractions of the operator string.

$$\langle\Psi^{(0)}|\hat{A}\hat{B}\hat{C}\hat{D}\hat{E}\hat{F}\ldots|\Psi^{(0)}\rangle = \sum_{\substack{\text{full}\\ \text{contractions}}} \langle\Psi^{(0)}|\{\hat{A}^{\bullet}\hat{B}^{\bullet}\hat{C}^{\bullet\bullet}\hat{D}^{\bullet\bullet}\hat{E}^{\bullet\bullet\bullet}\hat{F}^{\bullet\bullet\bullet}\ldots\}|\Psi^{(0)}\rangle \tag{2.46}$$

Wick's theorem offers a straightforward route to evaluate matrix elements for post-HF methods. In second quantization all matrix elements of arbitrary opera-

tors can be represented as expectation value of the HF ground state with respect to strings of excitation operators and the creation and annihilation operators of the respective operators. To obtain a matrix element, all possible contractions of the occurring creation and annihilation operators have to be formed. From the definition of the normal ordering in equation 2.43 and from the anti-commutation relations in equation 2.10 the contractions for all possible pairs of creation and or annihilation operators can be obtained as:

$$\hat{c}_i^{\dagger\bullet}\hat{c}_j^{\dagger\bullet} = \hat{c}_i^{\bullet}\hat{c}_j^{\bullet} = 0, \qquad \hat{c}_a^{\dagger\bullet}\hat{c}_b^{\dagger\bullet} = \hat{c}_a^{\bullet}\hat{c}_b^{\bullet} = 0, \qquad \hat{c}_i^{\dagger\bullet}\hat{c}_j^{\bullet} = \hat{c}_a^{\bullet}\hat{c}_b^{\dagger\bullet} = 0, \tag{2.47}$$

$$\hat{c}_i^{\dagger\bullet}\hat{c}_j^{\bullet} = -\hat{c}_j^{\bullet}\hat{c}_i^{\dagger\bullet} = \delta_{ij}, \qquad \hat{c}_a^{\dagger\bullet}\hat{c}_b^{\bullet} = -\hat{c}_b^{\bullet}\hat{c}_a^{\dagger\bullet} = \delta_{ab}. \tag{2.48}$$

Chapter 3

Algebraic Diagrammatic Construction Scheme for the Polarization Propagator

3.1 Original derivation

The algebraic diagrammatic construction (ADC) scheme for the polarization propagator is a quantum chemical method for the description of excited states [20, 30]. The ADC scheme has originally been derived using many-body Green's function theory [31]. The original derivation, which is briefly outlined, involves the spectral representation of the polarization propagator $\Pi_{pq,rs}(\omega)$ which is given as:

$$\Pi_{pq,rs}(\omega) = \sum_{n\neq 0} \left(\frac{\langle \Psi_0 | \hat{c}_p^\dagger \hat{c}_q | \Psi_n \rangle \langle \Psi_n | \hat{c}_p^\dagger \hat{c}_q | \Psi_0 \rangle}{\omega - (E_n - E_0)} - \frac{\langle \Psi_0 | \hat{c}_p^\dagger \hat{c}_q | \Psi_n \rangle \langle \Psi_n | \hat{c}_p^\dagger \hat{c}_q | \Psi_0 \rangle}{\omega + (E_n - E_0)} \right) \quad (3.1)$$

Here, $|\Psi_0\rangle$ and $|\Psi_n\rangle$ are the exact ground and n-th excited state of a molecular system with the respective energies E_0 and E_n. The polarization propagator has poles at the positive and negative excitation energies $\omega_n = E_n - E_0$ of the n-th excited state. In addition, the numerators contain the so-called transition amplitudes T_n from the ground to the n-th excited state. The transition amplitudes are defined as:

$$T_n^d = \langle \Psi_0 | \hat{d} | \Psi_n \rangle = \sum_{pq} d_{pq} \langle \Psi_0 | \hat{c}_p^\dagger \hat{c}_q | \Psi_n \rangle \quad (3.2)$$

with respect to a single-particle operator $\hat{d} = \sum_{pq} d_{pq} \hat{c}_p^\dagger \hat{c}_q$. Since both parts of $\Pi_{pq,rs}(\omega) = \Pi^+_{pq,rs}(\omega) + \Pi^-_{pq,rs}(\omega)$ contain all information on the excitation spectrum, it is sufficient to only consider one of them.

The representation of the polarization propagator in the exact eigenstates as given in equation 3.1, diagonalize the molecular Hamiltonian. Hence, it is called the diagonal form of $\Pi(\omega)$ and can be expressed in matrix notation as:

$$\Pi^+_{pq,rs}(\omega) = \sum_{n \neq 0} \frac{\langle \Psi_0 | \hat{c}_p^\dagger \hat{c}_q | \Psi_n \rangle \langle \Psi_n | \hat{c}_p^\dagger \hat{c}_q | \Psi_0 \rangle}{\omega - (E_n - E_0)} = \mathbf{x}^\dagger_{pq} \left(\mathbb{1}\omega - \mathbf{\Omega} \right)^{-1} \mathbf{x}_{rs}, \tag{3.3}$$

by introducing the vectors of transition amplitudes $\mathbf{x}_{pq} = \langle \Psi_0 | \hat{c}_p^\dagger \hat{c}_q | \Psi_n \rangle$ and the diagonal matrix $\mathbf{\Omega}$ of excitation energies ω_n. The ADC scheme postulates the existence of a non-diagonal representation of $\Pi^+(\omega)$:

$$\Pi(\omega) = \mathbf{F}^\dagger \left(\mathbb{1}\omega - \mathbf{M} \right)^{-1} \mathbf{F}, \tag{3.4}$$

with the secular matrix $\mathbf{M}$, the so-called ADC matrix, and the modified transition amplitudes $\mathbf{f}$. The index + has been dropped for brevity. $\mathbf{M}$ and $\mathbf{f}$ are expanded in a perturbation series:

$$\mathbf{M} = \mathbf{M}^{(0)} + \mathbf{M}^{(1)} + \mathbf{M}^{(2)} + \dots \tag{3.5}$$

$$\mathbf{F} = \mathbf{F}^{(0)} + \mathbf{F}^{(1)} + \mathbf{F}^{(2)} + \dots, \tag{3.6}$$

which is compared to a perturbation expansion of $\Pi(\omega)$. The diagrammatic analysis of the perturbation expansion of the polarization operator using the Møller-Plesset partitioning leads to algebraic expressions for the matrix elements of $\mathbf{M}_{IJ}$ and $\mathbf{f}_I$. Here, the indices I and J refer to excitation classes, i.e., singly, doubly and higher excitation classes. The n-th order ADC approximation (ADC(n)) contains all blocks of excitation classes required for the consistent describtion of $\Pi(\omega)$ in a given order n of perturbation theory. The highest excitation class m contained in

ADC(n) is [31]:

$$m = \frac{1}{2}n + 1, \quad (n \text{ even}) \tag{3.7}$$

$$m = \frac{1}{2}(n-1) + 1, \quad (n \text{ odd}). \tag{3.8}$$

Here, $m = 1$ refers to single excitations, which are called particle-hole (p,h) states, $m = 2$ refers to double excitations, which are two-particle-two-hole (2p,2h) states. The perturbative theoretical order required for each block in the elements of the series expansion for the ADC matrix $\mathbf{M}^{(n)}$ and modified transition amplitudes $\mathbf{F}^{(n)}$ up to third order are given in 3.1.

By solving the hermitian eigenvalue problem

$$\mathbf{MY} = \mathbf{Y\Omega}, \tag{3.9}$$

the excitation energies ω_I are obtained and using the eigenvectors $\mathbf{y_I}$ from the eigenvector matrix $\mathbf{Y}$, the transition moments can be obtained as:

$$T_I^d = \langle \Psi_0 | \hat{d} | \Psi_I \rangle = \mathbf{y}_I^\dagger \mathbf{F^d} \tag{3.10}$$

3.2 Intermediate state representation (ISR)

An alternative route to obtain the expressions for the ADC matrix and modified transition amplitudes is given by the so-called intermediate state representation (ISR) approach [20, 33]. In addition, the ISR approach offers access to excited state properties, which is later discussed in chapter 5. Here, similar to configuration interaction [24], a matrix representation of the electronic Hamiltonian is constructed. Instead of representing the Hamiltonian in the basis of Hartree-Fock determinants, the Hamiltonian is represented in the basis of intermediate states. These intermediate states can be interpreted as correlated excited determinants, which are formally constructed by the action of excitation operators $\hat{C}_I \equiv \{\hat{c}_a^\dagger \hat{c}_i; \hat{c}_a^\dagger \hat{c}_b^\dagger \hat{c}_i \hat{c}_j, a < b, i < j; \dots$ on the exact ground state $|\Psi_0\rangle$. In the following, the formal construction of the intermediate states is presented.

In the first step, the so-called precursor states $|\Psi_I^\#\rangle$ are introduced and orthog-

Table 3.1: Block structure of the n-th-order ADC matrix $\mathbf{M^{(n)}}$ and transition amplitudes $\mathbf{F^{(n)}}$ up to third order of perturbation theory [32]. The bold numbers indicate the order of perturbation theory for each block of the n-th-order ADC matrix and transition amplitudes.

$\mathbf{M^{(n)}}$	$\mathbf{p-h}$	$\mathbf{2p-2h}$
$\mathbf{p-h}$	$n=0:\ \mathbf{0}$ $n=1:\ \mathbf{1}$ $n=2:\ \mathbf{2}$ $n=3:\ \mathbf{3}$	$n=2:\ \mathbf{1}$ $n=3:\ \mathbf{2}$
$\mathbf{2p-2h}$	$n=2:\ \mathbf{1}$ $n=3:\ \mathbf{2}$	$n=2:\ \mathbf{0}$ $n=3:\ \mathbf{1}$

$\mathbf{F^{(n)}}$	
$n=0:\ \mathbf{0}$	
$n=1:\ \mathbf{1}$	
$n=2:\ \mathbf{2}$	
$n=3:\ \mathbf{3}$	
$n=2:\ \mathbf{1}$	
$n=3:\ \mathbf{2}$	

onalized with respect to the ground state:

$$|\Psi_I^{\#}\rangle = \hat{C}_I|\Psi_0\rangle - |\Psi_0\rangle\langle\Psi_0|\hat{C}_I|\Psi_0\rangle. \tag{3.11}$$

Successively, these precursor states are orthonormalized yielding the intermediate states $|\tilde{\Psi}_I\rangle$:

$$|\tilde{\Psi}_I\rangle = \sum_J |\Psi_J^{\#}\rangle(S^{-\frac{1}{2}})_{I,J}. \tag{3.12}$$

Here, the overlap matrix $\mathbf{S} = \{S_{I,J}\}$ has been introduced with the elements:

$$\begin{aligned} S_{I,J} = \langle\Psi_I^{\#}|\Psi_J^{\#}\rangle &= \left(\langle\Psi_0|\hat{C}_I^{\dagger} - \langle\Psi_0|\hat{C}_I^{\dagger}|\Psi_0\rangle\langle\Psi_0|\right)\left(\hat{C}_J|\Psi_0\rangle - |\Psi_0\rangle\langle\Psi_0|\hat{C}_J|\Psi_0\rangle\right) \\ &= \langle\Psi_0|\hat{C}_I^{\dagger}\hat{C}_J|\Psi_0\rangle - 2\langle\Psi_0|\hat{C}_I^{\dagger}|\Psi_0\rangle\langle\Psi_0|\hat{C}_J|\Psi_0\rangle \\ &\quad + \langle\Psi_0|\hat{C}_I^{\dagger}|\Psi_0\rangle\langle\Psi_0|\Psi_0\rangle\langle\Psi_0|\hat{C}_J|\Psi_0\rangle \\ &= \langle\Psi_0|\hat{C}_I^{\dagger}\hat{C}_J|\Psi_0\rangle - \langle\Psi_0|\hat{C}_I^{\dagger}|\Psi_0\rangle\langle\Psi_0|\hat{C}_J|\Psi_0\rangle \end{aligned} \tag{3.13}$$

From the intermediate states a matrix representation of the ground-state-energy-

shifted Hamiltonian $\tilde{H}$

$$\tilde{H} = \hat{H} - E_0 \tag{3.14}$$

is formed:

$$M_{IJ} = \langle \tilde{\Psi}_I | \hat{H} - E_0 | \tilde{\Psi}_J \rangle. \tag{3.15}$$

Again, solving the hermitian eigenvalue problem

$$\mathbf{Y}^t \mathbf{M} \mathbf{Y} = \mathbf{\Omega} \tag{3.16}$$

yields the excitation energies ω_I. So far, no approximations have been introduced and the equation 3.16 formally yields the exact excitation energies. However, by using the Møller-Plesset partitioning of the Hamiltonian and by expanding the exact ground state energy and exact ground state wavefunction in a perturbative theoretical series, approximative expressions for $\mathbf{M}$ can be obtained which are identical to the ADC matrix introduced earlier in section 3.1.

3.3 Construction of the ADC matrix using the ISR approach

To derive the ADC matrix expressions via the ISR approach, a series expansion of both the exact ground state energy and ground state wavefunction is inserted in 3.15. The auxiliary index λ is used to collect expressions with the same order of perturbation theory.

$$M_{I,J}^{(k+l+m)} \lambda^{k+l+m} = \sum_{K,L} \left(S_{I,K}^{-\frac{1}{2}} \right)^{(k)} \lambda^k \left(\langle \Psi_K^{\#} | \hat{H} - E_0 | \Psi_L^{\#} \rangle \right)^{(l)} \lambda^l \left(S_{L,J}^{-\frac{1}{2}} \right)^{(m)} \lambda^m \tag{3.17}$$

In the following the expressions on the right-hand-side of equation 3.17 required for the ADC(2) matrix are evaluated. For ADC(2) the indices $I, J, \ldots M$ are limited to the excitation space of single and double excitations (p-h, and 2p-2h) according to equation 3.7. Base on the block structure given in table 3.1, the p-h,p-h-block of the ADC(2) matrix is needed up to second order, the coupling blocks p-h,2p-2h and 2p-2h,p-h are required up to first order and the doubles excitation block is required in zeroth order.

First the single excitation precursor states $|\Psi_I^{\#}\rangle$ are considered, with $I \in \{\hat{c}_i^\dagger \hat{c}_a\}$:

$$|\Psi_I^{\#}\rangle^{(n)}\lambda^n = \hat{C}_I|\Psi_0^{(n)}\rangle\lambda^n - |\Psi_0^{(k)}\rangle\langle\Psi_0^{(l)}|\hat{C}_I|\Psi_0^{(m)}\rangle\lambda^{k+l+m}, \tag{3.18}$$

which in zeroth order are excited Hartree-Fock determinants:

$$|\Psi_I^{\#}\rangle^{(0)} = \hat{C}_I|\Psi_0^{(0)}\rangle - |\Psi_0^{(0)}\rangle \underbrace{\langle\Psi_0^{(0)}|\hat{C}_I|\Psi_0^{(0)}\rangle}_{=0}. \tag{3.19}$$

The first order term:

$$|\Psi_I^{\#}\rangle^{(1)} = \hat{C}_I|\Psi_0^{(1)}\rangle - \Big(|\Psi_0^{(1)}\rangle \underbrace{\langle\Psi_0^{(0)}|\hat{C}_I|\Psi_0^{(0)}\rangle}_{=0} + |\Psi_0^{(0)}\rangle \underbrace{\Big(\langle\Psi_0|\hat{C}_I|\Psi_0\rangle\Big)^{(1)}}_{=\rho_{ia}^{(1)}=0}\Big) \tag{3.20}$$

reduces to

$$|\Psi_I^{\#}\rangle^{(1)} = \hat{C}_I|\Psi_0^{(1)}\rangle, \tag{3.21}$$

and the second order term is given by:

$$|\Psi_I^{\#}\rangle^{(2)} = \hat{C}_I|\Psi_0^{(2)}\rangle - |\Psi_0^{(0)}\rangle \underbrace{\Big(\langle\Psi_0|\hat{C}_I|\Psi_0\rangle\Big)^{(2)}}_{=\rho_{ia}^{(2)}}\Big). \tag{3.22}$$

3.3.1 Overlap matrix

Using the expressions for the precursor states, the structure of the single excitation block of the overlap matrix $\{S_{I,J}\}$, with $I, J \in \{\hat{c}_i^\dagger \hat{c}_a\}$, up to second order is discussed, which is given as:

$$S_{I,J} = \sum_n S_{I,J}^{(n)}\lambda^n = \sum_{k,l} \lambda^{k+l}\langle\Psi_I^{\#}|^{(k)}|\Psi_J^{\#}\rangle^{(l)}. \tag{3.23}$$

In first order the block is diagonal:

$$S_{I,J}^{(0)} = \langle\Psi_0^{(0)}|\hat{C}_I^\dagger\hat{C}_J|\Psi_0^{(0)}\rangle = \delta_{IJ} \tag{3.24}$$

and the first order contributions vanish:

$$S^{(1)}_{I,J} = \langle \Psi^{(1)}_0 | \hat{C}^\dagger_I \hat{C}_J | \Psi^{(0)}_0 \rangle + \langle \Psi^{(0)}_0 | \hat{C}^\dagger_I \hat{C}_J | \Psi^{(1)}_0 \rangle = 0. \tag{3.25}$$

The elements of $\mathbf{S}$ in second order contain three contributions:

$$S^{(2)}_{I,J} = \langle \Psi^\#_I |^{(0)} | \Psi^\#_J \rangle^{(2)} + \langle \Psi^\#_I |^{(2)} | \Psi^\#_J \rangle^{(0)} + \langle \Psi^\#_I |^{(1)} | \Psi^\#_J \rangle^{(1)}, \tag{3.26}$$

of which for single excitations only the last term is non-zero. Thus, the elements of the second order block are

$$S^{(2)}_{I,J} = \langle \Psi^{(1)}_0 | \hat{C}^\dagger_I \hat{C}_J | \Psi^{(1)}_0 \rangle. \tag{3.27}$$

and the elements of $\mathbf{S}$ can be represented as:

$$S_{I,J} = \delta_{IJ} + S^{(2)}_{I,J} + O(3). \tag{3.28}$$

Here $O(3)$ contains third and higher order contributions. To obtain expressions for $\mathbf{S}^{-\frac{1}{2}}$ the function

$$S(x) = \mathbb{1} + x, \tag{3.29}$$

with $x = \mathbf{S}^{(2)} + O(3)$ is introduced. And $S^{-\frac{1}{2}}$ is expanded in a Taylor series:

$$\begin{aligned} S^{-\frac{1}{2}}(x) &= S^{-\frac{1}{2}}(0) + (S^{-\frac{1}{2}}(0))'(x-0) + \dots \\ &= \mathbb{1} - \frac{1}{2}x \\ &= \mathbb{1} - \frac{1}{2}\mathbf{S}^{(2)} + O(3) \end{aligned} \tag{3.30}$$

Thus, $S^{-\frac{1}{2}}_{I,J}$ is given as:

$$S^{-\frac{1}{2}}_{I,J} = \delta_{IJ} - \frac{1}{2} S^{(2)}_{I,J} + O(3) \tag{3.31}$$

3.3.2 Matrix representation in the precursor states

Now the matrix representation of the shifted Hamiltonian $\tilde{H} = \hat{H} - E_0$ in the precursor states with the Hamiltonian partitioning $\hat{H} = \hat{H}_0 + \lambda \hat{H}_1$ is discussed.

The so-called precursor matrix $\mathbf{M}^{\#}$ has the form:

$$\begin{aligned}\mathbf{M}_{IJ}^{\#\,(n)}\lambda^n =& \langle\Psi_I^{\#}|^{(k)}\lambda^k \left(\hat{H}_0 + \lambda\hat{H}_1 - E_0^{(l)}\lambda^l\right)|\Psi_J^{\#}\rangle^{(m)}\lambda^m \\ =& \left(\langle\Psi_I^{\#}|^{(k)}\hat{H}_0|\Psi_J^{\#}\rangle^{(m)}\right)\lambda^{(k+m)} + \left(\langle\Psi_I^{\#}|^{(k)}\hat{H}_1|\Psi_J^{\#}\rangle^{(m)}\right)\lambda^{(k+m+1)} \\ & - \left(S_{IJ}E_0\right)\lambda^{(n)}\end{aligned} \tag{3.32}$$

The expressions for $M_{IJ}^{\#\,(n)}$ up to second order are given as:

$$M_{IJ}^{\#\,(0)} = \langle\Psi_0^{(0)}|\hat{C}_I^\dagger\hat{H}_0\hat{C}_J|\Psi_0^{(0)}\rangle - \delta_{IJ}E_0^{(0)} \tag{3.33}$$

$$M_{IJ}^{\#\,(1)} = \langle\Psi_0^{(0)}|\hat{C}_I^\dagger\hat{H}_1\hat{C}_J|\Psi_0^{(0)}\rangle - \delta_{IJ}E_0^{(1)} \tag{3.34}$$

$$\begin{aligned}M_{IJ}^{\#\,(2)} =& \langle\Psi_0^{(1)}|\hat{C}_I^\dagger\hat{H}_1\hat{C}_J|\Psi_0^{(0)}\rangle + \langle\Psi_0^{(0)}|\hat{C}_I^\dagger\hat{H}_1\hat{C}_J|\Psi_0^{(1)}\rangle \\ & + \langle\Psi_0^{(1)}|\hat{C}_I^\dagger\hat{H}_0\hat{C}_J|\Psi_0^{(1)}\rangle - \delta_{IJ}E_0^{(2)} - S_{IJ}^{(2)}E_0^{(0)}\end{aligned} \tag{3.35}$$

3.4 Explicit expressions for ADC(2)

From the results for the overlap matrix in section 3.3.1 and the precursor matrix in 3.3.2, the terms required for the ADC(2) matrix can be obtained using equation 3.17. In addition, to extract explicit expressions, the terms of the series expansion of the ground state and the ground state energy are required. The expressions for $E_0^{(0)}$, $E_0^{(1)}$ have already been given in section 2.3.2 as well as the remaining terms $E_0^{(2)}$ and $|\Psi_0^{(1)}\rangle$. However, for the last two, the matrix elements in equations 2.40 and 2.41 have to be evaluated, which can be done using Wick's theroem.

The first order correction to the wavefunction is given as:

$$|\Psi_0^{(1)}\rangle = \sum_{\substack{i<j\\a<b}} |\Psi_{ij}^{ab}\rangle \frac{\langle\Psi_{ij}^{ab}|\hat{H}_1|\Psi_0^{(0)}\rangle}{E_0^{(0)} - E_{\Psi_{ij}^{ab}}^{(0)}} \tag{3.36}$$

The matrix element of $\hat{H}_1$, can be written as:

$$\langle\Psi_{ij}^{ab}|\hat{H}_1|\Psi_0^{(0)}\rangle = \frac{1}{4}\sum_{pqrs}\langle pq||rs\rangle\langle\Psi_0^{(0)}|\hat{c}_j^\dagger\hat{c}_i^\dagger\hat{c}_b\hat{c}_a\hat{c}_p^\dagger\hat{c}_q^\dagger\hat{c}_s\hat{c}_r|\Psi_0^{(0)}\rangle \tag{3.37}$$

Here, the single operator part of $\hat{H}_1$ has been omitted since the matrix element

yields zero. Using Wick's theorem, the expectation value $\langle\Psi_0^{(0)}|\hat{c}_j^\dagger\hat{c}_i^\dagger\hat{c}_b\hat{c}_a\hat{c}_p^\dagger\hat{c}_q^\dagger\hat{c}_s\hat{c}_r|\Psi_0^{(0)}\rangle$ can be evaluated as:

$$\langle\Psi_0^{(0)}|\hat{c}_j^\dagger\hat{c}_i^\dagger\hat{c}_b\hat{c}_a\hat{c}_p^\dagger\hat{c}_q^\dagger\hat{c}_s\hat{c}_r|\Psi_0^{(0)}\rangle = \delta_{js}\delta_{ir}\delta_{bp}\delta_{aq} - \delta_{js}\delta_{ir}\delta_{bq}\delta_{ap} - \delta_{jr}\delta_{is}\delta_{bp}\delta_{aq} + \delta_{jr}\delta_{is}\delta_{bq}\delta_{ap} \tag{3.38}$$

Thus, the matrix element in equation 3.37 can be obtained as:

$$\begin{aligned}\langle\Psi_{ij}^{ab}|\hat{H}_1|\Psi_0^{(0)}\rangle =& \frac{1}{4}\sum_{pqrs}\langle pq||rs\rangle\big(\delta_{js}\delta_{ir}\delta_{bp}\delta_{aq} - \delta_{js}\delta_{ir}\delta_{bq}\delta_{ap} \\ & - \delta_{jr}\delta_{is}\delta_{bp}\delta_{aq} + \delta_{jr}\delta_{is}\delta_{bq}\delta_{ap}\big) \\ =& \frac{1}{4}\left(\langle ab||ij\rangle - \langle ba||ij\rangle - \langle ab||ji\rangle + \langle ba||ji\rangle\right) = \langle ab||ij\rangle\end{aligned} \tag{3.39}$$

By lifting the restrictions $i < j$ and $a < b$ in equation 3.36, the first order correction to the wavefunction is finally obtained as:

$$|\Psi_0^{(1)}\rangle = -\frac{1}{4}\sum_{ijab}|\Psi_{ij}^{ab}\rangle\frac{\langle ab||ij\rangle}{\epsilon_a + \epsilon_b - \epsilon_i - \epsilon_j}, \tag{3.40}$$

which can be further simplified by introducing the so-called t-amplitudes:

$$t_{abij} = \frac{\langle ab||ij\rangle}{\epsilon_a + \epsilon_b - \epsilon_i - \epsilon_j} = t_{ijab}^\star. \tag{3.41}$$

Similar, the second order correction to the energy can be obtained as:

$$E_0^{(2)} = -\frac{1}{4}\sum_{ijab}t_{ijab}^\star\frac{1}{4}\sum_{pqrs}\langle pq||rs\rangle\langle\Psi_0^{(0)}|\hat{c}_p^\dagger\hat{c}_q^\dagger\hat{c}_s\hat{c}_r|\Psi_{ij}^{ab}\rangle = -\frac{1}{4}\sum_{ijab}t_{ijab}^\star\langle ij||ab\rangle \tag{3.42}$$

In the same way, the matrix elements occurring in the terms for the overlap and precursor matrix in sections 3.3.1 and 3.3.2 can be evaluated and the results are presented in the following sections.

3.4.1 Zeroth order and first order

Equation 3.17 yields for zeroth order:

$$M^{(0)}_{I,J} = \sum_{K,L} \left(S^{-\frac{1}{2}}_{I,K}\right)^{(0)} M^{\#\,(0)}_{IJ} \left(S^{-\frac{1}{2}}_{L,J}\right)^{(0)}, \tag{3.43}$$

which simplifies to:

$$M^{(0)}_{I,J} = \langle \Psi^{(0)}_0 | \hat{C}^\dagger_I \hat{H}_0 \hat{C}_J | \Psi^{(0)}_0 \rangle - \delta_{IJ} E^{(0)}_0 = \sum_p \epsilon_p \langle \Psi^{(0)}_0 | \hat{C}^\dagger_I \hat{c}^\dagger_p \hat{c}_p \hat{C}_J | \Psi^{(0)}_0 \rangle - \delta_{IJ} E^{(0)}_0 \tag{3.44}$$

Equation 3.44 yields for the p-h,p-h-block:

$$M^{(0)}_{ia,jb} = (\epsilon_a - \epsilon_i)\, \delta_{ab} \delta_{ij} \tag{3.45}$$

and for the 2p-2h,2p-2h-block:

$$M^{(0)}_{iajb,kcld} = (\epsilon_a + \epsilon_b - \epsilon_i - \epsilon_j)\, \delta_{ac} \delta_{bd} \delta_{ik} \delta_{jl}. \tag{3.46}$$

Similar, the first order term is given as:

$$\begin{aligned} M^{(1)}_{I,J} =& \sum_{K,L} \left(S^{-\frac{1}{2}}_{I,K}\right)^{(0)} M^{\#\,(1)}_{IJ} \left(S^{-\frac{1}{2}}_{L,J}\right)^{(0)} \\ =& \langle \Psi^{(0)}_0 | \hat{C}^\dagger_I \hat{H}_1 \hat{C}_J | \Psi^{(0)}_0 \rangle - \delta_{IJ} E^{(1)}_0, \end{aligned} \tag{3.47}$$

which yields after evaluating the matrix element of $\hat{H}_1$ for the p-h,p-h-block:

$$M^{(1)}_{ia,jb} = -\langle aj||bi\rangle + E^{(1)}_0 \delta_{ij} \delta_{ab} - \delta_{ij} \delta_{ab} E^{(1)}_0 = -\langle aj||bi\rangle. \tag{3.48}$$

Evaluating the matrix element in equation 3.47 for the coupling blocks yields:

$$M^{(1)}_{ia,kcld} = \langle kl||id\rangle \delta_{ac} - \langle kl||ic\rangle \delta_{ad} - \langle al||cd\rangle \delta_{ik} + \langle ak||cd\rangle \delta_{il} \tag{3.49}$$

$$M^{(1)}_{iajb,kc} = \langle kb||ij\rangle \delta_{ac} - \langle ka||ij\rangle \delta_{bc} - \langle ab||cj\rangle \delta_{ik} + \langle ab||ci\rangle \delta_{jk} \tag{3.50}$$

$$\tag{3.51}$$

3.4.2 Second order

First, the overlap matrix in second order is considered, which is only required for the p-h,p-h-block:

$$\begin{aligned} S^{(2)}_{ia,jb} =& \langle \Psi^{(1)}_0 | \hat{c}^\dagger_i \hat{c}_a \hat{\hat{c}}^\dagger_b \hat{c}_j | \Psi^{(1)}_0 \rangle \\ =& \frac{1}{16} \sum_{\substack{klmn \\ cdef}} t^\star_{cdkl} t_{mnef} \langle \Psi^{cd}_{kl} | \hat{c}^\dagger_i \hat{c}_a \hat{c}^\dagger_b \hat{c}_j | \Psi^{ef}_{mn} \rangle \\ =& \frac{1}{16} \sum_{\substack{klmn \\ cdef}} t^\star_{cdkl} t_{mnef} \langle \Psi^{(0)}_0 | \hat{c}^\dagger_l \hat{c}^\dagger_k \hat{c}_d \hat{c}_c \hat{c}^\dagger_i \hat{c}_a \hat{c}^\dagger_b \hat{c}_j \hat{c}_e \hat{c}_f \hat{c}^\dagger_m \hat{c}^\dagger_n | \Psi^{(0)}_0 \rangle. \end{aligned} \tag{3.52}$$

Evaluating the expectation value $\langle \Psi^{(0)}_0 | \hat{c}^\dagger_l \hat{c}^\dagger_k \hat{c}_d \hat{c}_c \hat{c}^\dagger_i \hat{c}_a \hat{c}^\dagger_b \hat{c}_j \hat{c}_e \hat{c}_f \hat{c}^\dagger_m \hat{c}^\dagger_n | \Psi^{(0)}_0 \rangle$ using Wick's theorem yields:

$$S^{(2)}_{ia,jb} = \frac{1}{4} \sum_{cdkl} |t_{cdkl}|^2 \delta_{ij} \delta_{ab} - \frac{1}{2} \sum_{kcd} t_{cdik} t^\star_{cdjk} \delta_{ab} - \frac{1}{2} \sum_{klc} t_{ackl} t^\star_{bckl} \delta_{ij} + \sum_{kc} t_{acik} t^\star_{bcjk} \tag{3.53}$$

Now, the matrix elements of $\hat{H}_1$, which contribute to the second order precursor matrix given in equation 3.35 are evaluated for the p-h,p-h-block:

$$\begin{aligned} \langle \Psi^{(1)}_0 | \hat{c}^\dagger_i \hat{c}_a \hat{H}^{(1)} \hat{c}^\dagger_b \hat{c}_j | \Psi^{(0)}_0 \rangle =& \frac{1}{4} \sum_{pqrs} \sum_{klcd} t^\star_{cdkl} \langle pq||rs \rangle \langle \Psi^{cd}_{kl} | \hat{c}^\dagger_i \hat{c}_a \hat{c}^\dagger_p \hat{c}^\dagger_q \hat{c}_s \hat{c}_r \hat{c}^\dagger_b \hat{c}_j | \Psi^{(0)}_0 \rangle \\ =& -\frac{1}{4} \delta_{ij} \delta_{ab} \sum_{cdkl} \langle cd||kl \rangle t^\star_{cdkl} + \frac{1}{2} \delta_{ij} \sum_{ckl} \langle ac||kl \rangle t^\star_{bckl} \\ &+ \frac{1}{2} \delta_{ab} \sum_{cdk} \langle cd||ik \rangle t^\star_{cdjk} - \sum_{ck} \langle ac||ik \rangle t^\star_{bcjk}, \end{aligned} \tag{3.54}$$

$$\begin{aligned} \langle \Psi^{(0)}_0 | \hat{c}^\dagger_i \hat{c}_a \hat{H}^{(1)} \hat{c}^\dagger_b \hat{c}_j | \Psi^{(1)}_0 \rangle =& \frac{1}{4} \sum_{pqrs} \sum_{klcd} \langle pq||rs \rangle t_{cdkl} \langle \Psi^{(0)}_0 | \hat{c}^\dagger_i \hat{c}_a \hat{c}^\dagger_p \hat{c}^\dagger_q \hat{c}_s \hat{c}_r \hat{c}^\dagger_b \hat{c}_j | \Psi^{cd}_{kl} \rangle \\ =& -\frac{1}{4} \delta_{ij} \delta_{ab} \sum_{cdkl} \langle kl||cd \rangle t_{cdkl} + \frac{1}{2} \delta_{ij} \sum_{ckl} \langle kl||bc \rangle t_{ackl} \\ &+ \frac{1}{2} \delta_{ab} \sum_{cdk} \langle jk||cd \rangle t_{cdki} - \sum_{ck} \langle jk||bc \rangle t_{acik}. \end{aligned} \tag{3.55}$$

The matrix element of $\hat{H}_0$, which is the third term on the right-hand side of equation 3.35 can be evaluated as:

$$\begin{aligned}\langle\Psi_0^{(1)}|\hat{c}_i^\dagger\hat{c}_a\hat{H}^{(0)}\hat{c}_b^\dagger\hat{c}_j|\Psi_0^{(1)}\rangle =&\frac{1}{16}\sum_{pqrs}\sum_{\substack{klmn\\cdef}} t^\star_{cdkl}t_{efmn}\langle\Psi^{cd}_{kl}|\hat{c}_i^\dagger\hat{c}_a\hat{c}_p^\dagger\hat{c}_p\hat{c}_b^\dagger\hat{c}_j|\Psi^{ef}_{mn}\rangle\\ =&\frac{1}{4}\delta_{ij}\delta_{ab}\sum_{cdkl} t^\star_{cdkl}t_{cdkl}(E_0^{(0)}+\epsilon_c+\epsilon_d-\epsilon_k-\epsilon_l+\epsilon_a-\epsilon_i)\\ &-\frac{1}{2}\delta_{ab}\sum_{cdk} t_{cdik}t^\star_{cdjk}(E_0^{(0)}+\epsilon_a+\epsilon_c+\epsilon_d-\epsilon_i-\epsilon_j-\epsilon_k)\\ &-\frac{1}{2}\delta_{ij}\sum_{ckl} t_{ackl}t^\star_{bckl}(E_0^{(0)}+\epsilon_c+\epsilon_a+\epsilon_b-\epsilon_k-\epsilon_l-\epsilon_i)\\ &+\sum_{ck} t_{acik}t^\star_{bcjk}(E_0^{(0)}+\epsilon_a+\epsilon_b+\epsilon_c-\epsilon_i-\epsilon_k-\epsilon_j).\end{aligned} \tag{3.56}$$

The result in equation 3.56 can be rewritten by collecting the orbital energies in the brackets in such a way that they cancel the denominators of the t-amplitudes. This yields exactly half of the matrix elements defined in 3.54 and 3.55 with opposite sign and a remainder:

$$\begin{aligned}\langle\Psi_0^{(1)}|\hat{c}_i^\dagger\hat{c}_a\hat{H}^{(0)}\hat{c}_b^\dagger\hat{c}_j|\Psi_0^{(1)}\rangle =& -\frac{1}{2}\left(\langle\Psi_0^{(1)}|\hat{c}_i^\dagger\hat{c}_a\hat{H}^{(1)}\hat{c}_b^\dagger\hat{c}_j|\Psi_0^{(0)}\rangle+\langle\Psi_0^{(0)}|\hat{c}_i^\dagger\hat{c}_a\hat{H}^{(1)}\hat{c}_b^\dagger\hat{c}_j|\Psi_0^{(1)}\rangle\right)\\ &+\frac{1}{4}\delta_{ij}\delta_{ab}\sum_{cdkl} t^\star_{cdkl}t_{cdkl}(E_0^{(0)}+\epsilon_a-\epsilon_i)-\frac{1}{4}\delta_{ab}\sum_{cdk} t_{cdik}t^\star_{cdjk}(E_0^{(0)}+2\epsilon_a-\epsilon_i-\epsilon_j)\\ &-\frac{1}{4}\delta_{ij}\sum_{ckl} t_{ackl}t^\star_{bckl}(E_0^{(0)}+\epsilon_a+\epsilon_b-2\epsilon_i)+\frac{1}{2}\sum_{ck} t_{acik}t^\star_{bcjk}(E_0^{(0)}+\epsilon_a+\epsilon_b-\epsilon_i-\epsilon_j).\end{aligned} \tag{3.57}$$

The terms containing $E_0^{(0)}$ cancel exactly the last term in equation 3.35. Thus, the terms for the second order p-h,p-h-block of the precursor matrix can be summed

up to:

$$\begin{aligned} M^{\#}_{ia,jb}{}^{(2)} &= \frac{1}{2}\left(\langle\Psi_0^{(1)}|\hat{c}_i^\dagger\hat{c}_a\hat{H}^{(1)}\hat{c}_b^\dagger\hat{c}_j|\Psi_0^{(0)}\rangle + \langle\Psi_0^{(0)}|\hat{c}_i^\dagger\hat{c}_a\hat{H}^{(1)}\hat{c}_b^\dagger\hat{c}_j|\Psi_0^{(1)}\rangle\right) \\ &+\frac{1}{4}\delta_{ij}\delta_{ab}\sum_{cdkl} t^\star_{cdkl}t_{cdkl}(\epsilon_a-\epsilon_i) - \frac{1}{4}\delta_{ab}\sum_{cdk} t_{cdik}t^\star_{cdjk}(2\epsilon_a-\epsilon_i-\epsilon_j) \\ -\frac{1}{4}\delta_{ij}\sum_{ckl} t_{ackl}t^\star_{bckl}(\epsilon_a+\epsilon_b-2\epsilon_i) &+ \frac{1}{2}\sum_{ck} t_{acik}t^\star_{bcjk}(\epsilon_a+\epsilon_b-\epsilon_i-\epsilon_j) - \delta_{ab}\delta_{ij}E_0^{(2)}, \end{aligned} \tag{3.58}$$

which can further be simplified to:

$$\begin{aligned} M^{\#}_{ia,jb}{}^{(2)} =& \frac{1}{2}\left(\langle\Psi_0^{(1)}|\hat{c}_i^\dagger\hat{c}_a\hat{H}^{(1)}\hat{c}_b^\dagger\hat{c}_j|\Psi_0^{(0)}\rangle + \langle\Psi_0^{(0)}|\hat{c}_i^\dagger\hat{c}_a\hat{H}^{(1)}\hat{c}_b^\dagger\hat{c}_j|\Psi_0^{(1)}\rangle\right) \\ &+ \frac{1}{2}S^{(2)}_{ia,jb}(\epsilon_a+-\epsilon_i) + \frac{1}{2}S^{(2)}_{ia,jb}(\epsilon_b-\epsilon_j) - \delta_{ab}\delta_{ij}E_0^{(2)}. \end{aligned} \tag{3.59}$$

According to equation 3.17 the contributions to the second order ADC matrix are:

$$\begin{aligned} M^{(2)}_{ia,jb} =& \sum_{klcd}\left(S^{-\frac{1}{2}}_{ia,kc}\right)^{(2)}\left(\langle\Psi^{\#}_{ck}|\hat{H}-E_0|\Psi^{\#}_{dl}\rangle\right)^{(0)}\left(S^{-\frac{1}{2}}_{ld,jb}\right)^{(0)} \\ &+ \sum_{klcd}\left(S^{-\frac{1}{2}}_{ia,kc}\right)^{(0)}\left(\langle\Psi^{\#}_{ck}|\hat{H}-E_0|\Psi^{\#}_{dl}\rangle\right)^{(0)}\left(S^{-\frac{1}{2}}_{ld,jb}\right)^{(2)} \\ &+ M^{\#}_{ia,jb}{}^{(2)}, \end{aligned} \tag{3.60}$$

which simplifies to:

$$\begin{aligned} M^{(2)}_{ia,jb} &= \sum_{kc}\left(S^{-\frac{1}{2}}_{ia,kc}\right)^{(2)}(\epsilon_b-\epsilon_j)\,\delta_{bc}\delta_{jk} + \sum_{kc}(\epsilon_a-\epsilon_i)\,\delta_{ac}\delta_{ik}\left(S^{-\frac{1}{2}}_{kc,jb}\right)^{(2)} + M^{\#}_{ia,jb}{}^{(2)} \\ &= -\frac{1}{2}S_{ia,jb}\,(\epsilon_b-\epsilon_j) - \frac{1}{2}S_{ia,jb}\,(\epsilon_a-\epsilon_i) + M^{\#}_{ia,jb}{}^{(2)}. \end{aligned} \tag{3.61}$$

The first two terms on the right-hand side of equation 3.61 cancel against parts of $M^{\#}_{ia,jb}{}^{(2)}$:

$$M^{(2)}_{ia,jb} = \frac{1}{2}\left(\langle\Psi_0^{(1)}|\hat{c}_i^\dagger\hat{c}_a\hat{H}^{(1)}\hat{c}_b^\dagger\hat{c}_j|\Psi_0^{(0)}\rangle + \langle\Psi_0^{(0)}|\hat{c}_i^\dagger\hat{c}_a\hat{H}^{(1)}\hat{c}_b^\dagger\hat{c}_j|\Psi_0^{(1)}\rangle\right) - \delta_{ab}\delta_{ij}E_0^{(2)} \tag{3.62}$$

Eventually, the last part in equation 3.62, $E_0^{(2)}$ cancels against the first terms on the right-hand side of equations 3.54 and 3.55 and the final result is given as:

$$\begin{aligned} M^{(2)}_{ia,jb} = = & \frac{1}{4}\delta_{ij}\sum_{ckl}\Big(t_{ackl}\langle kl||bc\rangle + t_{klbc}\langle kl||ac\rangle\Big) \\ & + \frac{1}{4}\delta_{ab}\sum_{cdk}\Big(t_{cdik}\langle jk||cd\rangle + t_{jkcd}\langle cd||ik\rangle\Big) \\ & - \frac{1}{2}\sum_{ck}\Big(t_{acik}\langle jk||bc\rangle + t_{jkbc}\langle ac||ik\rangle\Big). \end{aligned} \tag{3.63}$$

3.4.3 Summary

Finally, all contributions to the ADC(2) matrix are summarized:

$$M_{ia,jb} = M^{(0)}_{ia,jb} + M^{(1)}_{ia,jb} + M^{(2)\,A}_{ia,jb} + M^{(2)\,B}_{ia,jb} + M^{(2)\,C}_{ia,jb} \tag{3.64}$$
$$M_{ia,kcld} = M^{(1)}_{ia,kcld} \tag{3.65}$$
$$M_{iajb,kc} = M^{(1)}_{iajb,kc} \tag{3.66}$$
$$M_{iajb,kcld} = M^{(0)}_{iajb,kcld} \tag{3.67}$$

and the explicit expressions are given as:

$$M^{(0)}_{ia,jb} = (\epsilon_a - \epsilon_i)\,\delta_{ab}\delta_{ij} \tag{3.68}$$
$$M^{(1)}_{ia,jb} = -\langle aj||bi\rangle \tag{3.69}$$
$$M^{(2)\,A}_{ia,jb} = \frac{1}{4}\delta_{ij}\sum_{ckl}\left(\frac{\langle ac||kl\rangle\langle kl||bc\rangle}{\epsilon_a+\epsilon_c-\epsilon_k-\epsilon_l} + \frac{\langle ac||kl\rangle\langle kl||bc\rangle}{\epsilon_b+\epsilon_c-\epsilon_k-\epsilon_l}\right) \tag{3.70}$$
$$M^{(2)\,B}_{ia,jb} = \frac{1}{4}\delta_{ab}\sum_{cdk}\left(\frac{\langle cd||ik\rangle\langle jk||cd\rangle}{\epsilon_c+\epsilon_d-\epsilon_i-\epsilon_k} + \frac{\langle cd||ik\rangle\langle jk||cd\rangle}{\epsilon_c+\epsilon_d-\epsilon_j-\epsilon_k}\right) \tag{3.71}$$
$$M^{(2)\,C}_{ia,jb} = -\frac{1}{2}\sum_{ck}\left(\frac{\langle ac||ik\rangle\langle jk||bc\rangle}{\epsilon_a+\epsilon_c-\epsilon_i-\epsilon_k} + \frac{\langle ac||ik\rangle\langle jk||bc\rangle}{\epsilon_b+\epsilon_c-\epsilon_j-\epsilon_k}\right) \tag{3.72}$$
$$M^{(1)}_{ia,kcld} = \langle kl||id\rangle\delta_{ac} - \langle kl||ic\rangle\delta_{ad} - \langle al||cd\rangle\delta_{ik} + \langle ak||cd\rangle\delta_{il} \tag{3.73}$$
$$M^{(1)}_{iajb,kc} = \langle kb||ij\rangle\delta_{ac} - \langle ka||ij\rangle\delta_{bc} - \langle ab||cj\rangle\delta_{ik} + \langle ab||ci\rangle\delta_{jk} \tag{3.74}$$
$$M^{(0)}_{iajb,kcld} = (\epsilon_a + \epsilon_b - \epsilon_i - \epsilon_j)\,\delta_{ac}\delta_{bd}\delta_{ik}\delta_{jl}. \tag{3.75}$$

3.5 Expressions from perturbation theory

In this section, expressions from perturbation theory, which are required in the following chapters are given. All terms enter the third order ADC density matrices given in tables 4.3 and 4.5. In addition, $\rho^{(2)}$ enters the ISR excited state and state-to-state densities given in table 5.1.

$$\rho_{ij}^{(2)} = -\frac{1}{4}\left(1+\mathcal{P}_{ij}\right)\sum_{kab} t^{\star}_{ijab} t_{jkab} \tag{3.76}$$

$$\rho_{ia}^{(2)} = -\frac{1}{2\left(\epsilon_a-\epsilon_i\right)}\left(\sum_{jbc} t^{\star}_{ijab}\langle ja||bc\rangle + t_{jkab}\sum_{jkb}\langle jk|ib\right) \tag{3.77}$$

$$\rho_{ab}^{(2)} = \frac{1}{4}\left(1+\mathcal{P}_{ab}\right)\sum_{ijc} t^{\star}_{ijac} t_{ijbc} \tag{3.78}$$

$$T^{D}_{ijab} = \frac{\sum_{kc} t^{\star}_{ikac}\langle kb||jc\rangle - \frac{1}{2}\left(\sum_{cd} t^{\star}_{ijcd}\langle ab||cd\rangle + \sum_{kl} t_{klab}\langle ij||kl\rangle\right)}{\epsilon_a+\epsilon_b-\epsilon_i-\epsilon_j} \tag{3.79}$$

Chapter 4

Analytical Derivatives of the Energy of the Algebraic Diagrammatic Construction Scheme

4.1 Analytical derivatives in quantum chemistry

Analytical derivatives have become a standard tool in quantum chemistry. To illustrate the concepts and the techniques used in the derivation and implementation of analytical gradients in modern quantum chemistry methods, a brief overview of some of the major contribution to the topic is given.

4.1.1 Hellmann-Feynman theorem

The Hellmann-Feynman theorem [34, 35] is the first important realization for analytical derivatives in quantum chemistry. It holds for the energy E of the exact wavefunction $|\Psi\rangle$:

$$E = \langle \Psi | \hat{H} | \Psi \rangle \tag{4.1}$$

and it states that the derivative with respect to (w.r.t.) any perturbation ξ can be obtained as the expectation value of the perturbed Hamiltonian.

$$\frac{\partial E}{\partial \xi} = \langle \Psi | \frac{\partial \hat{H}}{\partial \xi} | \Psi \rangle \tag{4.2}$$

It can easily be extended to approximate wavefunctions depending on variationally optimized parameters $\mathbf{\Theta} = \{\theta_1, \ldots, \theta_n\}$. Since $\hat{H}$ is independent of the parameters $\mathbf{\Theta}$, the total derivative of the energy w.r.t. ξ is

$$\frac{dE(\mathbf{\Theta}, \xi)}{d\xi} = \frac{d\langle \Psi(\mathbf{\Theta}, \xi) | \hat{H} | \Psi(\mathbf{\Theta}, \xi) \rangle}{d\xi} = \langle \Psi(\mathbf{\Theta}, \xi) | \frac{\partial \hat{H}}{\partial \xi} | \Psi(\mathbf{\Theta}, \xi) \rangle + \sum_k^n \frac{\partial E(\mathbf{\Theta}, \xi)}{\partial \theta_k} \frac{d\theta_k}{d\xi}. \tag{4.3}$$

Because of the variational conditions

$$\frac{\partial E(\mathbf{\Theta}, \xi)}{\partial \theta_k} = 0, \tag{4.4}$$

the elements of the sum in (4.3) vanish. For the same reasons the theorem also holds for perturbation-independent parameters.

An example for optimized parameters are the variationally determined coefficients of a configuration interaction (CI) wavefunction expansion. However, CI-wavefunctions generally do not fully satisfy the Hellmann-Feynman theorem, since they depend implicitly on the parameters of the underlying reference state Φ_0 [36].

4.1.2 Z-vector approach

For analytical derivatives of wavefunctions depending on non-optimized parameters the so-called non-Hellmann-Feynman contributions have in principle to be evaluated for each pair of parameter and perturbation individually. Handy and Schaefer realized that dealing with the direct perturbation dependence of the non-optimized parameters can be avoided by introducing a perturbation-independent set of response equations [37]. This so-called Z-vector approach has greatly improved the efficiency of analytical derivative calculations.

4.1.3 Lagrange formalism

A generalization and rigorous derivation of the Z-vector approach can be obtained using a Lagrange formalism. The Lagrange formalism is an elegant and efficient way to avoid the evaluation of non-Hellmann-Feynman contributions and has become a standard method for the derivation of analytical gradients in quantum chemistry [22, 23, 36].

Considering an energy expression E depending on an external perturbation ξ, variationally optimized parameters $\mathbf{\Theta}$ and non-optimized parameters $\mathbf{\Delta}$, the total derivative of E w.r.t. ξ is given by

$$\frac{dE(\mathbf{\Theta}, \mathbf{\Delta}, \xi)}{d\xi} = \frac{\partial E}{\partial \xi} + \frac{\partial E}{\partial \mathbf{\Delta}} \frac{d\mathbf{\Delta}}{d\xi}. \tag{4.5}$$

Now the Lagrangian

$$\mathcal{L}(\mathbf{\Delta}, \mathbf{\Theta}, \xi, \mathbf{K}) = E + \sum_i \kappa_i f_i(\mathbf{\Delta}) \tag{4.6}$$

is introduced. Here $\{\kappa_k\} = \mathbf{K}$ are undetermined Lagrange multipliers and $\{f_k(\mathbf{\Delta}) = 0\}$ are equations defining the non-optimized parameters. From the definition of the Lagrangian follows, that $\mathcal{L}$ is stationary w.r.t. $\mathbf{K}$, since $\frac{\partial \mathcal{L}}{\partial \kappa_k} = f_k(\mathbf{\Delta}) = 0$. If the Lagrange multipliers can be determined such that they solve the system of equations

$$\left\{ \frac{\partial \mathcal{L}}{\partial \delta_k} = 0 \right\}, \tag{4.7}$$

then $\mathcal{L}$ is stationary w.r.t. all parameters and fulfilling the Hellmann-Feynman theorem. Thus, using the partial derivative of the Lagrangian the total derivative of E w.r.t. ξ can be obtained.

$$\frac{dE}{d\xi} = \frac{d\mathcal{L}}{d\xi} = \frac{\partial \mathcal{L}}{\partial \xi} \tag{4.8}$$

4.2 Analytical energy derivatives of wavefunction-based methods

In this work the Lagrange formalism is used in analogy to [23] to obtain expressions for energy derivatives of different ADC models. Some aspects of the derivation are independent of the respective method and will be discussed beforehand in this section.

4.2.1 Energy functional

Energy expressions of wavefunction-based methods can be written in terms of one- and two-electron integrals ($h_{pq} = \langle p|\hat{h}|q\rangle$ and $\langle pq||rs\rangle$) and the one- and two-particle reduced density matrices $\gamma = \{\gamma_{pq}\}$ and $\Gamma = \{\Gamma_{pqrs}\}$ (1RDM and 2RDM)

$$E = \sum_{pq} h_{pq}\gamma_{pq} + \frac{1}{4}\sum_{pqrs}\langle pq||rs\rangle\Gamma_{pqrs}. \tag{4.9}$$

4.2.2 Partial derivative

The partial derivative of the energy w.r.t. to an external perturbation ξ, the Hellmann-Feynman term, is given as

$$\frac{\partial E}{\partial \xi} = \sum_{pq} h^{\xi}_{pq}\gamma_{pq} + \frac{1}{4}\sum_{pqrs}\langle pq||rs\rangle^{\xi}\Gamma_{pqrs}. \tag{4.10}$$

The perturbed one- and two-electron integrals can be obtained by transforming the perturbed integrals from the atomic orbital basis $\{\chi_\mu\}$ (AO) to the molecular orbital basis $\{\phi_p\}$ (MO) using the orbital transformation matrix $\mathbf{C}$.

$$\frac{\partial h_{pq}}{\partial \xi} = h^{\xi}_{pq} = \sum_{\mu\nu} C_{\mu p} h^{\xi}_{\mu\nu} C_{\nu q} \tag{4.11}$$

$$\frac{\partial \langle pq||rs\rangle}{\partial \xi} = \langle pq||rs\rangle^{\xi} = \sum_{\mu\nu\sigma\tau} C_{\mu p} C_{\nu q} \langle \mu\nu||\sigma\tau\rangle^{\xi} C_{\sigma r} C_{\tau s} \tag{4.12}$$

4.2.3 Total derivative

Applying the chain rule, the total derivative of post-Hatree-Fock energy expressions, which depend on $\mathbf{C}$ and parameters $\mathbf{T} = \{t_z\}$ from a correlation treatment, w.r.t. ξ is given as

$$\frac{dE(\mathbf{C}, \mathbf{T}, \xi)}{d\xi} = \frac{\partial E}{\partial \xi} + \frac{\partial E}{\partial \mathbf{C}} \frac{d\mathbf{C}}{d\xi} + \frac{\partial \mathbf{E}}{\partial \mathbf{T}} \frac{dE}{d\xi}. \tag{4.13}$$

If the parameters $\mathbf{T}$ are obtained non-variationally, i.e. through perturbation theory, the third term on the right-hand side of equation 4.13, the partial derivative w.r.t. $\mathbf{T}$ does not vanish.

However, as first realized by Handy and Schaefer [37], the total derivative can be evaluated for all post-Hartree-Fock methods in the same way as the partial derivative and requires in addition only a set of Lagrange multipliers $\mathbf{\Omega} = \{\omega_{pq}\}$ and the derivative of the overlap matrix $\mathbf{S} = \{S_{pq}\} = \{\langle \phi_p | \phi_q \rangle\}$ which can also be obtained by transforming from the AO basis

$$\frac{\partial S_{pq}}{\partial \xi} = S^{\xi}_{pq} = \sum_{\mu\nu} C_{\mu p} S^{\xi}_{\mu\nu} C_{\nu q}. \tag{4.14}$$

By introducing effective one- and two-particle reduced density matrices γ^e and Γ^e, the total derivative can be written as

$$\frac{dE}{d\xi} = \sum_{pq} h^{\xi}_{pq} \gamma^e_{pq} + \frac{1}{4} \sum_{pqrs} \langle pq||rs \rangle^{\xi} \Gamma^e_{pqrs} + \sum_{pq} \omega_{pq} S^{\xi}_{pq}. \tag{4.15}$$

Three different parts contribute to the effective density matrices in 4.15 and their explicit form can be derived using the Lagrange formalism as shown in the next section.

4.2.4 Lagrangian of wavefunction-based methods

A Lagrangian for wavefunction-based methods can be used to avoid the computation of partial derivatives w.r.t. non-optimized wavefunction parameters. It can be constructed using the conditions for the equations of the underlying reference state and the correlation treatment as introduced in equation 4.6. If canonical Hartree-

Fock is used the Fock matrix $\mathbf{F} = \{f_{pq}\}$ is diagonal and the overlap matrix $\mathbf{S}$ is the unity matrix, which can be expressed as

$$f_{pq} - \delta_{pq}\epsilon_p = 0 \text{ and } S_{pq} - \delta_{pq} = 0. \tag{4.16}$$

It is necessary to find in a similar way equations $\{f_z\}$, that satisfy the condition

$$f_z(t_z) = 0 \tag{4.17}$$

for the parameters $\mathbf{T} = \{t_z\}$. Using 4.16 and 4.17, a general Lagrangian for methods based on canonical Hartree-Fock can be constructed as [23]

$$L(\mathbf{C}, \mathbf{T}, \mathbf{\Lambda}, \mathbf{\Omega}, \tilde{\mathbf{T}}) = E(\mathbf{C}, \mathbf{T}) + \sum_{pq} \lambda_{pq}(f_{pq} - \delta_{pq}\epsilon_p) + \sum_{pq} \omega_{pq}(S_{pq} - \delta_{pq}) + \sum_{z} \tilde{t}_z f_z(t_z). \tag{4.18}$$

Here, $\mathbf{\Lambda} = \{\lambda_{pq}\}$, $\mathbf{\Omega} = \{\omega_{pq}\}$, and $\tilde{\mathbf{T}} = \{\tilde{t}_z\}$ are sets of undetermined Lagrange multipliers. It should be noted, that the Lagrange multiplier matrices $\mathbf{\Lambda}$ and $\mathbf{\Omega}$ are symmetric. The first term of equation 4.18 is the energy $E(\mathbf{C}, \mathbf{T})$ given in 4.9 and the remaining terms are zero if the conditions 4.16 and 4.17 are satisfied.

From the definition of the Lagrangian it follows directly that L is stationary w.r.t. the Lagrange multipliers:

$$\begin{aligned} \frac{\partial L}{\partial \lambda_{pq}} &= f_{pq} - \delta_{pq}\epsilon_p = 0 \\ \frac{\partial L}{\partial \omega_{pq}} &= S_{pq} - \delta_{pq} = 0 \\ \frac{\partial L}{\partial t_z} &= f_z(t_z) = 0 \end{aligned} \tag{4.19}$$

The undetermined Lagrange multipliers can be chosen freely and are defined by imposing

$$\frac{\partial L}{\partial \mathbf{C}} \stackrel{!}{=} 0 \tag{4.20}$$

and

$$\frac{\partial L}{\partial \mathbf{T}} \stackrel{!}{=} 0, \tag{4.21}$$

meaning, that L is stationary w.r.t. all non-variational parameters. Thus, the

Lagrangian is stationary w.r.t. to *all* wavefunction parameters (and Lagrange multipliers) and the total derivative of L becomes equal to the partial derivative. Hence, from the definition of L in 4.18 follows that the total derivative of the energy E w.r.t. a perturbation ξ is given by

$$\frac{dE}{d\xi} = \frac{dL}{d\xi} \stackrel{!}{=} \frac{\partial L}{\partial \xi}, \tag{4.22}$$

if the Lagrange multipliers satisfy equations 4.20 and 4.21.

The partial derivative of L w.r.t. ξ is given by

$$\frac{\partial L}{\partial \xi} = \frac{\partial E}{\partial \xi} + \sum_{pq} \lambda_{pq} \frac{\partial f_{pq}}{\partial \xi} + \sum_{pq} \omega_{pq} \frac{\partial S_{pq}}{\partial \xi} + \sum_{i} \tilde{t}_i \frac{\partial f_i(t_i)}{\partial \xi}, \tag{4.23}$$

and can be sorted and rewritten as

$$\begin{aligned} \frac{\partial L}{\partial \xi} = & \sum_{pq} h^{\xi}_{pq} \left(\gamma_{pq}(T) + \gamma^{O}_{pq}(\Lambda) + \gamma^{A}_{pq}(\tilde{T}) \right) \\ & + \frac{1}{4} \sum_{pqrs} \langle pq||rs \rangle^{\xi} \left(\Gamma_{pqrs}(T) + \Gamma^{O}_{pqrs}(\Lambda) + \Gamma^{A}_{pqrs}(\tilde{T}) \right) \\ & + \sum_{pq} \omega_{pq} S^{\xi}_{pq}. \end{aligned} \tag{4.24}$$

By comparing with 4.24 the effective density matrices from equation 4.15 can be identified as

$$\gamma^{e} = \gamma(\mathbf{T}) + \gamma^{O}(\mathbf{\Lambda}) + \gamma^{A}(\tilde{\mathbf{T}}) \tag{4.25}$$

and

$$\Gamma^{e} = \Gamma(\mathbf{T}) + \Gamma^{O}(\mathbf{\Lambda}) + \Gamma^{A}(\tilde{\mathbf{T}}). \tag{4.26}$$

$\gamma(\mathbf{T})$ and $\Gamma(\mathbf{T})$ are the so-called unrelaxed densities which are identical to those in equation 4.10 and only depend on the parameters from the correlation treatment. The remaining terms on the right-hand side of equation 4.25 and 4.26 depend on the Lagrange multipliers. $\gamma^{O}(\mathbf{\Lambda})$ and $\Gamma^{O}(\mathbf{\Lambda})$ are the so-called orbital response contributions, and depend on the set of Lagrange multipliers, which guarantees stationarity of the Lagrangian w.r.t. changes in the parameters of the orbital basis. Their explicit form is method-independent and is presented in the next section

(4.2.5). The remaining terms, $\gamma^A(\tilde{\mathbf{T}})$ and $\Gamma^A(\tilde{\mathbf{T}})$, the so-called amplitude response contributions, depend on the Lagrange multipliers which ensure stationarity of L w.r.t. the parameters of the correlation treatment and are thus method-specific. Their explicit form is discussed for each model individually in section 4.3.

4.2.5 Orbital response

To determine the Lagrange multipliers, which ensure stationarity w.r.t. to the parameters of the reference state, the so-called orbital response procedure is performed. Here, a system of linear equation has to be solved, determined by the imposed condition given in equation 4.20. This system of linear equations can be derived starting from the definition of the Lagrangian in equation 4.18.

$$L = E + \sum_{pq} \lambda_{pq}(f_{pq} - \delta_{pq}\epsilon_p) + \sum_{pq} \omega_{pq}(S_{pq} - \delta_{pq}) + \sum_{z} \tilde{t}_z f_z(t_z). \tag{4.27}$$

It is useful to express the energy, using the relation between the Fock matrix

$$f_{pq} = h_{pq} + \sum_{i} \langle pi||qi\rangle \tag{4.28}$$

and the core Hamiltonian h_{pq}, as

$$E = \sum_{pq} f_{pq}\tilde{\gamma}_{pq} + \frac{1}{4}\sum_{pqrs} \langle pq||rs\rangle \tilde{\Gamma}_{pqsr} \tag{4.29}$$

The introduced densities $\tilde{\gamma}$ and $\tilde{\Gamma}$ are identified as

$$\tilde{\gamma_{pq}} = \gamma_{pq} \tag{4.30}$$

$$\tilde{\Gamma}_{pqrs} = \Gamma_{pqrs} - \gamma_{ps}\delta_{qr}\delta_{q\in\mathrm{occ}} + \gamma_{pr}\delta_{qs}\delta_{q\in\mathrm{occ}} + \gamma_{qs}\delta_{pr}\delta_{p\in\mathrm{occ}} - \gamma_{qr}\delta_{ps}\delta_{p\in\mathrm{occ}}. \tag{4.31}$$

Here, $\tilde{\Gamma}$ is the so-called nonseparable part of the two-particle density matrix. In the same way, the explicit form of the orbital response contributions can be identified

as

$$\gamma^O_{pq} = \lambda_{pq} \tag{4.32}$$

$$\Gamma^O_{pqrs} = -\lambda_{ps}\delta_{qr}\delta_{q\in\mathrm{occ}} + \lambda_{pr}\delta_{qs}\delta_{q\in\mathrm{occ}} + \lambda_{qs}\delta_{pr}\delta_{p\in\mathrm{occ}} - \lambda_{qr}\delta_{ps}\delta_{p\in\mathrm{occ}}. \tag{4.33}$$

The Lagrangian is sorted, collecting all contributions besides the orbital response Lagrange multipliers in

$$\gamma'(\mathbf{T}, \tilde{\mathbf{T}}) = \gamma(\mathbf{T}) + \gamma^A(\tilde{\mathbf{T}}) \text{ and } \Gamma'(\mathbf{T}, \tilde{\mathbf{T}}) = \tilde{\Gamma}(\mathbf{T}) + \Gamma^A(\tilde{\mathbf{T}}) \tag{4.34}$$

and thus, written as

$$L = \sum_{pq} f_{pq}\gamma'_{pq} + \frac{1}{4}\sum_{pqrs}\langle pq||rs\rangle\Gamma'_{pqrs} + \sum_{pq}\lambda_{pq}(f_{pq} - \delta_{pq}\epsilon_p) + \sum_{pq}\omega_{pq}S_{pq}. \tag{4.35}$$

Now the partial derivatives w.r.t. the elements of the orbital transformation matrix $\mathbf{C}$ are evaluated. The Lagrangian depends on the elements of $\mathbf{C}$ through the Fock matrix, the two-electron integrals and the overlap matrix. The system of linear equations according to equation 4.20 has the form

$$0 = \sum_{pq}\frac{\partial f_{pq}}{\partial C_{\mu p}}\left(\gamma'_{pq} + \lambda_{pq}\right) + \frac{1}{4}\sum_{pqrs}\frac{\partial\langle pq||rs\rangle}{\partial C_{\mu p}}\Gamma'_{pqrs} + \sum_{pq}\omega_{pq}\frac{\partial S_{pq}}{\partial C_{\mu p}}. \tag{4.36}$$

To obtain programmable expressions from equation 4.36,

$$\frac{\partial L}{\partial C_{\mu p}} = 0, \text{is replaced by} \sum_{\mu} C_{\mu q}\frac{\partial L}{C_{\mu p}} = 0, \tag{4.37}$$

to avoid expressions with partially-transformed integrals and the partial derivatives are performed. Evaluating the required derivatives of the Fock matrix, the two-electron integrals and the overlap matrix is straightforward [23]. Equation 4.37

yields

$$\begin{aligned}\sum_{\mu} C_{\mu u} \frac{\partial L}{\partial C_{\mu t}} = &\sum_{pq} \left(\lambda_{pq} + \gamma'_{pq}\right) \left(\delta_{pt} f_{uq} + \delta_{qt} f_{pu} + \left(\langle pu||qt\rangle + \langle pt||qu\rangle\right) \delta_{t\in\text{occ.}}\right) \\ &+ \sum_{pqr} \frac{1}{2} \left(\Gamma'_{tpqr} \langle up||qr\rangle + \Gamma'_{qrtp} \langle qr||up\rangle\right) \\ &+ \sum_{pq} \omega_{pq} \left(\delta_{pt} S_{uq} + \delta_{qt} S_{pu}\right),\end{aligned} \tag{4.38}$$

which can be simplified by assuming real two-electron integrals and using $f_{pq} = \epsilon_p \delta_{pq}$, $S_{pq} = \delta_{pq}$, as well as the symmetry of $\mathbf{\Lambda}$ and $\mathbf{\Omega}$, to

$$\sum_{\mu} C_{\mu u} \frac{\partial L}{\partial C_{\mu t}} = \sum_{pq} 2 \left(\lambda_{tu} + \gamma''_{tu}\right) \left(\epsilon_u + \langle pu||qt\rangle \delta_{t\in\text{occ.}}\right) + \sum_{pqr} \Gamma''_{tpqr} \langle up||qr\rangle + 2\omega_{ut}. \tag{4.39}$$

It should be noted that the contributions from the Hartree-Fock energy to 4.39 cancel and thus,

$$\gamma''_{ij} = \gamma'_{ij} - \delta_{ij} \text{ and } \Gamma''_{ijkl} = \Gamma'_{ijkl} + \delta_{il}\delta_{kj} - \delta_{ik}\delta_{jl}. \tag{4.40}$$

Choosing the indices t and u in equation 4.39 from different orbital spaces yields:

$$\begin{aligned}0 &= \sum_{\mu} C_{\mu i} \frac{\partial L}{\partial C_{\mu j}} \\ &= 2 \left(\lambda_{ij} + \gamma''_{ij}\right) \epsilon_i + \sum_{pq} \left(\lambda_{pq} + \gamma''_{pq}\right) \langle pi||qj\rangle + \sum_{pqr} \Gamma''_{jpqr} \langle ip||qr\rangle + 2\omega_{ij}, \qquad (4.41) \\ 0 &= \sum_{\mu} C_{\mu a} \frac{\partial L}{\partial C_{\mu i}} \\ &= 2 \left(\lambda_{ia} + \gamma''_{ia}\right) \epsilon_a + \sum_{pq} \left(\lambda_{pq} + \gamma''_{pq}\right) \langle pi||qa\rangle + \sum_{pqr} \Gamma''_{ipqr} \langle ap||qr\rangle + 2\omega_{ia}, \qquad (4.42)\end{aligned}$$

$$0 = \sum_{\mu} C_{\mu i} \frac{\partial L}{\partial C_{\mu a}} = 2\left(\lambda_{ia} + \gamma''_{ia}\right)\epsilon_i + \sum_{pqr} \Gamma''_{apqr}\langle ip||qr\rangle + 2\omega_{ij}, \tag{4.43}$$

$$0 = \sum_{\mu} C_{\mu a} \frac{\partial L}{\partial C_{\mu b}} = 2\left(\lambda_{ab} + \gamma''_{ab}\right)\epsilon_a + \sum_{pqr} \Gamma''_{bpqr}\langle ap||qr\rangle + 2\omega_{ij}. \tag{4.44}$$

Subtracting equations 4.42 from 4.43 yields the set of equation which determines the Lagrange multipliers $\mathbf{\Lambda}$:

$$\begin{aligned} 0 &= 2\left(\lambda_{ia} + \gamma''_{ia}\right)\left(\epsilon_i - \epsilon_a\right) \\ &+ \sum_{pq}\left(\lambda_{pq} + \gamma''_{pq}\right)\left(\langle pa||qi\rangle - \langle pi||qa\rangle\right) + \sum_{pqr}\left(\Gamma''_{ipqr}\langle ap||qr\rangle - \Gamma''_{apqr}\langle ip||qr\rangle\right). \end{aligned} \tag{4.45}$$

If no approximations restricting the active orbital space are employed, λ_{ij} and λ_{ab} are zero, since the energy is invariant w.r.t. orbital rotations within the space of occupied or virtual orbitals. However, for frozen core or frozen virtual approximations λ_{ij} and λ_{ab} can be obtained through the equations:

$$\begin{aligned} 0 &= \sum_{\mu} C_{\mu i}\frac{\partial L}{\partial C_{\mu j}} - \sum_{\mu} C_{\mu j}\frac{\partial L}{\partial C_{\mu i}} \\ &= 2\left(\lambda_{ij} + \gamma''_{ij}\right)\left(\epsilon_i - \epsilon_j\right) + \sum_{pqr}\left(\Gamma''_{jpqr}\langle ip||qr\rangle - \Gamma''_{ipqr}\langle jp||qr\rangle\right), \end{aligned} \tag{4.46}$$

$$\begin{aligned} 0 &= \sum_{\mu} C_{\mu a}\frac{\partial L}{\partial C_{\mu b}} - \sum_{\mu} C_{\mu b}\frac{\partial L}{\partial C_{\mu a}} \\ &= 2\left(\lambda_{ab} + \gamma''_{ab}\right)\left(\epsilon_a - \epsilon_b\right) + \sum_{pqr}\left(\Gamma''_{bpqr}\langle ap||qr\rangle - \Gamma''_{apqr}\langle bp||qr\rangle\right) \end{aligned} \tag{4.47}$$

and then enter equation 4.45.

After the occupied-virtual block of $\mathbf{\Lambda}$ has been determined iteratively, equations 4.41, 4.42, and 4.44 can be used to determine $\mathbf{\Omega}$.

4.3 Analytical energy derivatives for ADC

In this work for the first time analytical derivative expressions for the second order extended ADC model (ADC(2)-x) and third order ADC (ADC(3)) are presented. Expressions for the strict second order model ADC(2) have been published earlier

in [38]. Extending the computation of analytical energy derivatives for ADC(2) to the ADC(2)-x model requires only few additional terms in the density matrices and no additional Lagrange multipliers for the amplitude response. However, the ADC(3) energy in contrast to ADC(2) contains additional parameters from the perturbation treatment.

After the Lagrangian for an arbitrary ADC model is given, the expressions for the amplitude response for ADC(3) are presented. How the expressions for the density matrices can be derived is briefly demonstrated for the expressions of ADC(2) and successively the results for all models are summarized.

All expressions presented in this section are derived from the equations published for ADC(2) [31], ADC(2)-x [31] and ADC(3) [32] as they are implemented in the `adcman` module [20, 30, 39] embedded in the Q-Chem package of programs [40]. All occurring quantities are assumed to be real in the following sections.

4.3.1 ADC Lagrangian

The ADC excitation energy for an excited state I in terms of the excited state vectors $v_I = \left(v^I_{ia}, v^I_{ijab,\ldots}\right)^T$ is

$$\omega_I = v_I^\dagger \mathbf{M} v_I \tag{4.48}$$

and the total energy is obtained by adding the ground state energy

$$E = E_0 + \omega_I. \tag{4.49}$$

In the following the index I is omitted.

The Lagrangian for the energy of a given ADC(n) (MP(n)) model for $n \geqslant 1$ has the form

$$\begin{aligned} L^{ADC(n)} &= E_{HF} + \sum_{i>1}^{n} \left(E^{(i)} + v^\dagger \mathbf{M}^{(i)} v\right) + R_A^{ADC(n)} + R_O(\mathbf{\Lambda}, \mathbf{\Omega}) \\ &= E_{HF} + \sum_{pq} f_{pq} \gamma^{(n)}_{pq} + \frac{1}{4} \sum_{pqrs} \langle pq||rs\rangle \Gamma^{(n)}_{pqrs} + R_O(\mathbf{\Lambda}, \mathbf{\Omega}) \end{aligned} \tag{4.50}$$

with the orbital response contributions collected in

$$R_O(\mathbf{\Lambda}, \mathbf{\Omega}) = \sum_{pq} \lambda_{pq}(f_{pq} - \delta_{pq}\epsilon_p) + \sum_{pq} \omega_{pq} S_{pq}. \tag{4.51}$$

It should be noted that the ADC energy is invariant w.r.t. changes in the excitation vectors. The Lagrange multipliers and conditions $R_A^{ADC(n)}$ ensure stationarity w.r.t. parameters from the perturbation treatment that occur in the ADC(n) matrix and E_0(n), i.e. the t-amplitudes for MP(2), ADC(2) and ADC(2)-x, the T^D-amplitudes for MP(3) and additionally the second order density correction $\rho^{(2)}$ for ADC(3).

$$R_A^{ADC(0)} = R_A^{ADC(1)} = 0 \tag{4.52}$$

$$R_A^{ADC(2)} = R_A^{MP(2)} = \sum_{ijab} \bar{t}_{ijab} f(t_{ijab}) \tag{4.53}$$

$$R_A^{MP(3)} = R_A^{MP(2)} + \sum_{ijab} \bar{T}_{ijab}^D f(T_{ijab}^D) \tag{4.54}$$

$$R_A^{ADC(3)} = R_A^{MP(3)} + \sum_{pq} \bar{\rho}_{pq} f(\rho_{pq}^{(2)}) \tag{4.55}$$

To evaluate the derivative of the ADC energy, the expressions for the amplitude response have to be determined, meaning the partial derivatives of the Lagrangian w.r.t. to the non-variational parameters have to be evaluated. In addition, the expressions for the density matrices $\gamma^{(n)}$ and $\Gamma^{(n)}$ are required. The density matrices can be obtained by comparing the left- and right-hand side of

$$\sum_{i>1}^{n} \left(E^{(i)} + v^\dagger \mathbf{M}^{(i)} v\right) + R_A^{ADC(n)} = \sum_{pq} f_{pq} \gamma_{pq}^{(n)} + \frac{1}{4} \sum_{pqrs} \langle pq||rs\rangle \Gamma_{pqrs}^{(n)}. \tag{4.56}$$

4.3.2 Amplitude response for ADC(3)

Three different quantities from the perturbative expansion enter the ADC(3) matrix, i.e. the t-amplitudes, the T^D amplitudes and second order one-particle density $\rho^{(2)}$. To ensure the stationarity of the Lagrangian w.r.t. these parameters, Lagrange multipliers for the t-amplitudes ($\bar{t}$) and the T^D amplitudes ($\bar{T}^D$) have to be introduced. In this work, the MP(2) correction to the density matrix is used

and the stationarity w.r.t. the occupied-occupied and virtual-virtual blocks of $\rho^{(2)}$ is guaranteed through the Lagrange multipliers $\bar{t}$, since they contain only products of t-amplitudes. However, for the occupied-virtual part additional Lagrange multipliers are required.

The Lagrangian for ADC(3) is constructed as

$$\begin{aligned} L = E_{HF} &- \frac{1}{4}\sum_{ijab}\left(t_{ijab} + T^D_{ijab}\right)\langle ij||ab\rangle + \omega + R^O \\ &+ \sum_{ijab}\bar{t}_{ijab}\left(t_{ijab}\left(\epsilon_a + \epsilon_b - \epsilon_i - \epsilon_j\right) - \langle ij||ab\rangle\right) \\ &+ \sum_{ijab}\bar{T}^D_{ijab}\left(T^D_{ijab}\left(\epsilon_a + \epsilon_b - \epsilon_i - \epsilon_j\right) - y_{ijab}\right) \\ &+ \sum_{ia}\bar{\rho}_{ia}\left(\rho^{(2)}_{ia}\left(\epsilon_a - \epsilon_i\right) - d_{ia}\right). \end{aligned} \tag{4.57}$$

First, the Lagrange multipliers $\bar{T}^D$ are determined. Setting the partial derivative of L w.r.t. to T^D to zero yields:

$$\bar{T}^D_{ijab} = \frac{1}{4}\frac{\langle ij||ab\rangle - \frac{\partial\omega}{\partial T^D_{ijab}}}{\epsilon_a + \epsilon_a - \epsilon_i - \epsilon_j}. \tag{4.58}$$

The T^D-amplitudes enter the ADC(3) matrix in the same position as the t-amplitudes enter the ADC(2) matrix, in the p-h,p-h-block. Thus, equation 4.58 is identical to the equation determining the Lagrange multipliers $\bar{t}$ for the t-amplitudes in ADC(2). The derivative of the ADC(3) matrix w.r.t. to T^D is found as

$$\begin{aligned} \frac{\partial\omega^{ADC(3)}}{\partial T^D_{ijab}} = \frac{\partial\omega^{ADC(2)}}{\partial t_{ijab}} = &\left(1 - \mathcal{P}_{ab}\right)\sum_c\langle ij||cb\rangle\sum_k v_{ka}v_{kc} \\ &+ \left(1 - \mathcal{P}_{ij}\right)\sum_k\langle kj||ab\rangle\sum_c v_{ic}v_{kc} \\ &- \left(1 - \mathcal{P}_{ij}\right)\left(1 - \mathcal{P}_{ab}\right)v_{ia}\sum_{ck}\langle jk||bc\rangle v_{kc}. \end{aligned} \tag{4.59}$$

By omitting the second term in the numerator, the derivative of ω, equation 4.58 determines the Lagrange multipliers $\bar{T}^D$ for MP(3) (and $\bar{t}$ for MP(2) respectively),

which are the t-amplitudes scaled by the factor $\frac{1}{4}$. Thus, they do not need to be evaluated separately for the MP(2) [41] and MP(3) [42] energy derivatives respectively.

Now, the equations for the Lagrange multipliers $\bar{\rho}_{ia}$ are determined by evaluating the partial derivative of L w.r.t. the occupied-virtual part of $\rho^{(2)}$:

$$\begin{aligned}\bar{\rho}_{ia} = \frac{-\frac{\partial \omega}{\partial \rho^{(2)}_{ia}}}{\epsilon_a - \epsilon_i} = \frac{2}{\epsilon_a - \epsilon_i}\Bigg(&\sum_{jk}\langle ji||ka\rangle \sum_{c} v_{jc}v_{kc} \\ &- \sum_{jb} v_{jb} \sum_{k}\langle ji||kb\rangle v_{ka} \\ &+ \sum_{bc}\langle ib||ca\rangle \sum_{k} v_{kb}v_{kc} \\ &- \sum_{jc} v_{jc} \sum_{b}\langle jb||ca\rangle v_{ib}\Bigg)\end{aligned} \tag{4.60}$$

It should be noted that, if higher-order corrections for the one-particle density in the ADC(3) matrix are introduced, using the so-called Dyson expansion method (DEM) [43], the partial derivatives w.r.t. occupied-occupied and virtual-virtual blocks of ρ have to be evaluated as well and different conditions determining ρ have to be included in the Lagrangian.

Finally, the Lagrange multipliers $\bar{t}$ are determined. Here, it is important to notice that both, T^D and $\rho^{(2)}$, depend on the t-amplitudes. Hence, terms containing their respective Lagrange multipliers enter $\bar{t}$ and T^D and $\rho^{(2)}$ have to be determined, before $\bar{t}$ can be evaluated. The expressions for $\bar{t}$ are lengthy and comprise four different parts. First, the contribution from the ground state energy, which is simply a two-electron integral, secondly the partial derivative of ω w.r.t. the t-amplitudes, which is by far the longest part, and as third and fourth contributions, the partial derivatives of the equations determining T^D and $\rho^{(2)}_{ia}$.

The partial derivative of L w.r.t. t-amplitudes yields:

$$\bar{t}_{ijab} = \frac{\frac{\partial}{\partial t_{ijab}}\left(\sum_{klcd}\frac{1}{4}\langle kl||cd\rangle t_{klcd} - \omega + \sum_{klcd}\bar{T}^D_{klcd}y_{klcd} + \sum_{kc}\bar{\rho}_{kc}d_{kc}\right)}{\epsilon_a + \epsilon_b - \epsilon_i - \epsilon_j}. \tag{4.61}$$

The contributions to $\bar{t}$ from the partial derivative of ω are split further and equation

4.61 is written as:

$$\bar{t}_{ijab} = \frac{\langle ij||ab\rangle + \sum_{n=1}^{6} {}^{n}\tilde{t}_{ijab} + \tilde{t}^{T^D}_{ijab} + \tilde{t}^{\rho}_{ijab}}{\epsilon_a + \epsilon_b - \epsilon_i - \epsilon_j} \tag{4.62}$$

The terms occurring in equation 4.62 are presented in table 4.4 in the next section together with the expressions for the density matrices $\gamma^{(n)}$ and $\Gamma^{(n)}$ for different ADC and MP models.

4.3.3 Explicit expressions

To demonstrate how the expressions for the density matrices can be obtained, the expressions up to ADC(2) are derived, starting from the excitation energy in terms of the excited state vectors.

First, the symmetry properties of the two-electron integrals and the two-particle density matrices are noted. Assuming real quantities, both are antisymmetric w.r.t. to exchanging the first with the second, as well as the third with the fourth index. In addition, they are symmetric w.r.t. to exchanging two indices, the first and second, with the third and fourth at the same time:

$$\langle pq||rs\rangle = -\langle qp||rs\rangle = \langle qp||sr\rangle = \langle rs||pq\rangle \tag{4.63}$$

and

$$\Gamma_{pqrs} = -\Gamma_{qprs} = \Gamma_{qpsr} = \Gamma_{rspq}. \tag{4.64}$$

Using equations 4.63 and 4.64 the sum

$$\sum_{pqrs} \Gamma_{pqrs}\langle pq||rs\rangle \tag{4.65}$$

can be split into the six so-called canonical blocks, which are referred to as OOOO,

OOOV, OOVV, OVOV, OVVV and VVVV block:

$$\begin{aligned}\sum_{pqrs}\Gamma_{pqrs}\langle pq||rs\rangle = &\sum_{ijkl}\Gamma_{ijkl}\langle ij||kl\rangle + 4\sum_{ijka}\Gamma_{ijka}\langle ij||ka\rangle \\ &+ 2\sum_{ijab}\Gamma_{ijab}\langle ij||ab\rangle + 4\sum_{ijab}\Gamma_{iajb}\langle ia||jb\rangle \\ &+ 4\sum_{iabc}\Gamma_{iabc}\langle ia||bc\rangle + \sum_{abcd}\Gamma_{abcd}\langle ab||cd\rangle.\end{aligned} \tag{4.66}$$

Recognizing the factors on the right-hand side of 4.66 is important to assign the correct coefficients to the contributions of the 2RDM.

Now, the expressions of the 1RDM and 2RDM are derived. The first order $\gamma^{(1)} = \gamma^{(0)}$ and $\Gamma^{(1)}$ stem from the zeroth and first order contributions to ω:

$$\begin{aligned}\omega^{(0-1)} =&\sum_{ab} f_{ab}\sum_{i} v_{ia}v_{ib} - \sum_{ij} f_{ji}\sum_{a} v_{ia}v_{ja} + \sum_{ijab}\langle ia||bj\rangle v_{ja}v_{ib} \\ =&\sum_{pq} f_{pq}\gamma^{(0)}_{pq} + \frac{1}{4}\sum_{pqrs}\langle pq||rs\rangle\Gamma^{(1)}_{pqsr}\end{aligned} \tag{4.67}$$

and it is obvious that

$$\gamma^{(0)}_{ab} = \sum_{k} v_{ka}v_{kb}, \qquad \gamma^{(0)}_{ij} = -\sum_{c} v_{jc}v_{ic}, \qquad \Gamma^{(1)}_{iajb} = v_{ja}v_{ib}. \tag{4.68}$$

The density matrices for the correlated part of the total ADC(2) energy are defined by

$$-\frac{1}{4}\sum_{ijab} t_{ijab}\langle ij||ab\rangle + \omega^{ADC(2)} + R_A^{ADC(2)} = \sum_{pq} f_{pq}\gamma^{(2)}_{pq} + \frac{1}{4}\sum_{pqrs}\langle pq||rs\rangle\Gamma^{(2)}_{pqrs}. \tag{4.69}$$

The first term on the left-hand side comprises the ground state energy and it can readily be seen that its contribution to the OOVV part of the 2RDM is $-\frac{1}{2}t_{ijab}$. The third term, $R_A^{ADC(2)}$, contains the Lagrange multipliers $\bar{t}$:

$$R_A^{ADC(2)} = \sum_{ijab}\bar{t}_{ijab}\left(t_{ijab}\left(\sum_{c} f_{ac} + \sum_{c} f_{bc} - \sum_{k} f_{ik} - \sum_{k} f_{jk}\right) - \langle ij||ab\rangle\right) \tag{4.70}$$

Resorting the indices in equation 4.70 yields:

$$\begin{aligned} R_A^{ADC(2)} = &- \sum_{ijab} \langle ij||ab\rangle \bar{t}_{ijab} \\ &+ \sum_{ab} f_{ab} \sum_{ijc} (\bar{t}_{ijbc} t_{ijac} + \bar{t}_{ijac} t_{ijbc}) \\ &- \sum_{ij} f_{ij} \sum_{kab} (\bar{t}_{jkab} t_{ikab} + \bar{t}_{ikab} t_{jkab}) \end{aligned} \tag{4.71}$$

The second order contribution to the excitation energy comprises four distinct terms:

$$\omega^{(2)} = \omega_{11} + \omega_{12} + \omega_{21} + \omega_{22}. \tag{4.72}$$

The first one, ω_{11}, is given as

$$\begin{aligned} \omega_{11} = &\frac{1}{4} \sum_{ab} \left(\sum_{klc} t_{klac} \langle kl||bc\rangle + \sum_{klc} \langle kl||ac\rangle t_{klbc} \right) \sum_i v_{ia} v_{ib} \\ &+ \frac{1}{4} \sum_{ij} \left(\sum_{kcd} t_{ikcd} \langle jk||cd\rangle + \sum_{kcd} \langle ik||cd\rangle t_{jkcd} \right) \sum_a v_{ia} v_{ja} \\ &- \frac{1}{2} \sum_{ijab} \left(\sum_{kc} t_{ikac} \langle jk||bc\rangle + \sum_{kc} \langle ik||ac\rangle t_{jkbc} \right) v_{ia} v_{jb}. \end{aligned} \tag{4.73}$$

Again, by resorting the indices and using the derived expressions above for $\gamma^{(0)}$ one finds:

$$\begin{aligned} \omega_{11} = &\sum_{ijab} \langle ij||ab\rangle \frac{1}{4} \left(\sum_c t_{ijcb} \gamma_{ca}^{(0)} - \sum_c t_{ijca} \gamma_{cb}^{(0)} \right) \\ &- \sum_{ijab} \langle ij||ab\rangle \frac{1}{4} \left(\sum_k \gamma_{ik}^{(0)} t_{kjab} - \sum_k \gamma_{jk}^{(0)} t_{kiab} \right) \\ &- \sum_{ijab} \langle ij||ab\rangle \frac{1}{4} \Bigg(v_{ia} \sum_{kc} t_{jkbc} v_{kc} - v_{ja} \sum_{kc} t_{ikbc} v_{kc} \\ &\qquad - v_{ib} \sum_{kc} t_{jkac} v_{kc} + v_{jb} \sum_{kc} t_{ikac} v_{kc} \Bigg). \end{aligned} \tag{4.74}$$

The next two contributions to $\omega^{(2)}$

$$\omega_{12} = \sum_{ijka} \langle ij||ka\rangle \sum_{b} v_{kb} v_{ijba} + \sum_{iabc} \langle ia||bc\rangle \sum_{j} v_{ja} v_{jibc} \tag{4.75}$$

and

$$\omega_{21} = \sum_{ijka} \langle ia||jk\rangle \sum_{b} v_{jkba} v_{ib} + \sum_{iabc} \langle ab||ic\rangle \sum_{j} v_{jiab} v_{jc}, \tag{4.76}$$

can be summed up to

$$\omega_{12} + \omega_{21} = 2\sum_{ijka} \langle ij||ka\rangle \sum_{b} v_{kb} v_{ijba} + 2\sum_{iabc} \langle ia||bc\rangle \sum_{j} v_{ja} v_{jibc} \tag{4.77}$$

and the last contribution is

$$\omega_{22} = 2\sum_{ab} f_{ab} \sum_{ijc} v_{ijac} v_{ijbc} - 2\sum_{ij} f_{ji} \sum_{kab} v_{ikab} v_{jkab}. \tag{4.78}$$

As a result, we can identify the one and two-particle density matrices for ADC(2) including the zeroth and first order contributions from equation 4.68 as

$$\gamma^{(2)}_{ab} = \gamma^{(0)}_{ab} + (1 - \mathcal{P}_{ab}) \sum_{ijc} \bar{t}_{ijbc} t_{ijac} + 2\sum_{ijc} v_{ijac} v_{ijbc}, \tag{4.79}$$

$$\gamma^{(2)}_{ij} = \gamma^{(0)}_{ij} - (1 - \mathcal{P}_{ij}) \sum_{kab} \bar{t}_{jkab} t_{ikab} - 2\sum_{kab} v_{jkab} v_{ikab} \tag{4.80}$$

and

$$\begin{aligned} \Gamma^{(2)}_{ijab} = &-\frac{1}{2} t_{ijab} - 2\bar{t}_{ijab} \\ &+ \frac{1}{2} (1 - \mathcal{P}_{ab}) \sum_{c} t_{ijbc} \gamma^{(0)}_{ca} - \frac{1}{2} (1 - \mathcal{P}_{ij}) \sum_{k} \gamma^{(0)}_{jk} t_{kiab} \\ &- \frac{1}{2} (1 - \mathcal{P}_{ij}) (1 - \mathcal{P}_{ab}) v_{ia} \sum_{kc} t_{jkbc} v_{kc}, \end{aligned} \tag{4.81}$$

$$\Gamma^{(2)}_{ijka} = 2\sum_{b} v_{kb} v_{ijba}, \qquad \Gamma^{(2)}_{iabc} = 2\sum_{j} v_{ja} v_{jibc}, \tag{4.82}$$

$$\Gamma^{(2)}_{iajb} = \Gamma^{(1)}_{iajb} \tag{4.83}$$

Table 4.1: Explicit expressions for the one- and two-particle density matrices for ADC(1) as defined in equation 4.56. All quantities are assumed to have real values.

$$\gamma^{(1)}_{ij} = \gamma^{(0)}_{ij} = -\sum_c v_{jc} v_{ic}$$

$$\gamma^{(1)}_{ab} = \gamma^{(0)}_{ab} = \sum_k v_{ka} v_{kb}$$

$$\Gamma^{(1)}_{ijab} = v_{ia} v_{jb}$$

and the explicit form of $\bar{t}$ for ADC(2) is given in equation 4.59. The evaluation of the ADC(2)-x energy derivatives only requires additional terms in the OOOO, OVOV and VVVV blocks of the 2RDM.

The same procedure has been used to derive the expressions for the density matrices and Lagrange multipliers for ADC(2)-x and ADC(3). The results are collected in tables 4.1 - 4.4.

Table 4.4: Explicit expressions for the ADC(3) amplitude Lagrange multipliers. For the definition of the intermediate r^v see table 4.5. All quantities are assumed to have real values.

$$\bar{t}_{ijab} = \frac{\langle ij||ab\rangle + \sum_{n=1}^{6} {}^n\tilde{t}_{ijab} + \tilde{t}^D_{ijab} + \tilde{t}^\rho_{ijab}}{\epsilon_a + \epsilon_b - \epsilon_i - \epsilon_j}$$

$$\begin{aligned}
{}^1\tilde{t}_{ijab} = &\sum_{kl} t_{lkab} \sum_m \langle km||ij\rangle \gamma^{(0)}_{ml} \, (1 - \mathcal{P}_{ab}) \sum_k v_{ka} \sum_l \langle ij||kl\rangle \sum_{mc} t_{mlcb} v_{mc} \\
&+ (1 - \mathcal{P}_{ij}) \left(\frac{1}{2} \sum_k \gamma^{(0)}_{ki} \sum_{lm} \langle jk||lm\rangle t_{lmab} + 2 \sum_k t_{kjab} \sum_{lm} \gamma^{(0)}_{lm} \langle li||mk\rangle \right) \\
&+ (1 - \mathcal{P}_{ij}) \, (1 - \mathcal{P}_{ab}) \left(-\frac{1}{2} v_{ia} \sum_{kc} v_{kc} \sum_{lm} \langle lm||kj\rangle t_{lmcb} \right. \\
&\left. + 2 \sum_k v_{ka} \sum_{kl} \langle li||kl\rangle \sum_c t_{kjcb} v_{lc} \right)
\end{aligned}$$

Table 4.4: (continued)

$$
\begin{aligned}
{}^{2}\tilde{t}_{ijab} =& 4\Bigg(\sum_{kc} \langle ij||kc\rangle \sum_{l} v_{lc} v_{lkab} - (1-\mathcal{P}_{ij}) \sum_{k} v_{kiab} \sum_{kc} \langle jl||kc\rangle v_{lc} \\
&+ (1-\mathcal{P}_{ij})\,(1-\mathcal{P}_{ab}) \sum_{kl} \langle kj||lb\rangle \sum_{c} v_{kc} v_{ilac} \Bigg)
\end{aligned}
$$

$$
\begin{aligned}
{}^{3}\tilde{t}_{ijab} =& -(1-\mathcal{P}_{ab}) \sum_{c} \langle ij||cb\rangle \gamma^{(0)}_{ac} + (1-\mathcal{P}_{ij}) \sum_{k} \langle kj||ab\rangle \gamma^{(0)}_{ik} \\
&+ (1-\mathcal{P}_{ij})\,(1-\mathcal{P}_{ab})\, v_{ia} \sum_{kc} \langle jk||bc\rangle v_{kc}
\end{aligned}
$$

$$
\begin{aligned}
{}^{4}\tilde{t}_{ijab} =& (1-\mathcal{P}_{ij}) \Bigg(2 \sum_{k} t_{kjab} \sum_{cd} \langle ic||kd\rangle \gamma^{(0)}_{cd} - 2 \sum_{kl} t_{lkab} \sum_{c} v_{ic} \sum_{d} v_{ld} \langle jc||kd\rangle \\
&- \sum_{c} v_{ic} \sum_{k} t_{kjab} \sum_{ld} v_{ld} \langle lc||kd\rangle - \sum_{k} t_{kjab} \sum_{c} v_{kc} \sum_{ld} v_{ld} \langle lc||id\rangle \Bigg) \\
&+ (1-\mathcal{P}_{ab}) \Bigg(-2 \sum_{c} t_{ijcb} \sum_{kl} \langle ka||lc\rangle \gamma^{(0)}_{kl} - 2 \sum_{cd} t_{ijdc} \sum_{k} v_{ka} \sum_{l} v_{ld} \langle kb||lc\rangle \\
&- \sum_{k} v_{ka} \sum_{c} t_{ijcb} \sum_{ld} v_{ld} \langle kd||lc\rangle - \sum_{c} t_{ijcb} \sum_{k} v_{kc} \sum_{ld} v_{ld} \langle kd||la\rangle \Bigg) \\
&+ (1-\mathcal{P}_{ij})\,(1-\mathcal{P}_{ab}) \Bigg(\sum_{c} \gamma^{(0)}_{ac} \sum_{kc} \langle kc||jd\rangle t_{ikbd} + \sum_{kc} \langle jc||kb\rangle \sum_{d} t_{ikda} \gamma^{(0)}_{dc} \\
&\quad - \sum_{k} \gamma^{(0)}_{ik} \sum_{lc} \langle lb||kc\rangle t_{jlac} - \sum_{kc} \langle jc||kb\rangle \sum_{l} t_{liac} \gamma^{(0)}_{lk} \\
&\quad - \sum_{c} v_{ic} \sum_{k} \langle jc||kb\rangle r^{v}_{ka} - v_{jb} \sum_{kc} v_{kc} \sum_{ld} \langle lc||id\rangle t_{klad} \\
&\quad - \sum_{k} v_{ka} \sum_{c} \langle jc||kb\rangle r^{v}_{ic} - v_{jb} \sum_{kc} v_{kc} \sum_{ld} \langle la||kd\rangle t_{ilcd} \\
&\quad + 2 \sum_{kcd} v_{ka} \langle kc||id\rangle \left(\sum_{l} v_{lc} t_{ljdb} \right) + 2 \sum_{klc} v_{ic} \langle kc||la\rangle \left(\sum_{d} v_{kd} t_{ljdb} \right) \Bigg)
\end{aligned}
$$

Table 4.4: (continued)

$$
\begin{aligned}
{}^{5}\tilde{t}_{ijab} = -4\Bigg(& \sum_{kc}\langle kc||ab\rangle \sum_{d} v_{kd} v_{ijcd} - (1-\mathcal{P}_{ab}) \sum_{c} v_{ijcb} \sum_{kd} \langle kc||da\rangle v_{kd} \\
& + (1-\mathcal{P}_{ij})\,(1-\mathcal{P}_{ab}) \sum_{kl}\langle kj||lb\rangle \sum_{c} v_{kc} v_{ilac} \Bigg)
\end{aligned}
$$

$$
\begin{aligned}
{}^{6}\tilde{t}_{ijab} = & - \sum_{cd} t_{ijcd} \sum_{e} \langle de||ab\rangle \gamma^{(0)}_{cd} - (1-\mathcal{P}_{ij}) \sum_{c} v_{ic} \sum_{d} \langle cd||ab\rangle \sum_{ke} t_{kjed} v_{ke} \\
& - (1-\mathcal{P}_{ab}) \left(\frac{1}{2} \sum_{c} \gamma^{(0)}_{ac} \sum_{de} \langle bc||de\rangle t_{ijde} + 2 \sum_{c} t_{ijcb} \sum_{de} \gamma^{(0)}_{de} \langle da||ec\rangle \right) \\
& - (1-\mathcal{P}_{ij})\,(1-\mathcal{P}_{ab}) \left(\frac{1}{2} v_{ia} \sum_{kc} v_{kc} \sum_{de} \langle cb||de\rangle t_{kjde} \right. \\
& \left. - 2 \sum_{c} v_{ic} \sum_{de} \langle cd||ea\rangle \sum_{k} t_{kjdb} v_{ke} \right)
\end{aligned}
$$

$$
\begin{aligned}
\tilde{t}^{T^D}_{ijab} = (1-\mathcal{P}_{ij})\,(1-\mathcal{P}_{ab}) \Bigg(& 4 \sum_{kc} \bar{T}^{D}_{ikac} \langle jc||kb\rangle \\
& + 2 \sum_{cd} \bar{T}^{D}_{ijcd} \langle cd||ab\rangle + \sum_{kl} \bar{T}^{D}_{klab} \langle kl||ij\rangle \Bigg)
\end{aligned}
$$

$$
\tilde{t}^{\rho}_{ijab} = -(1-\mathcal{P}_{ij}) \textstyle\sum_{c} \langle jc||ab\rangle \bar{\rho}_{ic} - (1-\mathcal{P}_{ab}) \sum_{k} \langle ij||kb\rangle \bar{\rho}_{ka}
$$

$$
\begin{aligned}
\bar{T}^{D}_{ijab} = & (1-\mathcal{P}_{ab}) \sum_{c} \langle ij||cb\rangle \gamma^{(0)}_{ac} + (1-\mathcal{P}_{ij}) \sum_{k} \langle kj||ab\rangle \gamma^{(0)}_{ik} \\
& - (1-\mathcal{P}_{ij})\,(1-\mathcal{P}_{ab})\, v_{ia} \sum_{ck} \langle jk||bc\rangle v_{kc} \\
\bar{\rho}_{ia} = & \frac{-2}{\epsilon_a - \epsilon_i} \Bigg(\sum_{jk} \langle ji||ka\rangle \gamma^{(0)}_{jk} + \sum_{jb} v_{jb} \sum_{k} v_{ka} \langle ji||kb\rangle \\
& - \sum_{bc} \langle ib||ca\rangle \gamma^{(0)}_{bc} + \sum_{jb} v_{jb} \sum_{c} v_{ic} \langle jc||ba\rangle \Bigg)
\end{aligned}
$$

Table 4.2: Explicit expressions for the one- and two-particle density matrices for ADC(2) and ADC(2)-x as defined in equation 4.56. All quantities are assumed to have real values.

$$\gamma_{ij}^{(2)-x} = \gamma_{ij}^{(2)} = \gamma_{ij}^{(0)} - (1 - \mathcal{P}_{ij}) \sum_{kab} \bar{t}_{jkab} t_{ikab} - 2 \sum_{kab} v_{jkab} v_{ikab}$$

$$\gamma_{ab}^{(2)-x} = \gamma_{ab}^{(2)} = \gamma_{ab}^{(0)} + (1 - \mathcal{P}_{ab}) \sum_{ijc} \bar{t}_{ijbc} t_{ijac} + 2 \sum_{ijc} v_{ijac} v_{ijbc}$$

$$\Gamma_{iajb}^{(2)} = \Gamma_{iajb}^{(1)} = v_{ia} v_{jb}$$

$$\Gamma_{iajb}^{(2)-x} = \Gamma_{iajb}^{(2)} - 4 \sum_{kc} v_{kicb} v_{kjca}$$

$$\begin{aligned} \Gamma_{ijab}^{(2)-x} = \Gamma_{ijab}^{(2)} = -\frac{1}{2} \Bigg(& t_{ijab} - 4\bar{t}_{ijab} + (1 - \mathcal{P}_{ab}) \sum_{c} t_{ijbc} \gamma_{ca}^{(0)} \\ & - (1 - \mathcal{P}_{ij}) \sum_{k} \gamma_{jk}^{(0)} t_{kiab} - (1 - \mathcal{P}_{ij}) (1 - \mathcal{P}_{ab}) v_{ia} \sum_{kc} t_{jkbc} v_{kc} \Bigg) \end{aligned}$$

$$\Gamma_{ijkl}^{(2-x)} = 2 \sum_{ab} v_{ijab} v_{klab}$$

$$\Gamma_{abcd}^{(2-x)} = 2 \sum_{ij} v_{ijcd} v_{ijab}$$

$$\begin{aligned} \bar{t}_{ijab} = \frac{1}{\epsilon_a + \epsilon_b - \epsilon_i - \epsilon_j} \Bigg(& (1 - \mathcal{P}_{ab}) \sum_{c} \langle ij||cb\rangle \gamma_{ac}^{(0)} + (1 - \mathcal{P}_{ij}) \sum_{k} \langle kj||ab\rangle \gamma_{ik}^{(0)} \\ & - (1 - \mathcal{P}_{ij}) (1 - \mathcal{P}_{ab}) v_{ia} \sum_{ck} \langle jk||bc\rangle v_{kc} \Bigg) \end{aligned}$$

Table 4.3: Explicit expressions for the one-particle density matrix and Lagrange multipliers for ADC(3) as defined in equation 4.56. All quantities are assumed to have real values. Expressions for T^D and $\rho^{(2)}$ are given in equations 3.76-3.79.

$$
\begin{aligned}
\gamma^{(3)}_{ij} =& -\sum_{a} v_{ia} v_{ja} - \sum_{kab} v_{jkab} v_{ikab} \\
& - (1 + \mathcal{P}_{ij}) \left(\sum_{kab} \bar{t}_{jkab} t_{ikab} + \sum_{kab} \bar{T}^D_{jkab} T^D_{ikab} + \sum_{a} \bar{\rho}_{ia} \rho_{ja} \right) \\
\gamma^{(3)}_{ab} =& \sum_{i} v_{ia} v_{ib} + 2 \sum_{ijc} v_{ijac} v_{ijbc} \\
& + (1 + \mathcal{P}_{ab}) \left(\sum_{ijc} \bar{t}_{ijac} t_{ijbc} + \sum_{ijc} \bar{T}^D_{ijac} T^D_{ijbc} + \frac{1}{2} \sum_{i} \bar{\rho}_{ia} \rho^{(2)}_{ib} \right)
\end{aligned}
$$

Table 4.5: Explicit expressions the two-particle density matrix. For the definitions of the intermediates see table 4.3. All quantities are assumed to have real values. Expressions for T^D and $\rho^{(2)}$ are given in equations 3.76-3.79.

$$
\begin{aligned}
\Gamma^{(3)}_{ijkl} =& 2 \sum_{ab} v_{ijab} v_{klab} + \frac{1}{2} \left(1 + \mathcal{P}^{kl}_{ij}\right) \left(2 \sum_{ab} \bar{t}^D_{ijab} t_{klab} \right. \\
& - \frac{1}{2} \left(1 - \mathcal{P}_{ij}\right) \sum_{m} \gamma^{(0)}_{jm} \sum_{ab} t_{miab} t_{klab} \\
& + \left(1 - \mathcal{P}_{kl}\right) \sum_{c} v_{kc} \sum_{b} t_{ijcb} \sum_{ma} t_{mlab} v_{ma} \\
& \left. + \left(1 - \mathcal{P}_{ij}\right) \left(1 - \mathcal{P}_{kl}\right) \left(\rho^{(2)}_{jl} \gamma^{(0)}_{ik} - \sum_{b} \left(\sum_{a} t^2_{ljab} v_{ia} \right) v_{kb} \right) \right) \\
\Gamma^{(3)}_{ijka} =& 2 \sum_{b} v_{kb} v_{ijba} - \sum_{l} v_{la} \sum_{bc} t_{ljba} v_{lkbc} \\
& + \left(1 - \mathcal{P}_{ij}\right) \left(- 2 \sum_{c} v_{ic} \sum_{lb} t_{ljba} v_{lkbc} + v_{ja} \sum_{lbc} t_{libc} v_{klbc} \right. \\
& \left. + \rho^{(2)}_{ja} \gamma^{(0)}_{ik} + v_{ia} \sum_{b} \rho^{(2)}_{jb} v_{kb} + \frac{1}{2} \sum_{b} t_{ijba} \bar{\rho}_{kb} \right)
\end{aligned}
$$

Table 4.5: (continued)

$$
\begin{aligned}
\Gamma^{(3)}_{ijab} = \frac{1}{2}\Bigg(& - t_{ijab} - t^{D}_{ijab} - 4\bar{t}_{ijab} \\
& + (1 - \mathcal{P}_{ab}) \sum_{c} \left(t^{D}_{ijcb} + t_{ijcb} \right) \gamma^{(0)}_{ca} \\
& - (1 - \mathcal{P}_{ij}) \sum_{k} \left(t^{D}_{kjab} + t_{kjab} \right) \gamma^{(0)}_{ki} \\
& - (1 - \mathcal{P}_{ab}) (1 - \mathcal{P}_{ij}) \, v_{ia} \sum_{kc} t^{D}_{kjcb} \left(v_{kc} + r^{v}_{jb} \right) \Bigg)
\end{aligned}
$$

$$
\begin{aligned}
\Gamma^{(3)}_{iajb} = & - v_{ja} v_{ib} - 4 \sum_{kc} v_{kicb} v_{kjca} + \rho^{(2)}_{ij} \gamma^{(0)}_{ab} + \rho^{(2)}_{ab} \gamma^{(0)}_{ij} \\
& + \frac{1}{2} \left(1 + \mathcal{P}^{jb}_{ia} \right) \Bigg(- 4 \sum_{kc} t_{kidb} \bar{t^{D}}_{kjca} \\
& + 4 \sum_{c} \sum_{kd} \left(t_{kjcd} t_{kidb} \right) \sum_{l} v_{lc} v_{la} - \sum_{k} \sum_{lc} \left(t_{klca} t_{licb} \right) \sum_{d} v_{kd} v_{jd} \\
& + \sum_{l} v_{la} \sum_{d} t_{lidb} r^{v}_{jd} + \sum_{d} v_{jd} \sum_{l} t_{lidb} r^{v}_{la} \\
& + v_{ja} \sum_{c} \rho^{(2)}_{cb} v_{ic} - v_{ib} \sum_{k} \rho^{(2)}_{kj} v_{ka} - 2 \sum_{k} v_{ka} \sum_{c} t^{2}_{jkcb} v_{ic} \\
& + \frac{1}{2} \sum_{c} v_{jc} \sum_{d} v_{id} \sum_{kl} \left(t_{klda} t_{klcb} \right) + \frac{1}{2} \sum_{l} \sum_{k} \left(\sum_{cd} t_{kicd} t_{ljcd} v_{ka} \right) v_{lb} \Bigg)
\end{aligned}
$$

$$
\begin{aligned}
\Gamma^{(3)}_{iabc} = & 2 \sum_{j} v_{ja} v_{jibc} + \sum_{d} v_{id} \sum_{jk} t_{jkbc} v_{jkad} \\
& + (1 - \mathcal{P}_{bc}) \Bigg(- 2 \sum_{j} v_{jb} \sum_{kd} t_{kidc} v_{jkad} + v_{ib} \sum_{jkd} t_{jkcd} v_{jkad} \\
& - \rho^{(2)}_{ic} \gamma^{(0)}_{ab} + v_{ib} \sum_{j} \rho^{(2)}_{jc} v_{ja} + \frac{1}{2} \sum_{b} t_{jibc} \bar{\rho}_{ja} \Bigg)
\end{aligned}
$$

Table 4.5: (continued)

$$
\begin{aligned}
\Gamma^{(3)}_{abcd} =& 2 \sum_{ij} v_{ijcd} v_{ijab} + \frac{1}{2} \left(1 + \mathcal{P}^{cd}_{ab}\right) \left(2 \sum_{ij} \bar{t}^{D}_{ijab} t_{ijcd} \right. \\
&+ \frac{1}{2} \left(1 - \mathcal{P}_{ab}\right) \sum_{e} \gamma^{(0)}_{eb} \sum_{jk} t_{jkea} t_{jkcd} \\
&+ \left(1 - \mathcal{P}_{ab}\right) \sum_{k} v_{ka} \sum_{j} t_{kjcd} \sum_{ie} t_{ijeb} v_{ie} \\
&\left. + \left(1 - \mathcal{P}_{ab}\right) \left(1 - \mathcal{P}_{cd}\right) \left(\rho^{(2)}_{bd} \gamma^{(0)}_{ac} - \sum_{j} \left(\sum_{i} t^{2}_{ijdb} v_{ia} \right) v_{jc} \right) \right)
\end{aligned}
$$

$$
v_{ia} = \sum_{jb} v^{n}_{jb} t_{ijab} \quad t^{2}_{ijab} = \sum_{kc} t_{ikac} t_{jkbc}
$$

Chapter 5

Obtaining Optical Properties Using the Intermediate State Representation

5.1 Intermediate state representation of general operators

Molecular properties and state-to-state transition properties with respect to an operator $\hat{D}$ can be obtained as expectation values of a state or between two states

$$D_n = \langle \Psi_n | \hat{D} | \Psi_n \rangle, \qquad T_{nm} = \langle \Psi_n | \hat{D} | \Psi_m \rangle. \tag{5.1}$$

In the same way as the ISR is used to expand the ground-state-energy-shifted Hamiltonian, a representation of an arbitrary one-particle operator

$$\hat{D} = \sum_{pq} d_{pq} \hat{c}_p^\dagger \hat{c}_q, \tag{5.2}$$

shifted by the ground-state property $D_0 = \langle \Psi_0 | \hat{D} | \Psi_0 \rangle$ can be constructed as [33]:

$$\mathbf{D}_{IJ} = \langle \tilde{\Psi}_I | \hat{D} - D_0 | \tilde{\Psi}_J \rangle \tag{5.3}$$

and $\mathbf{D}$ can be expanded in a perturbation series:

$$\mathbf{D} = \mathbf{D}^{(0)} + \mathbf{D}^{(1)} + \mathbf{D}^{(2)} + \dots \tag{5.4}$$

The matrix $\mathbf{D}$ for a given order of perturbation theory has the same structure as the respective ADC matrix of the same order. Explicit expressions for the elements of $\mathbf{D}$ can be determined using the same procedure as demonstrated for the ADC matrix and have been published in [33]. Using the ISR of $\hat{D}$ and the eigenvectors $\{v_n = \left(v^n_{ia}, v^n_{ijab,\dots}\right)^t\}$ from the ADC eigenvalue problem, the moments in equation 5.1 can be evaluated as:

$$D_n = v_n^\dagger \mathbf{D} v_n + D_0, \qquad T_{nm} = v_n^\dagger \mathbf{D} v_m, \quad \text{with: } n \neq m. \tag{5.5}$$

Instead of constructing $\mathbf{D}$ for different operators, the elements from equation 5.3 can be used to derive the expressions for the excited-state and the state-to-state transition densities. By comparing equations 5.5 with equations 5.1 one finds:

$$D_n = \langle \Psi_n | \sum_{pq} d_{pq} \hat{c}_p^\dagger \hat{c}_q \hat{D} | \Psi_n \rangle = \sum_{pq} d_{pq} \underbrace{\langle \Psi_n | \hat{c}_p^\dagger \hat{c}_q | \Psi_n \rangle}_{=\rho^n_{pq}} = v_n^\dagger \mathbf{D} v_n + D_0 \tag{5.6}$$

and

$$T_{nm} = \langle \Psi_n | \sum_{pq} d_{pq} \hat{c}_p^\dagger \hat{c}_q \hat{D} | \Psi_m \rangle = \sum_{pq} d_{pq} \underbrace{\langle \Psi_n | \hat{c}_p^\dagger \hat{c}_q | \Psi_m \rangle}_{=\rho^{nm}_{pq}} = v_n^\dagger \mathbf{D} v_m. \tag{5.7}$$

Thus, the expressions for the excited state contribution to the density ρ^n and the transition density ρ^{nm} can be obtained by collecting and sorting all terms in equations 5.5, which contain the same matrix elements d_{pq}, i.e. d_{ij}, d_{ia}, d_{ai} and d_{ab}. Finally, the expectation values are obtained as:

$$D_n = \sum_{pq} \left(\rho^n_{pq} + \rho^0_{pq}\right) d_{pq}, \qquad T_{nm} = \sum_{pq} \rho^{nm}_{pq} d_{pq}, \quad \text{with: } n \neq m. \tag{5.8}$$

Here, ρ^n does not contain the contributions from the ground state density ρ^0.

In addition, the excited-state and transition densities can be used for the analysis of excited states [44]. Explicit expressions for ρ^n and ρ^{nm} are given in table 5.1.

5.2 Excited state absorption

For the theoretical description of excited-state absorption spectra in addition to the excitation energies, the state-to-state transition dipole moments between the excited states are required. These can be evaluated as expectation values of the dipole operator, which is given along a coordinate α as:

$$\hat{\mu}^{\alpha} = \sum_{pq} \mu_{pq}^{\alpha} \hat{c}_p^{\dagger} \hat{c}_q \tag{5.9}$$

According to equation 5.8 the transition dipole moments can be obtained as:

$$\mu_{nm}^{\alpha} = \sum_{pq} \rho_{pq}^{nm} \mu_{pq}^{\alpha}. \tag{5.10}$$

From the transition dipole moment, the oscillator strength f_{nm} can be computed, which corresponds to the absorption probability between state n and m in the experiment, with the state-to-state excitation energy ω_{nm} :

$$f_{nm} = \frac{2}{3}\omega_{nm} \sqrt{\sum_{\alpha=x,y,z} {\mu_{nm}^{\alpha}}^2} \tag{5.11}$$

5.3 Non-linear optical properties

Expressions from time-dependent response theory for the first and higher order frequency-dependent polarizabilities contain functions of the following form:

$$f^{\alpha\beta}(\omega) = \langle \Psi_n | \hat{\mu}^{\alpha} \left[\hat{H} - \omega \right]^{-1} \hat{\mu}^{\beta} | \Psi_m \rangle, \quad \alpha, \beta \in \{x, y, z\}. \tag{5.12}$$

The ISR approach offers two ways to evaluate such expressions. The first one uses the excitation energies, the static and the state-to-state transition dipole moments accessible through the ISR of the dipole operator to directly evaluate $f^{\alpha\beta}(\omega)$ in the limit of the number of calculated eigenvectors of the ADC matrix [14]. The second one leads to a closed-form expression for $f^{\alpha\beta}(\omega)$ [45], which can be solved iteratively and numerical exact. In this work, both approaches are used to obtain two-photon absorption cross-sections in section 5.4. In addition,

the same techniques can also be used to compute the polarizability and higher order hyperpolarizabilties. A closed-form expression of the complex polarizability is presented in section 5.5.

5.4 Two-photon absorption

The expression for the two-photon absorption (TPA) matrix $\mathbf{S} = \{S_{\alpha\beta}\}$, with $\alpha, \beta \in \{x, y, z\}$, stems from time-dependent response theory. For resonant TPA, meaning the simultaneous absorption of two photons with the same energy, the elements of $\mathbf{S}$ for the final excited state f with the excitation energy ω_f have the form [46]:

$$S_{\alpha\beta} = \langle\Psi_0|\hat{\mu}^{\alpha}\left[\hat{H} - \frac{\omega_f}{2}\right]^{-1}\hat{\mu}^{\beta}|\Psi_f\rangle + \langle\Psi_0|\hat{\mu}_{\beta}\left[\hat{H} - \frac{\omega_f}{2}\right]^{-1}\hat{\mu}_{\alpha}|\Psi_f\rangle. \tag{5.13}$$

From the two-photon absorption matrix, TPA cross-sections δ_{TP} for linear-polarized light can be calculated according to [46]:

$$\delta_{TP} = \frac{1}{30}\sum_{\mu\nu} 2S_{\mu\mu}S^{\star}_{\mu\nu} + 2S_{\mu\nu}S^{\star}_{\mu\nu} + 2S_{\mu\nu}S^{\star}_{\nu\mu}. \tag{5.14}$$

In this section the two alternative routes to evaluate the expressions for $\mathbf{S}$ based on the ISR approach are presented, which have been outlined in section 5.3.

5.4.1 Sum-over-states

Inserting the resolution of the identity (RI) of exact states $\sum_{n}^{\infty}|\Psi_n\rangle\langle\Psi_n|$ in equation 5.13 yields a sum-over-states (SOS) [14] expression for $\mathbf{S}$ [47]:

$$S_{\alpha\beta} = \sum_{n}^{\infty}\frac{\langle\Psi_0|\hat{\mu}^{\alpha}|\Psi_n\rangle\langle\Psi_n|\hat{\mu}^{\beta}|\Psi_f\rangle}{\omega_n - \frac{\omega}{2}} + \alpha \leftrightarrow \beta, \tag{5.15}$$

with $\omega_0 = E_0$. Equation 5.15 simplifies to

$$S_{\alpha\beta} = \sum_{n}^{\infty}\frac{\mu^{\alpha}_{0n}\mu^{\beta}_{nf}}{\omega_n - \frac{\omega}{2}} + \alpha \leftrightarrow \beta \tag{5.16}$$

and can directly be evaluated after the computation of the eigenvalues of the ADC-matrix and the successive computation of the static dipole and state-to-state transition dipole moments via the ISR approach as described in section 5.1, and the ground-to-excited state transition dipole moments via the modified transition amplitudes.

5.4.2 Closed-form expression

Inserting the RI of the intermediate states $\sum_{I}^{\infty} |\tilde{\Psi}_I\rangle\langle\tilde{\Psi}_I|$ in two positions in equation 5.13 leads to the following expression:

$$S_{\alpha\beta} = \sum_{I,J}^{N} \langle\Psi_0|\hat{\mu}^{\alpha}|\tilde{\Psi}_I\rangle\langle\tilde{\Psi}_I| \left[\hat{H} - \frac{\omega_f}{2}\right]^{-1} |\tilde{\Psi}_J\rangle\langle\tilde{\Psi}_J|\mu_{\beta}|\Psi_f\rangle + \alpha \leftrightarrow \beta. \tag{5.17}$$

This can be rewritten in matrix form yielding:

$$S_{\alpha\beta} = \mathbf{F}_{\alpha}^{\dagger} \left(\mathbf{M} - \mathbb{1}\omega\right)^{-1} \mathbf{B}_{\beta}\mathbf{Y}_{\mathbf{f}} + \frac{\mu_{00}^{\alpha}\mu_{0f}^{\beta}}{E_0 - \frac{\omega}{2}} + \alpha \leftrightarrow \beta. \tag{5.18}$$

Here, $\mathbf{B}_{\beta}$ is the IS representation of the dipole operator in direction β, $\mathbf{F}_{\alpha}^{\dagger}$ is the matrix of modified transition amplitudes along coordinate α, and $\mathbf{Y}_f$ is the eigenvector of the final state the f. It should be noted that the RI of intermediate states contains the ground state as zeroth order excitation class, but the contribution from the ground state is not included in this matrix representation and has to be added separately.

To solve the term involving the inverse shifted ADC matrix in 5.18, the vector $\mathbf{x}_{\alpha}^{\dagger}$ is introduced:

$$\mathbf{x}_{\alpha}^{\dagger} = \mathbf{F}_{\alpha}^{\dagger} \left(\mathbf{M} - \mathbb{1}\frac{\omega}{2}\right)^{-1}. \tag{5.19}$$

which is the solution of the system of linear equations:

$$\mathbf{x}_{\alpha}^{\dagger} \left(\mathbf{M} - \mathbb{1}\frac{\omega}{2}\right) = \mathbf{F}_{\alpha}^{\dagger}. \tag{5.20}$$

Equation 5.20 has to be solved iteratively for each component $\alpha \in \{x, y, z\}$. The resulting vectors can be used to compute pseudo-densities according to equation

5.7

$$\rho^{\alpha f} = \mathbf{x}_{\alpha}^{\dagger}\mathbf{D}\mathbf{Y}_{f}, \tag{5.21}$$

which then can be contracted with the matrix elements of the dipole operator along β and the elements of $\mathbf{S}$ are obtained as:

$$S_{\alpha\beta} = \sum_{pq} \rho^{\alpha f}\mu_{pq}^{\beta} + \frac{\mu_{00}^{\alpha}\mu_{0f}^{\beta}}{E_0 - \frac{\omega}{2}} + \alpha \leftrightarrow \beta. \tag{5.22}$$

5.5 Complex frequency-dependent polarization

The use of conventional algorithms like the Davidson method [48] for the solution of the eigenvalue problem of ADC faces limitations for the theoretical description of absorption experiments if the involved states are in the high-energy region of the spectrum or if the spectral features stem from a large number of excited states. These algorithms usually compute the energetically-lowest excited states and thus, if higher-lying states are of interest, require the computation of a potentially large number of eigenstates, which play no role in the absorption phenomena. In addition, to compare with experimental spectra, the stick spectra obtained from solving eigenvalue equations and the computation of oscillator strengths are convoluted with a Gaussian or Lorentzian to simulate experimental line broadening. If the spectral region has a high density of states, meaning that a large number of states contribute to the spectral features, other approaches are more efficient.

An alternative route to simulate absorption spectra is the so-called complex polarization propagator approach (CPP) [49]. It is based on introducing a complex dampening factor in the frequency-dependent electric dipole polarizability $\alpha(\omega) = \{\alpha^{\mathbf{ij}}(\omega)\}$, with $i, j \in \{x, y, z\}$. Here, the complex polarization is computed incrementally for the spectral range of interest and the absorption probability can directly be obtained from the complex part of $\alpha(\omega)$. For the efficient computation of $\alpha(\omega)$, specially designed numerical algorithms have been presented and implemented for different quantum chemical methods like HF/DFT [49] and CC [50]. This algorithm enables the computation of $\alpha(\omega)$ simultaneously for several hundred frequencies with comparable computational costs of a single-frequency calculation.

To adapt the CPP approach to ADC, a closed-form ISR expression of $\alpha(\omega)$ is presented together with a proof-of-principle implementation using numerical standard techniques. This implementation evaluates $\alpha(\omega)$ for each frequency individually.

The elements of the complex frequency-dependend polarizability with the imaginary dampening factor γ have the form:

$$\alpha^{ij}(\omega) = \langle\Psi_0|\hat{\mu}^j \left[\hat{H} - 1\left(\omega + \mathrm{i}\gamma\right)\right]^{-1} \hat{\mu}^i|\Psi_0\rangle + \langle\Psi_0|\hat{\mu}^j \left[\hat{H} + 1\left(\omega + \mathrm{i}\gamma\right)\right]^{-1} \hat{\mu}^i|\Psi_0\rangle. \tag{5.23}$$

In analogy to equation 5.18, through insertion of the RI of the intermediate states $\sum_I^\infty |\tilde{\Psi}_I\rangle\langle\tilde{\Psi}_I|$ equation 5.23 becomes:

$$\alpha^{ij}(\omega) = \mathbf{F}_i^\dagger \left(\mathbf{M} - \mathbb{1}\left(\omega + \mathrm{i}\gamma\right)\right)^{-1} \mathbf{F}_j + \mathbf{F}_j^\dagger \left(\mathbf{M} + \mathbb{1}\left(\omega + \mathrm{i}\gamma\right)\right)^{-1} \mathbf{F}_i \tag{5.24}$$

and the contributions from the ground state cancel out. Like the expression for the TPA matrix $\mathbf{S}$, the expressions in equation 5.24 can be evaluated by solving the systems of linear equations:

$$\left(\mathbf{M} - \mathbb{1}\left(\omega + \mathrm{i}\gamma\right)\right) \mathbf{x}_j^- = \mathbf{F}_j, \tag{5.25}$$

$$\left(\mathbf{M} + \mathbb{1}\left(\omega + \mathrm{i}\gamma\right)\right) \mathbf{x}_i^+ = \mathbf{F}_i. \tag{5.26}$$

These systems of linear equations can be separated into a real and imaginary part as shown for the first one, with the solution vector $\mathbf{x}_j^- = \mathbf{x} + \mathrm{i}\mathbf{y}$:

$$\begin{aligned} \left(\mathbf{M} - \omega\right) \mathbf{x} - \gamma\mathbf{y} &= \mathbf{F}_j \\ \mathrm{i}\left(\mathbf{M} - \omega\right) \mathbf{y} + \mathrm{i}\gamma\mathbf{x} &= \mathbf{0}, \end{aligned} \tag{5.27}$$

since the matrices $\mathbf{F}_i$ and $\mathbf{F}_j$ are real, the imaginary part is trivial and the solution for $\mathbf{x}$ can be inserted in the real part of equation 5.27. This leads to:

$$\frac{1}{\gamma}\left(\mathbf{M} - \omega\right)^2 \mathbf{y} - \gamma\mathbf{y} = \mathbf{F}_j, \tag{5.28}$$

which can be rewritten as

$$\left(\mathbf{M}'^2 - \gamma\right)\mathbf{y} = \gamma\mathbf{F}_j, \tag{5.29}$$

with $\mathbf{M}' = \mathbf{M} - \omega$. Equation 5.29 can be solved in the same way as the equtions for the TPA matrix using iterative methods.

Table 5.1: Explicit expressions for the ISR transition density in second order. The expressions contain the second order correction to the ground state density $\rho^{(2)}$ and the t-amplitudes. The presented expressions have been obtained by rewriting the original equations from [33] as outlined in section 5.1. Expressions for $\rho^{(2)}$ are given in equations 3.76-3.78.

$$\begin{aligned}
\rho_{ij}^{nm} &= \gamma_{ij}^1 + 2\gamma_{ij}^2 + \frac{1}{2}\sum_k \gamma_{ik}^1 \left(\rho_{kj}^{(2)} + \sum_l \rho_{il}^{(2)}\gamma_{lj}^1\right) \\
&\quad - \sum_{kcd} t_{jkcd}\frac{1}{2}\sum_l \gamma_{kl}^1 \left(t_{ilcd} - \sum_b t_{ikbd}\gamma_{bc}^1\right) \\
&\quad - \frac{1}{2}\left(\sum_a v_{ja}^m \sum_{kc} t_{ikac} r_{kc}^{v^n} + \sum_a v_{ia}^n \sum_{kc} t_{jkac} r_{kc}^{v^m}\right) - \sum_a r_{ja}^{v^n} r_{ia}^{v^m} \\
\rho_{ab}^{nm} &= \gamma_{ab}^1 + 2\gamma_{ab}^2 - \frac{1}{2}\sum_c \gamma_{ac}^1 \left(\rho_{cb}^{(2)} + \sum_d \rho_{ad}^{(2)}\gamma_{db}^1\right) \\
&\quad - \sum_{klc} t_{klac}\frac{1}{2}\sum_d \gamma_{dv}^1 \left(t_{klbd} - \sum_j t_{jlbc}\gamma_{kj}^1\right) \\
&\quad + \frac{1}{2}\left(\sum_i v_{ia}^m \sum_{kc} t_{ikbc} r_{kc}^{v^n} + \sum_i v_{ib}^n \sum_{kc} t_{ikac} r_{kc}^{v^m}\right) - \sum_a r_{ia}^{v^n} r_{ib}^{v^m}
\end{aligned}$$

$$\begin{aligned}
\rho_{ia}^{nm} &= \gamma_{ia}^{nm} + \sum_b \rho_{ib}^{(2)}\gamma_{ba}^1 + \sum_j \rho_{ja}^{(2)}\gamma_{ij}^1 + \sum_{jb} t_{ijab}\gamma_{bj}^{mn} \\
&\quad - \sum_b v_{ib}^n \sum_{klc} t_{klca} v_{klcb}^m - \sum_j v_{ja}^n \sum_{kcd} t_{ikcd} v_{jkcd}^m \\
\rho_{ai}^{nm} &= \gamma_{ai}^{mn} + \sum_b \rho_{ib}^{(2)}\gamma_{ab}^1 + \sum_j \rho_{ja}^{(2)}\gamma_{ji}^1 + \sum_{jb} t_{ijab}\gamma_{jb}^{nm} \\
&\quad - \sum_b v_{ib}^m \sum_{klc} t_{klca} v_{klcb}^n - \sum_j v_{ja}^m \sum_{kcd} t_{ikcd} v_{jkcd}^n
\end{aligned}$$

Table 5.1: (continued)

$$\gamma^1_{ij} = -\sum_a v^n_{ja} v^m_{ia} \quad \gamma^1_{ab} = \sum_i v^n_{ia} v^m_{ib} \quad \gamma^2_{ij} = -\sum_{kab} v^n_{jkab} v^m_{ikab} \quad \gamma^2_{ab} = \sum_{ijc} v^n_{ijac} v^m_{ijbc}$$

$$\gamma^{nm}_{ia} = -2\sum_{bj} v^n_{jb} v^m_{ijab} \quad \gamma^{mn}_{ia} = -2\sum_{bj} v^m_{jb} v^n_{ijab}$$

$$r^{v^n}_{ia} = \sum_{jb} v^n_{jb} t_{ijab} \quad r^{v^m}_{ia} = \sum_{jb} t_{ijab} v^m_{jb}$$

Chapter 6

Implementation

The expressions for the analytical energy derivatives and the optical properties have been implemented in the `adcman` module [30], which is a `C++` project containing different variants of ADC and is embedded in the quantum chemical program package Q-Chem [40]. However, due to the modular structure of `adcman` and the related libraries, it can be integrated into other quantum chemical programs as well.

Of central importance is the open-source tensor library `libtensor` [51], which handles all algebraic operations using optimized linear algebra routines at its core. It splits large tensors into smaller blocks, which are stored on different levels of memory, i.e., core memory and disk-space, enabling parallel algorithms. In addition, `libtensor` provides a convenient interface facilitating straightforward implementations of tensor expressions and treats symmetries which are encountered in quantum chemical calculations, i.e., permutation and spin symmetry as well as point-group symmetry.

6.1 Analytical energy derivatives

The evaluation of the analytical energy derivatives is for all implemented ADC models performed in the same way. First, the eigenvalue problem of the respective ADC matrix is solved using the Davidson algorithm [48]. In the next step, the Lagrange multipliers are computed. In the case of ADC(3) the Lagrange multipliers for the MP(2) density and the T^D amplitudes have to be evaluated first, because

they are required for the computation of the t-amplitude Lagrange multipliers $\bar{t}$. Successively, the amplitude-relaxed one- and two-particle density matrices are computed, which are used as input for the orbital response. The orbital response Lagrange multipliers $\{\lambda_{ia}\}$ are found as the solution of a linear system of equations, which is solved using the DIIS algorithm [52]. From the result, the fully relaxed density matrices are computed together with the Lagrange multipliers $\{\omega_{pq}\}$. In the last step, the fully relaxed density matrices and the Lagrange multipliers $\{\omega_{pq}\}$ are transformed in the AO basis and contracted with the perturbed integrals in Q-Chem, to obtain the energy derivative.

6.2 Optical properties

For the calculation of excited-state properties, the excited-state densities are computed using the eigenvectors of the ADC matrix according to the expressions presented in table 5.1. To compute the excited-state absorption oscillator strengths, the densities are contracted with the matrix elements of the dipole operator in the MO basis to obtain excited-state and state-to-state transition dipole moments. If the eigenvectors from the ADC(3) matrix are combined with the second order ISR densities, the resulting model is called ADC(3/2)

6.2.1 Two-photon absorption

The sum-over-states expressions for the TPA matrix are directly evaluated using the excited-state and state-to-state dipole moments. For the closed-form expression, first the vector of modified transition moments for a certain coordinate α of the dipole operator is computed, which is the inhomogeneity of equation 5.20 and the system of linear equations is solved with the DIIS algorithm. The resulting vector and the eigenvector of the final state are used to compute a pseudo-density using the equations from table 5.1. Finally, this pseudo-density is contracted with the MO representation of the dipole operator along another coordinate β to obtain the TPA matrix element $\mathbf{S}_{\alpha\beta}$.

6.3 List of implemented features

- geometry optimizations using ADC(1), ADC(2), ADC(2)-x and ADC(3)
- excited state absorption using ADC(1), ADC(2), ADC(2)-x and ADC(3/2)
- two-photon absorption matrices for ADC(2) and ADC(2)-x

Part II

Applications

Chapter 7

Benchmark and Test Calculations

7.1 Nuclear derivatives

Using the implementation described in section 6.1 of the expressions presented in chapter 4, nuclear derivatives and excited state equilibrium structures have been computed. To test the implementation, analytical energy derivatives are compared to numerical derivatives. In addition, the performance of the first-time implemented energy derivatives for ADC(2)-x and ADC(3) is evaluated using reference values of other quantum chemical methods for a series of small molecules.

7.1.1 Numerical derivatives

Numerical derivatives have been computed using single point calculations for all implemented ADC models, i.e., ADC(2), ADC(2)-x and ADC(3). Analytical derivatives with respect to the interatomic bond lengths in the diatomic molecule BH and the x-coordinate of a C and H atom in *trans*-butadiene have been computed for comparison with numerical derivatives. Usually numerical differentiation is performed using two single point calculations, however to ascertain the correct implementation of the analytical derivative which in the case of ADC(3) depends on a large number of small contributions, higher order approximations of numerical derivatives have been used for comparison.

Finite differences

Derivatives can be approximated numerically. The simplest approach is to calculate the difference quotient:

$$f'(x) \approx \frac{f(x) - f(x+h)}{h}, \tag{7.1}$$

which requires the evaluation of f at two points: x and $x + h$. However, a more accurate approximation of $f'(x)$ using two single points can be obtained from the so-called central difference:

$$f'(x) \approx \frac{f(x+h) - f(x-h)}{2h}. \tag{7.2}$$

The expression for the central difference can be found through the Taylor series around $(x + h)$ and $(x - h)$:

$$f(x+h) = f(x) + hf'(x) + 2hf''(x)\ldots \tag{7.3}$$
$$f(x-h) = f(x) - hf'(x) + 2hf''(x)\ldots, \tag{7.4}$$

of which the difference yields:

$$f(x+h) - f(x-h) = 2hf'(x) - h^3 f'''(x)\ldots \tag{7.5}$$

Thus, it follows:

$$\Rightarrow f'(x) = \frac{f(x+h) - f(x-h)}{2h} + \mathcal{O}(h^2) \tag{7.6}$$

and $\mathcal{O}(h^2)$ contains the higher order terms of the Taylor series, which are at least proportional to h^2. In the same way, higher-order numerical approximations for the derivative can be obtained by comparing the Taylor series around $x + nh$ and $x - nh$, with $n = 1, 2, \ldots$.

Difference between numerical and analytical gradients

For the BH molecule the derivatives have been computed at the interatomic distance of 1.208 Å. The numerical derivative have been obtained from single point

Table 7.1: Analytical derivative and absolute difference between analytical and numerical nuclear derivatives of the S_1 of the BH molecule with respect to the interatomic distance in atomic units. The numerical derivatives have been calculated using 2, 4, 6 and 8 single point calculations with an increment of ±0.001 Å starting at the interatomic distance of 1.208 Å, at which the analytical derivative has been computed. The calculations have been performed using the 6-31G basis set.

Number of single points	ADC(2)	ADC(2)-x	ADC(3)
analytical derivative	0.009482	0.016433	0.018564
2	4.25E-07	4.25E-07	4.71E-07
4	1.09E-08	7.74E-08	7.74E-08
6	9.99E-09	8.01E-08	4.48E-08
8	8.86E-09	8.20E-08	4.61E-08

calculations with a step size of 0.001 Å. For butadiene the x-coordinates of a C and H atom have been altered with the same step size as for BH, starting from a MP(2) optimized equilibrium ground state structure using the cc-pVDZ basis set. The difference between the numerical derivatives using two, four, six and eight single point calculations and the analytical gradient are presented in tables 7.1 and 7.2.

The numerical derivatives computed using the difference of two single point calculations deviate in all cases from the analytical derivatives by a value of around 5.00E-07 a.u., which becomes smaller for the approximations based on more points. For both molecules, the difference between the numerical derivative based on 8 single points and the analytical result is around 1.00E-07 a.u. which is one order of magnitude smaller than the convergence criteria of the numerical algorithm used for the excitation energies. Thus, it is assumed that the analytical gradient implementation is correct.

7.1.2 Benchmark on small diatomic molecules

For the comparison of the ADC(2)-x and the ADC(3) energy derivatives with other methods, a set of singlet and triplet excited state equilibrium distances of four diatomic molecules: N_2, CO, BF and BH, displayed in table 7.3 is used. It has been presented in the first publication of ADC(2) gradients [38], together with

Table 7.2: Analytical derivative and absolute difference between analytical and numerical nuclear derivatives of the $2A_g^-$ state with respect to the x-coordinate of a C and H atom in butadiene in atomic units. The numerical derivatives have been calculated using 2 and 8 single point calculations with an increment of ±0.001 Å starting at the ground state MP(2)/cc-pVDZ equilibrium geometry, at which the analytical derivative has been computed. The calculations have been performed using the 6-31G* basis set.

coordinate	ADC(2)	ADC(2)-x	ADC(3)
	analytical derivative		
C-x	0.113281	0.193974	0.188352
H-x	0.005200	0.005774	0.006386
	2 point		
C-x	5.56E-07	5.20E-07	5.56E-07
H-x	5.28E-07	5.13E-07	5.74E-07
	8 point		
C-x	1.52E-07	1.32E-07	5.20E-08
H-x	1.08E-07	1.16E-07	9.96E-08

Table 7.3: The equilibrium distances of singlet and triplet excited states of the four diatomic molecules: N_2, CO, BF and BH. The results for ADC(2), ADC(2)-x and ADC(3) have been obtained using the analytical derivative implementation presented in this work and the aug-cc-pwCVQZ basis set. The results for CC, CCSD, CCSDR(3) and CC3 have been taken from [38] and experimental results are from [53].

		ADC(2)	ADC(2)-x	ADC(3)	CCSD	CCSDR(3)	CC3	Exp.
N_2	$A^3\Sigma_u^+$	1.291	1.272	1.291	1.268		1.293	1.287
	$a'^1\Sigma_u^-$	1.290	1.288	1.272	1.248	1.269	1.280	1.275
	$a^1\Pi_g$	1.246	1.236	1.208	1.201	1.215	1.222	1.220
	$w^1\Delta_u$	1.281	1.281	1.267	1.242	1.263	1.274	1.268
CO	$a^3\Pi$	1.214	1.215	1.194	1.194		1.211	1.206
	$A^1\Pi$	1.278	1.250	1.210	1.222	1.233	1.245	1.235
BF	$a^3\Pi$	1.316	1.314	1.301	1.306		1.311	1.308
	$A^1\Pi$	1.312	1.312	1.294	1.301	1.305	1.307	1.304
BH	$A^1\Pi$	1.206	1.218	1.218	1.219	1.221	1.222	1.219

ADC(2) and CC(2) equilibrium distances. All values in the test set have been obtained using the aug-cc-pwCVQZ basis set [54–56], for which the results are expected to be close to the basis set limit, and the results for all ADC models have been obtained using the very same basis. All ADC(2) results are found to be identical to the first implementation in [38] except for smaller deviations < 0.001 Å, which is the accuracy, in which the restults in [38] have been presented.

In addition to computed excited state equilibrium structures, experimental values are given, which have been published in [53]. Of the excited singlet and striplet states of the four molecules, the first excited singlet state of each molecule has been chosen in addition to the first triplet states of N_2, CO and BF and the second and third excited singlet state of N_2.

For this choice of eight excited states the two third order CC methods CC3 and CCSDR(3) show the best agreement with the experimental bond lengths. Both, ADC(3) and CCSD, yield in average too short bond lengths for the excited states and perform comparable for this test set. ADC(2) and ADC(2)-x overestimate the excited state bond lengths and ADC(2) shows the largest errors. For the singlet excited states of N_2, ADC(3) yields results with an accuracy comparable to CC3, while CCSD underestimates these excited-state bond lengths by about 0.2 Å. All ADC models show the largest error for the first excited state of BF: ADC(2) largely overestimates the excited bond lengths by 0.43 Å and ADC(3) underestimates it by 0.25 Å, which is the largest absolute error for ADC(3) in the test set.

In all cases, ADC(2)-x improves over the strict second order results, which can be attributed to the higher order treatment of double excitations in ADC(2)-x. However, going to ADC(3) on average yields no improvement, in contrary the maximum and mean absolute error is larger than the one of ADC(2)-x. The underestimation of the ADC(3) bond lengths can be attributed to the underlying MP(3) ground state. MP(3) is known to yield too short ground state equilibrium distances for diatomic molecules [57], which leads to biased total energy potential energy surfaces.

7.1.3 Small organic molecules

To further evaluate the performance of the implemented ADC models, test calculations on small organic molecules have been performed. For comparison with

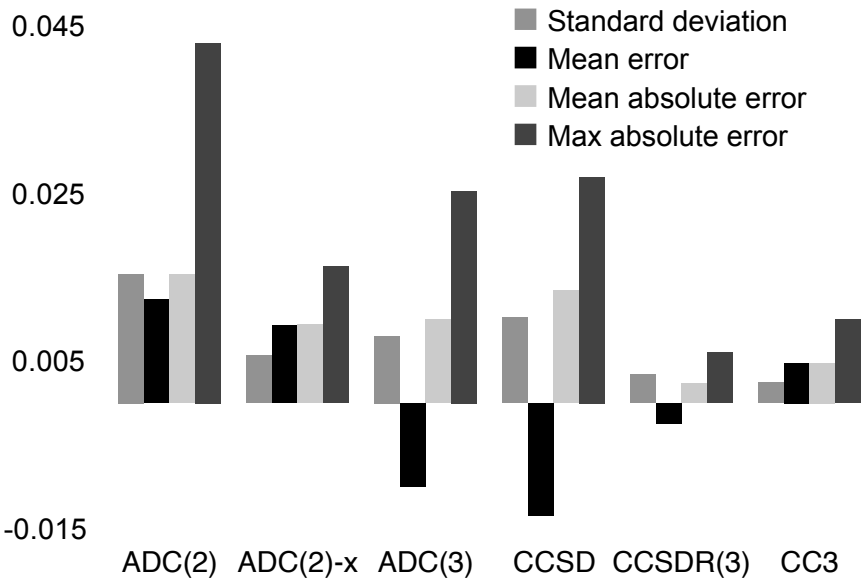

Figure 7.1: Errors in calculated bond lengths for 8 excited states of diatomic molcules compared to experimental data taken from [53]. For technical details see text.

Table 7.4: Excited state equilibrium geometries for the first two excited states of *trans*-butadiene. The ADC(2)-x and ADC(3) results have been obtained using the 6-31G* basis set and CASPT2 results are taken from [58].

	CASPT2	ADC(2)-x	ADC(3)
	$1^1B_u^+$ $\pi \rightarrow \pi*$		
C=C	1.421	1.425	1.424
C—C	1.399	1.400	1.397
	$2^1A_g^-$ $\pi \rightarrow \pi*$		
C=C	1.418	1.563	1.543
C—C	1.498	1.381	1.399

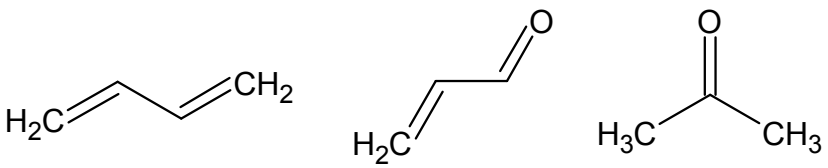

Figure 7.2: The structures of *trans*-butadiene, acrolein and acetone.

CASPT2 results from [58], the equilibrium structures of the first excited state of three molecules, i.e., acetone, acrolein and *trans*-butadiene (butadiene), have been computed using the ADC(2)-x and ADC(3) models using the 6-31G* basis set. In addition, the second excited state $2^1A_g^-$ of butadiene has been optimized. The excited state bond lengths are presented in table 7.4 and 7.5.

For the $1^1B_u^+$ state of butadiene, the results of ADC(2)-x and ADC(3) are very close to the CASPT2 results. In the $2^1A_g^-$ state equilibrium structure ADC(2)-x and ADC(3) drastically overestimate the bond length inversion in the excited state and the double bonds are stretched over the lengths of a single carbon-carbon bond. The overestimation of the double bonds by the ADC models can be explained by the failure in the underlying MP(2) and MP(3) ground state respectively. Due to the inversion of the bond lengths alternation pattern, the excited state structure is too far off the equilibrium ground state structure and the shape of the potential energy surface of the ground state in this region is incorrectly described by both MP(2) and MP(3). Hence, the total energies and total energy derivatives become unphysical.

For acetone and acrolein ADC(2)-x and ADC(3)-x yield different results. Compared to the CASPT2 structure, ADC(2)-x overestimates the carbon-oxygen bond. Again, this behavior stems from the ground state description of the method. The overestimation of the correlation effects and thus, bond lengths, in MP(2) results in too long bond distances. In addition, ADC(2)-x overestimates the bond lengths inversion of the carbon-carbon bonds. In contrast to ADC(2)-x, ADC(3) underestimates the carbon-oxygen bond length, but describes the changes in the carbon-carbon bonds qualitatively correct. Both bond lengths become similar in the excited state even though, the carbon-carbon single bond is slightly larger than the double bond, which is the opposite in CASPT2.

7.2 Excited-state absorption

The state-to-state transition dipole moments for the H_2O molecule have been computed with the aug-cc-pVDZ basis set, using ADC(2), ADC(2)-x and ADC(3/2). The results are compared to CC2 and CCSD results from [59]. The ADC(2) and CC2 results are practically identical and have the largest value for the three states

Table 7.5: Excited state equilibrium geometries for the first excited states of acrolein and acetone. The ADC(2)-x and ADC(3) results have been obtained using the 6-31G* basis set and CASPT2 results are taken from [58].

	CASPT2	ADC(2)-x	ADC(3)
Acrolein $n \rightarrow \pi*$			
C=O	1.345	1.392	1.300
C—C	1.384	1.359	1.399
C=C	1.393	1.418	1.385
Acetone $n \rightarrow \pi*$			
C=O	1.368	1.450	1.310
C—C	1.489	1.486	1.506

Table 7.6: Excited state absorption from the 1^1B_2 state of H_2O computed using ADC(2), ADC(2)-x and ADC(3) with the aug-cc-pVDZ basis set on the MP2/cc-pVTZ equilibrium ground state structure. CC2 and CCSD results are taken from [59].

State	Direction	CC2	CCSD	ADC(2)	ADC(2)x	ADC(3/2)
1^1A_2	X	7.103	6.652	7.162	6.819	6.349
2^1A_1	Y	4.825	4.534	4.887	4.717	4.370
3^1B_2	Z	3.483	3.147	3.445	3.256	3.038

of H_2O. CCSD lies between the ADC(2)-x and ADC(3) results, which have the smallest values. Overall the results are very similar, however, all states show the same trend of declining values in the order: ADC(2) = CC2 > ADC(2)-x > CCSD > ADC(3), which resembles the increasing order of perturbative theoretical treatment of the respective methods. ADC(2) and CC2 are based on a second order ground state and treat single excitation up to second order, and double excitations in zeroth order. Both ADC(2)-x and CCSD additionally treat the double excitations in first order and CCSD additionally incorporates a third order ground state. The highest order perturbative theoretical treatment is contained in ADC(3), which in contrast to CCSD includes a third order treatment of the single excitations.

Table 7.7: Two-photon absorption cross-sections δ_{TP} in atomic units for the lowest excited states of H_2O using ADC(2), ADC(2)-x with the aug-cc-pVDZ basis set on the MP2/6-31G* equilibrium ground state structure. A* indicates data from a different implementation [47].

	1^1B_1	1^1A_2	2^1A_1	2^1B_1	3^1A_1
ADC(2)*	6.94	60.27	13.76	50.91	498.27
ADC(2)-x*	6.81	65.90	13.81	62.84	586.12
ADC(2)	7.29	61.60	13.80	49.83	504.20
ADC(2)-x	7.13	67.26	13.09	62.18	593.76

7.3 Two-photon absorption cross-sections

In addition, two-photon absorption cross sections for H_2O with ADC(2) and ADC(2)-x are presented. The performance of the ADC models for the theoretical description of TPA cross-sections has already been extensively discussed in a previous publication [47]. However, in the previous work a different numerical procedure, the band-Lanczos algorithm, has been used to solve the involved expressions. The results are presented in table 7.7 and compared to the previous data. The small deviations stem from a different description of the ground state density, which is in the implementation of the previous work based on the so-called Dyson-expansion method (DEM). Overall the results proof the correct implementation of the DIIS algorithm in this work.

Chapter 8

Calculations on Model Systems

To show the applicability of the first-time implemented ADC(2)-x and ADC(3) analytical gradients and the two-photon absorption code, two medium-sized organic chromophores have been examined. Of the two chosen molecules, the first one, all-*trans*-octatetraene, is a model system for linear polyenes and poses problems for the description with ADC(3), since its first excited state involves large changes in the bond lengths compared to the equilibrium ground state structure. This is comparable to the case of *trans*-butadiene, which has been discussed in the previous chapter. The second one, bithiophene, is an important system in technical and medical applications.

8.1 All-*trans*-octatetraene

Linear all-*trans*-polyenes like all-*trans*-octatetraene (octatetraene) serve as model systems for polyene chromophores which play important roles in many biological photo-processes and in technical applications. For example, carotenoids possess various important roles in photobiology as light harvesting pigments, as photoprotective agents by quenching singlet and triplet states, and as scavengers of

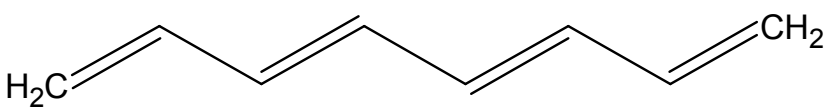

Figure 8.1: Structure of all-*trans*-octatetraene.

singlet oxygen [60, 61]. The study of the lowest excited states of linear polyenes has a long history in theory and experiment [62–75], since for a fundamental understanding of the photo-physical functions of polyene chromophores, precise knowledge of their excited states is crucial. Typically, the low-lying excited states of carotenoids are characterized by the irreducible representations of the molecular C_{2h} point group symmetry of the all-*trans* polyene models, i.e., A_g, B_g, A_u, B_u. In addition, the states are usually assigned an additional index, – or + [76], which specifies the anti-symmetric or symmetric linear combination of degenerate configurations. According to these rules, the electronic ground state of linear polyenes is referred to as $1^1\mathrm{A}_g^-$. The correct ordering of the lowest excited states of linear polyenes has been and is still a subject of much debate. However, it is generally agreed that for octatetraene and longer polymers the lowest excited state singlet state S_1 is the optically forbidden $2^1\mathrm{A}_g^-$ and the second excited singlet state S_2 is classified as $1^1\mathrm{B}_u^+$. The reasons for the ongoing debate lie in the difficulties both experimentalists and theoreticians face by the investigation of the excited states of linear polyenes. From a theoretical point of view, difficulties in the description of linear polyenes arise from the highly correlated nature of the ground state wave function, which are further manifested in a large double-excitation character of the excited state wave function of $2^1\mathrm{A}_g^-$ (S_1), while the $1^1\mathrm{B}_u^+$ (S_2) state corresponds to a clearly singly excited state. Therefore, to arrive at a balanced description of both states, high-level methods are required.

8.1.1 Ground state structure and vertical excitation energies

It has been shown, that the calculation of vertical excitation energies with ADC(2)-x and ADC(3) yields the correct ordering for the lowest excited states of linear polyenes [39, 77]. However, these results have been biased by the choice of the ground state geometry, which is known to have significant influence on the vertical excitation energies. In this work, vertical excitation energies have been computed using a CCSD(T)/cc-pVTZ ground state equilibrium structure to yield best-estimates for the vertical excitation energies using ADC(3) and the cc-pVTZ basis set for octatetraene. These results are compared in table 8.1 to the estimates for vertical excitation energies presented by Christensen et al. [78] and are in per-

Table 8.1: Vertical ADC(3)/cc-pVTZ excitation energies in eV for the $2^1A_g^-$ and $1^1B_u^+$ state at the CCSD(T)/cc-pVTZ ground state equilibrium structure. Experimental 'vertical excitation' energies have been taken from [78].

	ADC(3)	exp.
$2^1A_g^-$	3.94	4.0 ± 0.1
$1^1B_u^+$	4.65	4.6 ± 0.1

fect agreement with the experimental estimates, which have been obtained through elaborate experiments and reasonable assumption for the influence of experimental effects.

8.1.2 Excited state structure

The next step is, to go beyond the approximation of vertical absorption energies for the $2^1A_g^-$ state and to compute fluorescence energies, which can be compared to fluorescence experiments from free jet expansions. This can be done by using the newly implemented derivative program to optimize the $2^1A_g^-$ structure. The S_1 state has been optimized using ADC(3) and the so-called spin-flip variant of ADC(3) (SF-ADC(3)) and the cc-pVTZ basis set. The resulting excited state geometries and vertical fluorescence energies are presented in table 8.2 together with CASSCF results from [79] and experimental (0 - 0) transition energies from [80]. While the vertical absorption energies were in agreement with the experiments, the computed fluorescence energies, 2.59 eV for SF-ADC(3) and 0.81 for ADC(3) are compared to the experimental value of 3.59 eV by far too low. Comparing the results for the SF-ADC(3) excited-state carbon-carbon bond lengths with the CASSCF data, which is assumed to yield qualitatively correct results, it is obvious that the double bonds, especially the internal, in the SF-ADC(3) structure are too short. In the case of ADC(3) the description of the excited state geometry is even worse and the internal double bond is by far too long and is stretched almost to the lengths of a single carbon-carbon bond. The poor description of the ADC(3) excited state structure can be explained by the failure in the underlying MP(3) ground state energy. The excited state possesses an inversed bond-lengths-alternation pattern, and the changes in the structure compared to the equilibrium

Table 8.2: Bond lengths in Å for the carbon backbone in S_1 optimized geometries of all-*trans*-octatetraene and vertical $S_1 \rightarrow S_0$ excitation energies in eV. Experimental values have been taken from [80] and the CASSCF structure has been taken from [79]. The optimized structures for SF-ADC(3) and ADC(3) have been computed using the cc-pVTZ basis set.

	SF-ADC(3)	ADC(3)	CASSCF	Exp.
$2^1A_g^-$	2.59	0.81		3.59
C_1=C_2	1.423	1.438	1.438	
C_2—C_3	1.360	1.352	1.376	
C_3=C_4	1.415	1.483	1.437	
C_4—C_4'	1.393	1.340	1.392	

Table 8.3: Bond lengths in Å for the carbon backbone of different ground state geometries of octaetraene computed using the cc-pVTZ basis set.

	HF	CCSD(T)	SF-ADC(3)
C_1=C_2	1.3206	1.3409	1.3164
C_2—C_3	1.4596	1.4468	1.4426
C_3=C_4	1.3266	1.3474	1.3401
C_4—C_4'	1.4558	1.4416	1.4416

ground state structure are significant. MP(3) fails to correctly describe this part of the ground state potential energy surface, which leads to an unphysical description of the excited state PES. The spin-flip variant of ADC(3) has been reported to correct the unphysical behavior of MP(3) in the case of bond-breaking [81]. For the ground state equilibrium structure of octatetraene, SF-ADC(3) yields reasonable results, which are presented in table 8.4. However, the terminal double bond is described as too short compared to CCSD(T) and even shorter as in the uncorrelated Hartree-Fock structure. For the excited state, SF-ADC(3) improves over the ADC(3) result for the fluorescence energy, but, the result is still too low, and the excited state equilibrium geometry is incorrect.

Table 8.4: Two-photon absorption δ_{TP} cross-sections for the $2^1A_g^-$ state of octaetraene computed at the CCSD(T)/cc-pVTZ ground state equilibrium structure using the aug-cc-pVTZ basis. A * indicates results from using a different implementation [47].

	ADC(2)	ADC(2)-x	ADC(2)*	ADC(2)*
δ_{TP}	78660	1546	71170	871

8.1.3 Two-photon absorption

The two-photon absorption cross-sections for octatetraene have already been presented using a MP(2)/6-31G* optimized ground state structure and the 6-31+G* basis set [47]. Using the implementation in this work larger basis sets could be applied and the TPA cross-sections have been obtained at the CCSD(T)/cc-pVTZ ground state structure. The results for the $2^1A_g^-$ state using the aug-cc-pVTZ basis set are given in table 8.4 together with the data from the previous work.

8.2 *Trans*-bithiophene

Oligothiophenes play important roles in medical and technical applications. Thiophene derivatives are often used as electron donors in the field of organic solar cells [82–84] and oligo- and polythiophenes are used as imaging agents for the detection of β-amyloid protein deposits [85], of which the formation plays an important role in degenerative protein misfolding diseases like Alzheimer's disease. The key mechanism, which can also be studied in the bithiophene molecule, is the planarization of the non-planar bithiophene unit upon excitation. It is accompanied by a significant stokes shift in the fluorescence energy and induces conformational changes in its molecular environment.

8.2.1 Excited state structure and stokes shift

The first excited state of the *trans*-bithiophene (bithiophene) molecule has been optimized using ADC(2), ADC(2)-x and ADC(3)/cc-pVDZ and the planarization in the excited state is correctly described. The resulting vertical fluorescence energies are given in table 8.5 together with vertical excitation energies obtained at

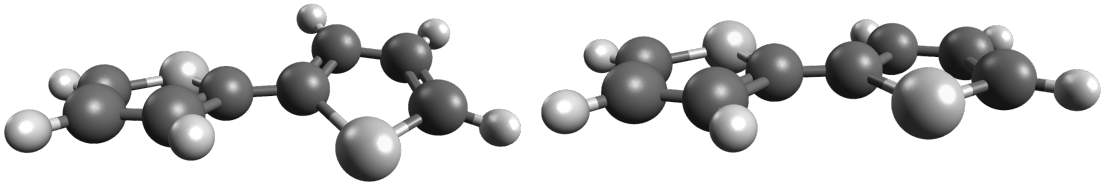

Figure 8.2: Non-planar ground state structure and planar structure of the first excited state of bithiophene.

the MP2/def2-TZVPP ground state structure. The vertical absorption energies of ADC(2)-x and ADC(3) are in good agreement with experimental findings as well as the vertical fluorescence energies at the ADC(2)-x and ADC(3)-optimized structure. The experimentally observed stokes shift of about 0.7 eV is well reproduced by all ADC models.

8.2.2 Two-photon absorption

Two-photon absorption spectroscopical measurements revealed an energetically high-lying two-photon allowed excited state [86]. The TPA cross-sections for bithiophene have been computed using ADC(2) and ADC(2)-x/cc-pVDZ at the MP2/def2-TZVPP ground state equilibrium structure and the results are given in table 8.5. The ADC(2) results show an excited state with a large TPA cross-section around 6 eV. However, the 2^1A_1 and 3^1A_1 have substantial double excitation character. Thus, they are overestimated by ADC(2), which can be seen by comparison with ADC(2)-x, which finds those states at substantially lower energies. ADC(2)-x is known to underestimate the doubly excited states and ADC(3) excitation energies have computed for comparison, which find a 0.55 eV higher excitation energy for the 2^1A_1 state. Based on the ADC(2)-x and ADC(3) results, the state with the largest two-photon activity can be assigned to the 2^1A_1 state at 4.96 eV, which is in good agreement with experimental results.

Table 8.5: Vertical fluorescence and absorption energies and oscillator strengths for the 1^1B_1 state of bithiophene in atomic units using ADC(2)-x and ADC(3)/cc-pVDZ. In addition, vertical excitation energies and TPA cross-sections δ_{TP} in atomic units for the lowest states with A_1 symmetry are given. The results have been obtained using the cc-pVDZ basis set for geometry optimizations and TPA cross-sections, which have been computed at the MP2/def2-TZVPP ground state structure. Experimental values have been taken from a: [87], b: [86].

	ADC(2)	ADC(2)-x	ADC(3)	Exp.
1^1B_1				
vert. abs.	4.74	4.14	4.58	4.13[a], 3.86 (0 - 0)[a]
osc.str.	0.47	0.36	0.43	
vert. fluo.	3.81	3.23	3.63	3.40[b]
osc. str.	0.50	0.38	0.45	
2^1A_1	5.50	4.41	4.96	4.96[a], 4.48 (0 - 0)[b]
δ_{TP}	1262	1361		
3^1A_1	6.07	4.59	5.38	
δ_{TP}	4806	122		

Chapter 9

Conclusion

9.1 Overview

Method development for the quantum chemical description of electronically excited states for medium-sized and large molecular systems is an essential field of modern theoretical chemistry. In this thesis, for the first time analytical derivative expressions for the energy of the algebraic diagrammatic construction scheme of the polarization propagator of third order and extended second order have been derived and presented enclosed in a comprehensive review of analytical derivative theory in quantum chemistry. In addition, an efficient program for the computation of two-photon absorption cross-sections for ADC(2) and ADC(2)-x has been presented. The computation of TPA cross-sections is based on the implementation of expressions for excited-state one-particle densities obtained through the intermediate state representation approach, which has been outlined in detail. Analytical derivative expressions for ADC(2), ADC(2)-x and ADC(3), and the introduced scheme for the calculation of the TPA cross-sections employing the DIIS algorithm have been integrated in the `adcman` module embedded in the Q-Chem package of programs. The integrity of the implemented features has been verified through numerical testing. Furthermore, a numerical scheme for the computation of the complex frequency-dependent electric dipole polarization has been outlined and a preliminary proof-of-principle implementation has been carried out.

The analytical derivatives have been used for excited-state geometry optimizations and have been applied in the first step to small test molecules. Benchmark

calculations on diatomic molecules have been used to evaluate the performance of the excited state equilibrium structures obtained with ADC(2), ADC(2)-x and ADC(3). For the chosen test set, ADC(2)-x showed a systematic improvement over ADC(2) and both ADC(2)-x and ADC(3) performed comparable to CCSD. Test calculations on small organic molecules revealed limitations of the applicability of ADC(2)-x and ADC(3) for the description of excited state potential energy surfaces, and the origin of the deficiencies has been imputed to the underlying MP(2) and MP(3) ground state respectively.

Two model systems have been studied using the newly implemented features. Both systems represent important classes of molecules with various biological functions, and technical and medical applications. In the study of the first one, all-*trans*-octatetraene, it could be shown that ADC(3) yields vertical excitation energies, which are in good agreement with experimental results. However, it has been seen that ADC(2)-x and ADC(3) fail to correctly describe the excited state geometry of the first excited state of linear polyenes like octatetraene. The study of bithiophene showed, that ADC(3) yields accurate results for vertical absorption and fluorescence energies and yields reasonable excited state geometries for the first excited singlet state. In addition, ADC(2)-x and ADC(3) results predict a two-photon-active excited state in the energy region, in which TPA experiments revealed a one-photon-forbidden state.

9.2 Outlook

The newly implemented features in combination with the highly efficient and fully parallel `adcman` program can be used to study medium-sized and larger organic chromophores. Geometry optimizations with ADC(3) for systems up to four hundred basis functions can be performed on sufficiently powerful computers within a few days. In addition, comparing the results of computed two-photon absorption cross-sections with ADC(2) and ADC(2)-x yields qualitative and quantitative insights for two-photon active states with large double excitation character. Furthermore, it is straightforward to extended the two-photon absorption program to the ADC(3/2) model due to the modular structure of the program.

Another promising perspective is the extension of the analytical derivatives to

other ADC variants, i.e. the core-valence separation and ionization and electron affinity ADC.

One of the most interesting questions is, how the deficiencies of the ADC(2)-x and ADC(3) energy derivative can be overcome. In general, the vertical excitation energies of ADC(2)-x and especially ADC(3) are very accurate and the failure to correctly describe certain excited state potential energy surfaces can be attributed to the ground state energy contribution of the total energy. Thus, it is obvious that in order to improve or remediate the excited state derivatives of ADC models, an improved treatment of the ground state energy is necessary. In principle, the combination of any ground state method with ADC is possible, since it plays no role in the hermitian eigenvalue problem. However, MP(n) is the intrinsic ground state to a given ADC(n) model and thus, other combinations have no formal justification. Nevertheless, pairing the excitation energy derivatives of ADC with the derivatives of other ground state methods is straightforward since derivatives can simply be added up and the modular structure of the `adcman` program offers the required flexibility. Thus, this is a route, which should be explored in the future.

Bibliography

[1] P. Mathis, editor. *Photosynthesis: From Light to Biosphere.* Kluwer Academic Pub. (**1996**).

[2] W. R. Briggs and J. L. Spudich, editors. *Handbook of Photosensory Receptors.* Wiley-VCH, Weinheim, Germany (**2005**).

[3] M.-M. Russew and S. Hecht. "Photoswitches: From Molecules to Materials". *Advanced Materials*, 22 (2010) pages 3348–3360.

[4] D. Wöhrle and O. R. Hild. "Organische Solarzellen. Energie der Zukunft". *Chemie in unserer Zeit*, 44 (2010) pages 174–189.

[5] A. L. Roes, E. A. Alsema, K. Blok and M. K. Patel. "Ex-ante environmental and economic evaluation of polymer photovoltaics". *Progress in Photovoltaics: Research and Applications*, 17 (2009) pages 372–393.

[6] P. H. P. Harbach and A. Dreuw. *The Art of Choosing the Right Quantum Chemical Excited-State Method for Large Molecular Systems.* Wiley-VCH Verlag GmbH & Co. KGaA (**2011**). pages 29–47.

[7] A. H. Zewail, F. C. de Schryver, S. De Feyter and G. Schweitzer. *Femtochemistry.* Wileyy-VCH (**2001**).

[8] A. Dreuw. "Quantum chemical methods for the description of photo-initiated processes in biological systems". *Chem. Phys. Chem.*, 7 (2006) page 2259.

[9] J. E. Ridley and M. C. Zerner. *Theor. Chim. Acta*, 32 (1973) pages 111–134.

[10] M. Kotzian, N. Rösch and M. C. Zerner. *Theor. Chim. Acta*, 81 (1992) pages 201–222.

[11] W. Weber and W. Thiel. *Theor. Chem. Acc.*, 103 (2000) page 495.

[12] J. del Bene, R. Ditchfield and J. A. Pople. *J. Chem. Phys.*, 55 (1971) pages 2236–2241.

[13] J. B. Foresman, M. Head-Gordon, J. A. Pople and M. J. Frisch. *J. Phys. Chem.*, 96 (1992) pages 135–149.

[14] A. L. Fetter and J. D. Walecka. *Quantum Theory of Many-Particle Systems.* McGraw-Hill, New York (**1971**).

[15] D. Hegarthy and M. A. Robb. *Mol. Phys.*, 38 (1979) pages 1795–1812.

[16] R. H. E. Eade and M. A. Robb. *Chem. Phys. Lett.*, 83 (1981) pages 362–368.

[17] E. Runge and E. K. U. Gross. *Phys. Rev. Lett.*, 52 (1984) pages 997–1000.

[18] M. E. Casida. *Recent Advances in Density Functional Methods, Part I.* World Scientific, Singapore (**1995**). pages 155–192.

[19] R. J. Bartlett and M. Musiał. "Coupled-cluster theory in quantum chemistry". *Rev. Mod. Phys.*, 79 (2007) pages 291–352.

[20] A. Dreuw and M. Wormit. "The algebraic diagrammatic construction scheme for the polarization propagator for the calculation of excited states". *Wiley Interdisciplinary Reviews: Computational Molecular Science*, 5 (2015) pages 82–95.

[21] P. Pulay. "Ab initio calculation of force constants and equilibrium geometries in polyatomic molecules". *Molecular Physics*, 17 (1969) pages 197–204.

[22] P. Pulay. "Analytical derivatives, forces, force constants, molecular geometries, and related response properties in electronic structure theory". *Wiley Interdisciplinary Reviews: Computational Molecular Science*, 4 (2014) pages 169–181.

[23] S. V. Levchenko, T. Wang and A. I. Krylov. "Analytic gradients for the spin-conserving and spin-flipping equation-of-motion coupled-cluster models with single and double substitutions". *The Journal of Chemical Physics*, 122 (2005) 224106.

[24] A. Szabo and N. S. Ostlund. *Modern Quantum Chemistry.* MacMillan Publishing (**1982**).

[25] T. Helgaker, P. Jrgensen, J. Olsen, T. Helgaker, P. Jrgensen and J. Olsen. *Second Quantization.* John Wiley & Sons, Ltd (**2000**). pages 1–33.

[26] C. Møller and M. S. Plesset. "Note on an Approximation Treatment of Many-Electron Systems". *Phys. Rev.*, 46 (1934) pages 618–622.

[27] E. Schrödinger. "Quantisierung als Eigenwertproblem". *Ann. d. Phys.*, 385 (1926) pages 437–490.

[28] T. Helgaker, P. Jrgensen, J. Olsen, T. Helgaker, P. Jrgensen and J. Olsen. *Perturbation Theory*. John Wiley & Sons, Ltd (**2000**). pages 724–816.

[29] G. C. Wick. "The Evaluation of the Collision Matrix". *Phys. Rev.*, 80 (1950) pages 268–272.

[30] M. Wormit, D. R. Rehn, P. H. Harbach, J. Wenzel, C. M. Krauter, E. Epifanovsky and A. Dreuw. "Investigating excited electronic states using the algebraic diagrammatic construction (ADC) approach of the polarisation propagator". *Molecular Physics*, 112 (2014) pages 774–784.

[31] J. Schirmer. *Phys. Rev. A*, 26 (1982) pages 2395–2416.

[32] A. B. Trofimov, G. Stelter and J. Schirmer. *J. Chem. Phys.*, 111 (1999) page 9982.

[33] J. Schirmer and A. B. Trofimov. *J. Chem. Phys.*, 120 (2004) page 11449.

[34] H. Hellmann. *Einführung in die Quantenchemie*. Leipzig: Franz Deuticke (**1937**).

[35] R. P. Feynman. "Forces in Molecules". *Phys. Rev.*, 56 (1939) pages 340–343.

[36] T. Helgaker and P. Jørgensen. "Configuration-interaction energy derivatives in a fully variational formulation". *Theoretical Chemistry Accounts: Theory, Computation, and Modeling (Theoretica Chimica Acta)*, 75 (1989) pages 111–127.

[37] N. C. Handy and H. F. S. III. "On the evaluation of analytic energy derivatives for correlated wave functions". *The Journal of Chemical Physics*, 81 (1984) pages 5031–5033.

[38] C. Hättig. "Structure Optimizations for Excited States with Correlated Second-Order Methods: {CC2} and ADC(2)". In H. Jensen, editor, "Response Theory and Molecular Properties (A Tribute to Jan Linderberg and Poul Jrgensen)", volume 50 of *Advances in Quantum Chemistry*. Academic Press (**2005**). pages 37 – 60.

[39] P. H. P. Harbach, M. Wormit and A. Dreuw. "The third-order algebraic diagrammatic construction method (ADC(3)) for the polarization propagator for closed-shell molecules: Efficient implementation and benchmarkinga)". *The Journal of Chemical Physics*, 141 (2014) 064113.

[40] Y. Shao, Z. Gan, E. Epifanovsky, A. T. Gilbert, M. Wormit, J. Kussmann, A. W. Lange, A. Behn, J. Deng, X. Feng *et al.* "Advances in molecular quantum chemistry contained in the Q-Chem 4 program package". *Molecular Physics*, 113 (2015) pages 184–215.

[41] M. J. Frisch, M. Head-Gordon and J. A. Pople. "A direct MP2 gradient method". *Chemical Physics Letters*, 166 (1990) pages 275–280.

[42] J. Gauss and D. Cremer. "Implementation of analytical energy gradients at third- and fourth-order Mller-Plesset perturbation theory". *Chemical Physics Letters*, 138 (1987) pages 131 – 140.

[43] J. Schirmer and G. Angonoa. "On Greens function calculations of the static selfenergy part, the ground state energy and expectation values". *The Journal of Chemical Physics*, 91 (1989) pages 1754–1761.

[44] F. Plasser, B. Thomitzni, S. A. Bppler, J. Wenzel, D. R. Rehn, M. Wormit and A. Dreuw. "Statistical analysis of electronic excitation processes: Spatial location, compactness, charge transfer, and electron-hole correlation". *Journal of Computational Chemistry*, 36 (2015) pages 1609–1620.

[45] A. Trofimov, I. Krivdina, J. Weller and J. Schirmer. "Algebraic-diagrammatic construction propagator approach to molecular response properties". *Chemical Physics*, 329 (2006) pages 1 – 10. Electron Correlation and Multimode Dynamics in Molecules(in honour of Lorenz S. Cederbaum).

[46] P. Cronstrand, Y. Luo and H. Ågren. "Multi-Photon Absorption of Molecules". volume 50 of *Advances in Quantum Chemistry*. Academic Press (**2005**). pages 1 – 21. doi:10.1016/S0065-3276(05)50001-7.

[47] S. Knippenberg, D. R. Rehn, M. Wormit, J. H. Starcke, I. L. Rusakova, A. B. Trofimov and A. Dreuw. "Calculations of nonlinear response properties using the intermediate state representation and the algebraic-diagrammatic construction polarization propagator approach: Two-photon absorption spectra". *The Journal of Chemical Physics*, 136 (2012) 064107.

[48] E. R. Davidson. *J. Comp. Phys.*, 17 (1975) pages 87–94.

[49] P. Norman, D. M. Bishop, H. Jo/rgen Aa. Jensen and J. Oddershede. "Near-resonant absorption in the time-dependent self-consistent field and multiconfigurational self-consistent field approximations". *The Journal of Chemical Physics*, 115 (2001) pages 10323–10334.

[50] S. Coriani, O. Christiansen, T. Fransson and P. Norman. "Coupled-cluster response theory for near-edge x-ray-absorption fine structure of atoms and molecules". *Phys. Rev. A*, 85 (2012) page 022507.

[51] E. Epifanovsky, M. Wormit, T. Ku, A. Landau, D. Zuev, K. Khistyaev, P. Manohar, I. Kaliman, A. Dreuw and A. I. Krylov. "New implementation of high-level correlated methods using a general block tensor library for high-performance electronic structure calculations". *Journal of Computational Chemistry*, 34 (2013) pages 2293–2309.

[52] P. Pulay. "Convergence acceleration of iterative sequences. the case of scf iteration". *Chemical Physics Letters*, 73 (1980) pages 393 – 398.

[53] K. P. Huber and G. Herzberg. *Molecular Spectra and Molecular Structure IV. Constants of Diatomic Molecules*. Van Nostrand, New York (**1979**).

[54] T. H. Dunning Jr. *J. Chem. Phys.*, 90 (1989) page 1007.

[55] D. E. Woon and T. H. Dunning. "Gaussian basis sets for use in correlated molecular calculations. IV. Calculation of static electrical response properties". *The Journal of Chemical Physics*, 100 (1994) pages 2975–2988.

[56] D. E. Woon and T. H. Dunning. "Gaussian basis sets for use in correlated molecular calculations. III. The atoms aluminum through argon". *The Journal of Chemical Physics*, 98 (1993) pages 1358–1371.

[57] T. H. Dunning and K. A. Peterson. "Use of Mo/ller-Plesset perturbation theory in molecular calculations: Spectroscopic constants of first row diatomic molecules". *The Journal of Chemical Physics*, 108 (1998) pages 4761–4771.

[58] C. S. Page and M. Olivucci. "Ground and excited state CASPT2 geometry optimizations of small organic molecules". *Journal of Computational Chemistry*, 24 (2003) pages 298–309.

[59] M. Pabst and A. Köhn. "Implementation of transition moments between excited states in the approximate coupled-cluster singles and doubles model". *The Journal of Chemical Physics*, 129 (2008) 214101.

[60] A. Young and G. Britton, editors. *Carotenoids in Photosynthesis*. Chapman and Hall, New York (**1993**).

[61] T. Polívka and V. Sundström. *Chem. Rev.*, 104 (2004) page 2021.

[62] B. S. Hudson and B. E. Kohler. "A low-lying weak transition in the polyene α,ω-diphenyloctatetraene". *Chem. Phys. Lett.*, 14 (1972) pages 299–304.

[63] B. S. Hudson and B. E. Kohler. "Linear Polyene Electronic Structure and Spectroscopy". *Ann. Rev. Phys. Chem.*, 25 (1974) pages 437–460.

[64] K. Schulten, I. Ohmine and M. Karplus. *J. Chem. Phys.*, 64 (1976) pages 4422–4441.

[65] B. S. Hudson, B. E. Kohler and K. Schulten. Academic Press, New York (**1982**). page 1.

[66] P. Tavan and K. Schulten. *Phys. Rev. B*, 36 (1987) page 4337.

[67] R. J. Cave and E. R. Davidson. *J. Chem. Phys.*, 91 (1987) page 4481.

[68] R. J. Cave and E. R. Davidson. *J. Chem. Phys.*, 92 (1988) page 614.

[69] G. Orlandi, F. Zerbetto and M. Z. Zgierski. *Chem. Rev.*, 91 (1991) page 867.

[70] W. J. Buma, B. E. Kohler and K. Song. *J. Chem. Phys.*, 94 (1991) page 6367.

[71] L. Serrano-Andres, M. Merchan, I. Nebot-Gil, R. Lindh and B. O. Roos. *J. Chem. Phys.*, 98 (1993) page 3151.

[72] L. Serrano-Andres, R. Lindh, B. O. Roos and M. Merchan. *J. Phys. Chem.*, 97 (1993) page 9360.

[73] R. P. Krawczyk, K. Malscha, G. Hohlneicher, R. C. Gillen and W. Domcke. "1^1B_u—2^1A_g conical intersection in trans-butadiene: ultrafast dynamics and optical spectra". *Chem. Phys. Lett.*, 320 (2000) pages 535–541.

[74] C.-P. Hsu, S. Hirata and M. Head-Gordon. "Excitation Energies from Time-Dependent Density Functional Theory for Linear Polyene Oligomers: Butadiene to Decapentaene". *J. Phys. Chem. A*, 105 (2001) pages 451–458.

[75] K. B. Wiberg, A. E. de Oliveira and G. Trucks. *J. Phys. Chem. A*, 106 (2002) page 4192.

[76] R. Pariser. *J. Chem. Phys.*, 24 (1956) page 250.

[77] J. H. Starcke, M. Wormit, J. Schirmer and A. Dreuw. "How much double excitation character do the lowest excited states of linear polyenes have?" *Chem. Phys.*, 329 (2006) pages 39–49.

[78] R. L. Christensen, M. G. I. Galinato, E. F. Chu, J. N. Howard, R. D. Broene and H. A. Frank. *J. Phys. Chem. A*, 112 (2008) page 12629.

[79] L. Serrano-Andrés, R. Lindh, B. O. Roos and M. Merchán. "Theoretical study of the electronic spectrum of all-trans-1,3,5,7-octatetraene". *J. Chem. Phys.*, 97 (1993) pages 9360–9368.

[80] H. Petek, A. J. Bell, Y. S. Choi, K. Yoshihara, B. A. Tounge and R. L. Christensen. "The 2 ^1A_g state of *trans,trans*-1,3,5,7octatetraene in free jet expansions". *The Journal of Chemical Physics*, 98 (1993) pages 3777–3794.

[81] D. Lefrancois, M. Wormit and A. Dreuw. "Adapting algebraic diagrammatic construction schemes for the polarization propagator to problems with multi-reference electronic ground states exploiting the spin-flip ansatz". *The Journal of Chemical Physics*, 143 (2015) 124107.

[82] F. Zhang, D. Wu, Y. Xu and X. Feng. "Thiophene-based conjugated oligomers for organic solar cells". *J. Mater. Chem.*, 21 (2011) pages 17590–17600.

[83] D. Blanger. *Polythiophenes as Active Electrode Materials for Electrochemical Capacitors*. John Wiley & Sons, Ltd (**2009**). pages 577–594. doi:10.1002/9780470745533.ch15.

[84] A. Mishra, C.-Q. Ma, J. L. Segura and P. Buerle. *Functional Oligothiophene-Based Materials: Nanoarchitectures and Applications*. John Wiley & Sons, Ltd (**2009**). pages 1–155. doi:10.1002/9780470745533.ch1.

[85] A. slund, C. J. Sigurdson, T. Klingstedt, S. Grathwohl, T. Bolmont, D. L. Dickstein, E. Glimsdal, S. Prokop, M. Lindgren, P. Konradsson *et al.* "Novel Pentameric Thiophene Derivatives for in Vitro and in Vivo Optical Imaging of a Plethora of Protein Aggregates in Cerebral Amyloidoses". *ACS Chemical Biology*, 4 (2009) pages 673–684. PMID: 19624097.

[86] D. Birnbaum and B. E. Kohler. "Location of a 1Ag state in bithiophene". *The Journal of Chemical Physics*, 96 (1992) pages 2492–2495.

[87] J. E. Chadwick and B. E. Kohler. "Optical Spectra of Isolated s-cis- and s-trans-Bithiophene: Torsional Potential in the Ground and Excited States". *The Journal of Physical Chemistry*, 98 (1994) pages 3631–3637.

List of Publications

- **Dirk R. Rehn**, M. Wormit and A. Dreuw, "Analytical gradients for the Algebraic Diagrammatic Construction scheme of the polarization propagator up to third order", In preparation

- T. Setzer, **Dirk R. Rehn**, M. Wormit and A. Dreuw. "Benchmark of excited-state transition moments using the ADC/ISR approach up to 3rd order" In preparation

- F. Plasser, B. Thomitzni, S. Bppler, J. Wenzel, **Dirk R. Rehn**, M. Wormit and A. Dreuw, "Statistical Analysis of Electronic Excitation Processes: Location, Compactness, and Electron-Hole Correlation" J. Comp. Chem., 2015, 36, 1609

- Yihan Shao, Zhengting Gan, Evgeny Epifanovsky, Andrew T.B. Gilbert, Michael Wormit, Joerg Kussmann, Adrian W. Lange, Andrew Behn, Jia Deng, Xintian Feng, Debashree Ghosh, Matthew Goldey, Paul R. Horn, Leif D. Jacobson, Ilya Kaliman, Rustam Z. Khaliullin, Tomasz Kuo, Arie Landau, Jie Liu, Emil I. Proynov, Young Min Rhee, Ryan M. Richard, Mary A. Rohrdanz, Ryan P. Steele, Eric J. Sundstrom, H. Lee Woodcock III, Paul M. Zimmerman, Dmitry Zuev, Ben Albrecht, Ethan Alguire, Brian Austin, Gregory J. O. Beran, Yves A. Bernard, Eric Berquist, Kai Brandhorst, Ksenia B. Bravaya, Shawn T. Brown, David Casanova, Chun-Min Chang, Yunqing Chen, Siu Hung Chien, Kristina D. Closser, Deborah L. Crittenden, Michael Diedenhofen, Robert A. DiStasio Jr., Hainam Do, Anthony D. Dutoi, Richard G. Edgar, Shervin Fatehi, Laszlo Fusti-Molnar, An Ghysels, Anna Golubeva-Zadorozhnaya, Joseph Gomes, Magnus W.D. Hanson-Heine, Philipp H.P. Harbach, Andreas W. Hauser, Edward G. Hohenstein, Zachary C. Holden, Thomas-C. Jagau, Hyunjun Ji, Benjamin Kaduk, Kirill Khistyaev, Jaehoon Kim, Jihan Kim, Rollin A. King, Phil Klunzinger, Dmytro Kosenkov, Tim Kowalczyk, Caroline M. Krauter, Ka Un Lao, Adele D. Laurent, Keith V. Lawler, Sergey V. Levchenko, Ching Yeh Lin, Fenglai Liu, Ester Livshits, Rohini C. Lochan, Arne Luenser, Prashant Manohar, Samuel F. Manzer, Shan-Ping Mao, Narbe Mardirossian, Aleksandr V.

Marenich, Simon A. Maurer, Nicholas J. Mayhall, Eric Neuscamman, C. Melania Oana, Roberto Olivares-Amaya, Darragh P. ONeill, John A. Parkhill, Trilisa M. Perrine, Roberto Peverati, Alexander Prociuk, **Dirk R. Rehn**, Edina Rosta, Nicholas J. Russ, Shaama M. Sharada, Sandeep Sharma, David W. Small, Alexander Sodt, Tamar Stein, David Stock, Yu-Chuan Su, Alex J.W. Thom, Takashi Tsuchimochi, Vitalii Vanovschi, Leslie Vogt, Oleg Vydrov, Tao Wang, Mark A. Watson, Jan Wenzel, Alec White, Christopher F. Williams, Jun Yang, Sina Yeganeh, Shane R. Yost, Zhi-Qiang You, Igor Ying Zhang, Xing Zhang, Yan Zhao, Bernard R. Brooks, Garnet K.L. Chan, Daniel M. Chipman, Christopher J. Cramer, William A. Goddard III, Mark S. Gordon, Warren J. Hehre, Andreas Klamt, Henry F. Schaefer III, Michael W. Schmidt, C. David Sherrill, Donald G. Truhlar, Arieh Warshel, Xin Xu, Alan Aspuru-Guzik, Roi Baer, Alexis T. Bell, Nicholas A. Besley, Jeng-Da Chai, Andreas Dreuw, Barry D. Dunietz, Thomas R. Furlani, Steven R. Gwaltney, Chao-Ping Hsu, Yousung Jung, Jing Kong, Daniel S. Lambrecht, WanZhen Liang, Christian Ochsenfeld, Vitaly A. Rassolov, Lyudmila V. Slipchenko, Joseph E. Subotnik, Troy Van Voorhis, John M. Herbert, Anna I. Krylov, Peter M.W. Gill, Martin Head-Gordon, "Advances in molecular quantum chemistry contained in the Q-Chem 4 program package" Mol. Phys., 2015, 113, 184

- M. Wormit, **Dirk R. Rehn**, P. H. P. Harbach, J. Wenzel, C. M. Krauter, E. Epifanovsky and A. Dreuw, "Investigating Excited Electronic States using the Algebraic Diagrammatic Construction (ADC) Approach of the Polarisation Propagator" Mol. Phys., 2014, 112, 774

- S. Knippenberg, **Dirk R. Rehn**, M. Wormit, J. H. Starcke, I.L.Rusakova, A. B. Trofimov and A. Dreuw, "Calculations of nonlinear response properties using intermediate state representation and algebraic-diagrammatic construction polarization propagator approach: Two-photon absorption spectra", J. Chem. Phys., 2012, 136, 064107

Danksagung

Ich bedanke mich an dieser Stelle sehr herzlich bei allen, die mich bei dieser Arbeit unterstützt haben.

Besonderer Dank gilt Prof. Dr. Andreas Dreuw, der mich für dieses Feld begeistert hat und mir die Möglichkeit bot, an interessanten Themen zu Forschen. Ich möchte mich für seine motivierende und mitreißende Art bedanken. Er war mir immer ein großartiger Betreuer und hat mich auch über das Fachliche hinaus unterstützt.

Ich bedauere sehr, dass ich nicht mehr die Möglichkeit habe, mich nach dem Abschluss meiner Arbeit ein weiteres mal persönlich bei Dr. Michael Wormit für seine wunderbare Art zu erklären und zu diskutieren bedanken kann. Ihm gebührt mein besonderer Dank und ich sehr bin froh, dass ich so lange mit ihm zusammen Arbeiten konnte.

Meinen Mentoren, Dr. Shirin Faraji, Prof. Dr. Lorenz Cederbaum und PD Dr. Markus Pernpointner danke ich für die Betreuung, die Gelegenheit meine Zwischenergebnisse zu präsentieren und für die anregenden Fragen bei unseren Treffen.

Jan Wenzel und Matthias Schneider danke ich für die sehr angenehme Athmosphäre, die während unserer gemeinsamen Zeit in unserem Büro herrschte und die Zeit mit Tim Stauch und Jie Han, stand dieser in nichts nach.

Der gesamten Arbeitsgruppe möchte ich danken für die sehr schöne Zeit.

Für das Korrekturlesen meiner Arbeit danke ich zuerst Jan Wenzel und Tim Stauch und Manuel Hodecker.

Natürlich möchte ich mich auch bei meiner Mutter und bei meiner Familie, meinem Bruder Ingo und meinem Bruder Hanno und dessen Frau Ulrike bedanken, die mich immer unterstützt haben.

Besonders bedanke ich mich auch bei meiner lieben Freundin Eva, die mir zur Seite stand und steht.

Ich danke allen meinen Freunden.

Eidesstattliche Versicherung gemäß §8 der Promotionsordnung der Naturwissenschaftlich-Mathematischen Gesamtfakultät der Universität Heidelberg

1. Bei der eingereichten Dissertation zu dem Thema
   „Development of Quantum Chemical Methods for Excited-State and Response Properties“
   handelt es sich um meine eigenständig erbrachte Leistung.

2. Ich habe nur die angegebenen Quellen und Hilfsmittel benutzt und mich keiner unzulässigen Hilfe Dritter bedient. Insbesondere habe ich wörtlich oder sinngemäß aus anderen Werken übernommene Inhalte als solche kenntlich gemacht.

3. Die Arbeit oder Teile davon habe ich bislang nicht an einer Hochschule des In- oder Auslands als Bestandteil einer Prüfungs- oder Qualifikationsleistung vorgelegt.

4. Die Richtigkeit der vorstehenden Erklärungen bestätige ich.

5. Die Bedeutung der eidesstattlichen Versicherung und die strafrechtlichen Folgen einer unrichtigen oder unvollständigen eidesstattlichen Versicherung sind mir bekannt.

Ich versichere an Eides statt, dass ich nach bestem Wissen die reine Wahrheit erklärt und nichts verschwiegen habe.

Ort/Datum Unterschrift